Università degli studi di Modena e Reggio Emilia

International Doctorate School in Clinical and Experimental Medicine
Clinical, Genetic and Molecular Medicine

XXVIII CYCLE

CHARACTERIZATION OF THE R7S MUTATION OF THE HEAT SHOCK PROTEIN HSPB3 AND OF TWO NOVEL MUTATIONS FOUND IN MYOPATHIC PATIENTS: UNDERSTANDING THE MECHANISMS LEADING TO DISEASE

PhD Thesis by:
Federica, Francesca Morelli

Supervisor:
Prof.ssa Serena Carra

Director of PhD school:
Prof. Giuseppe Biagini

Accademic Year 2014-2015

TABLE OF CONTENTS

INTRODUCTION

The Heat Shock Proteins

Almost 50 years ago, the Italian scientist Ferruccio Ritossa, who was working on chromosomal puffs using *Drosophila melanogaster* as animal model, discovered the heat shock response by serendipity. In fact, one of his co-workers raised the temperature of the incubator where Dr. Ritossa was growing his flies. The change in the temperature altered the puffing pattern and lead to the synthesis of new, unknown factors, which were later called heat shock proteins (HSPs) (De Maio 2011). HSPs are highly conserved and present in all organisms and in all cells of all organisms. While some HSPs are already expressed under resting conditions (constitutive HSPs), other HSPs are only induced upon stress conditions, including not only heat shock, but also oxidative stress, changes in pH, nutrients and others (De Maio 2011).

The heat shock proteins (HSPs) have been classified into six major families based on their molecular masses. However, after the discovery of the heat shock response different names have been assigned to the same gene product, thus creating confusion in the exact nomenclature of HSPs. In addition, almost identical names have been used to refer to different gene products. For example, HSPA1B has been called HSP70-2, whereas HSP70.2 refers to the testis specific HSPA2 member. Attempts have thus been made to simplify the nomenclature of HSPs. The first attempt to clarify the nomenclature of the HSPA/HSP70 family was published in 1996 (Tavaria et al. 1996) and the new nomenclature is based on the systematic gene symbols that have been assigned by the HUGO Gene Nomenclature Committee (HGNC) and are used as the primary identifiers in databases such as Entrez Gene and Ensemble. The six families are represented by: HSPH/HSP100 (100-110 kDa), HSP90/HSPC (83-90 kDa), HSP70/HSPA (66-78 kDa), HSP60/HSPD (60 kDa), HSP40/DNAJ (40 kDa) and small heat shock proteins (sHSPs)/HSPB (15-30 kDa) (see Table 1). The first name refers to the new nomenclature system, while the second one refers to the oldest nomenclature. Each family comprises several members, whose number also differs amongst the various organisms. For example, in the HSPA (HSP70) family, the number of members varies from 3 in *Escherichia coli* to 13 in humans.

Hsp100	Cytosol	Role in stress tolerance
Hsp90	Cytosol ER	Role in signal transduction, refolds and maintains role in cell cycle and proliferation
Hsp70	Cystosol ER Mitochondria	Autoregulation of the heat shock response, interorganellar transport, antiapoptotic activity
Hsp60	Mitochondria Cytosol	Refolds and prevents aggregation
Hsp40	Cytosol	Essential cochaperone activity with 70
Small hsps	Cytosol	Suppresses aggregation, heat inactivation

Table 1. The families of heat shock proteins (HSPs) (From: Byung et al. 2008).

Many functions have been attributed to HSPs. Certainly, the role of HSPs as molecular chaperones is their primary function that has been studied and well established both *in vivo* and *in vitro*. Molecular chaperones are proteins able to distinguish between proteins in their native protein conformation (native 3-dimensional structure, biologically functional) and misfolded/unfolded proteins; the latter are proteins not correctly folded that expose hydrophobic residues and, thus, become highly unstable. Protein unfolding and misfolding can be due to genetic mutations or to protein-denaturing stress. The molecular chaperones interact transiently with all these unfolded/misfolded proteins (called clients or substrates), and either assist the refolding of the bound substrates or, when correct folding cannot be achieved, prevent irreversible protein aggregation (Verghese et al. 2012; Saibil 2013). Aggregation is generally a multi-step process, in which exposed hydrophobic portions of the unfolded proteins interact with the exposed hydrophobic patches of other unfolded proteins, leading to irreversible protein aggregation (Requena et al. 2015). The accumulation of protein aggregates has been associated with toxicity and cell death in a number of diseases, which are referred to as protein conformation diseases and include e.g. the Alzheimer's, Parkinson's and Huntington's diseases.

Since protein aggregation leads to toxicity, the cells have evolved the "Protein Quality Control System" (PQC), which is composed by molecular chaperones and degradative systems, such as the ubiquitin-proteasome system (UPS) and the system of autophagy. The PQC has the primary purpose of preventing protein aggregation and, when the latter is not possible, it assists the removal of proteins with altered folding ("misfolded") or irreversibly aggregated (Hartl et al. 2011).

On the basis of their ability to bind to misfolded proteins, a protective role for molecular chaperones in misfolding disorders has been proposed (Stenoien et al. 1999; Cummings and Zoghbi 2000; Jana et al. 2000; Cummings et al. 2001; Sittler et al. 2001; Bailey et al. 2002; Chavez Zobel et al. 2003; Carra et al. 2005). Besides pathological conditions, chaperones also play an essential role for the maintenance, under physiological conditions, of the protein homeostasis (which consists in the maintenance of the equilibrium between protein synthesis, protein folding and protein degradation). Moreover, HSPs confer resistance to stress and thermotolerance, thereby allowing cells to adapt to and survive stressful conditions (De Maio 1999; Giffard et al. 2008).

Molecular chaperones exist in two different functional states characterized by a low or high affinity for misfolded substrates. A shift between the two states allows cycles of binding and release of the substrates providing repeated opportunities for renaturation or degradation of the substrates. According to the mechanism of action there are two classes of chaperones: ATP–independent chaperones (small HSPs) and ATP-dependent chaperones (HSP100, HSP70, HSP90, HSP60, HSP40), which require hydrolysis of ATP to bind to and release the substrate (Carra and Landry 2006). Chaperones interact together and generally work in multi-chaperone complexes that also include other co-factors such as the co-chaperones (see later). The cooperation of several chaperones, ATP-independent and ATP-dependent, with specific co-factors allows the refolding or degradation of the bound substrate, thereby ensuring the maintenance of proteostasis (Mogk et al. 2003; Mogk et al. 2003a; Ehrnsperger et al. 1997).

Besides working as chaperones, the HSPs are implicated in many cellular processes such as cellular differentiation, regulation of cell cycle and modulation of apoptosis (or programmed cell death). In this PhD thesis we will focus on the family of small HSPs.

The Small Heat Shock Proteins

The small heat shock proteins (sHSPs) belong to one of the six families of HSPs and are characterized by low molecular masses of ca. 12-43 kDa and by the presence of a highly conserved stretch of 80-100 amino acids in their C-terminal domain called the “α-crystallin domain” (ACD). Due to its high conservation, the ACD constitutes the signature of the family (Bakthisaran et al. 2015). sHSPs are found throughout the kingdom, from bacteria to plants to

mammals. The human genome encodes for ten sHSPs that are referred to as HSPBs, according to the new nomenclature (see Table 2).

HSPB name	Alternative names	Tissue expression
HspB1	Hsp27, Hsp25 (mouse) Not related to Drosophila Hsp27	smooth, skeletal and cardiac muscles, liver, kidney, lung, stomach, colon, testis, lens, brain
HspB2	MKBP	skeletal and cardiac muscles
HspB3	HspL27	smooth, skeletal and cardiac muscles
HspB4	αA-crystallin	Lens
HspB5	αB-crystallin	smooth, skeletal and cardiac muscles, liver, kidney, lung, stomach, colon, testis, lens, brain
HspB6	Hsp20, p20	smooth, skeletal and cardiac muscles, liver, kidney, lung, stomach, colon, brain
HspB7	cvHsp	skeletal and cardiac muscles
HspB8	Hsp22, H11, E2IG1; not related to Drosophila Hsp22	smooth, skeletal and cardiac muscles, kidney, lung, stomach, colon, testis, brain
HspB9	none	Testis
HspB10	ODFP, ODF1	Testis

MKBP, myotonic dystrophy protein kinase-binding protein; cvHsp, cardiovascular heat shock protein; ODFP , sperm outer dense fiber protein 1.

Table 2. Nomenclature of the mammalian sHSP family members (HSPB) and their tissue distribution (From: Carra and Landry 2006).

From the structural point of view, the sHSPs are composed of three distinct domains: the ACD, the N-terminus and the C-terminus and all regions are important for the function of these proteins. The ACD contains eight (in bacteria and plants) (Bagneris et al. 2009; Laganowsky et al. 2010) or seven (in mammals) (Bagneris et al. 2009; Baranova et al. 2011) β-strands, which are packed into two sheets forming a rather compact structure. The first sheet is formed by conservative β2, β3, β9, and β8 strands, whereas β6-β7, β5, and β4 strands form the second sheet (Baranova et al. 2011) (see Figure 1). Though these strands, sHSPs can interact together forming homo- or hetero-dimers or oligomers, based on whether they contain subunits from one single sHSP or different sHSPs (see Figure 2). For example, two antiparallel β6-β7 strands belonging to two neighbouring HSP monomers form a series of hydrogen bonds that stabilize the dimeric structure (Bagneris et al. 2009; Baranova et al. 2011) (see Figure 3). Homo- or hetero-dimers are considered as the basic unit of sHSP that exerts chaperone activity (one of the main functions of sHSPs; see later); instead, high

molecular weight oligomers (that can contain up to 24 subunits) are generally considered as reservoir of the cellular chaperone power (Merck et al. 1992; Feil et al. 2001). The residues located in the β3, β6-β7, β8, and β9 strands of sHSPs might participate in the interaction of sHSPs with their target proteins, although some controversies exist in the literature (Ghosh et al. 2006; Sreelakshmi et al. 2005). In fact, certain sites located in the ACD are involved in the interaction of sHSPs with substrates such as e.g. cytoskeletal proteins (Sun and MacRae 2005).

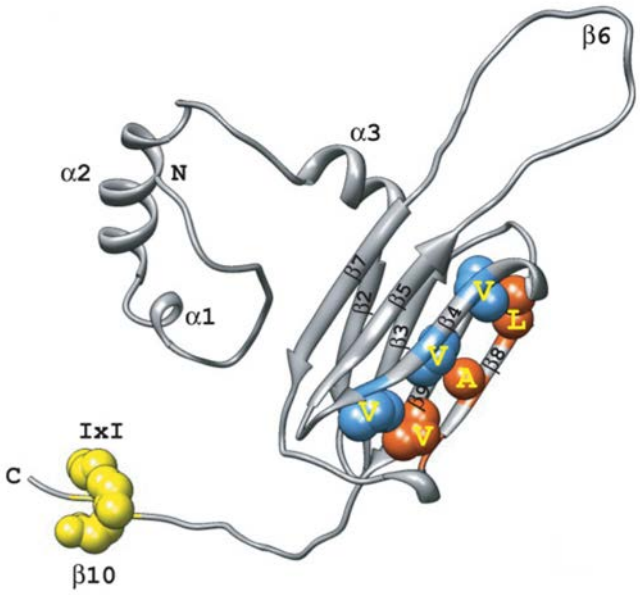

Figure 1. Schematic representation of β sheet. Ribbon diagram of the T. aestivum Hsp16.9 monomer (PDB code 1GME). The N- and C-terminal domains are indicated by N and C correspondingly; α-helices and β-strands are numbered. The amino acid residues responsible for the formation of the hydrophobic groove are shown as blue balls on β4 and as red balls on β8. The IXI motif (IXI) in the β10 strand is shown in yellow (From: Fuchs et al. 2010).

The ACD is flanked by the less conserved N-terminal domain (NTD) and by the C-terminal extension (CTE) (Kriehuber et al. 2010; Mymrikov et al. 2011). The NTD is variable in length and amino acid composition and is, thus, far less well conserved as compared to the ACD (Kriehuber et al. 2010). Due to the high motility and flexibility, the exact structure and location of the NCD within the three dimensional structure of the sHSPs remains unknown for the majority of sHSPs (Hilton et al. 2013). Structural studies done using αB-crystallin (HSPB5)(Jehle et al. 2011) show that the highly mobile NTD can interact with the ACD of the same monomer or form tight contacts with the NTD of neighbouring monomers, leading the formation and stabilization of higher order functional oligomers and, thus, modulating not

only sHSP structure, but also function (see later). Into the very N-terminal end of some sHSPs a not very conservative domain, called WDPF domain, is found. This motif has the following primary structure: (W/F)(D/F)PF-X0-8-(W/F)(D/E)(P/F)F, where X-denotes non-conservative residues (Lambert et al. 1999). The CTE is very variable in length and amino acid composition, highly flexible and mobile (Lindner et al. 2000; Treweek et al. 2010), not well ordered, and is therefore easily cleaved by proteolysis (Kumarasamy and Abraham 2008; Aquilina and Watt 2007). The CTE is located beyond the conservative ACD (Schäfer et al. 1999; Kato et al. 2001) and is usually rather short. The CTE is divided into two regions: the C-terminal fragment (Hilton et al. 2013) and C-terminal tail, composed by conservative sequence (I/V/L)-X-(I/V/L) (usually designated as IXI motif).

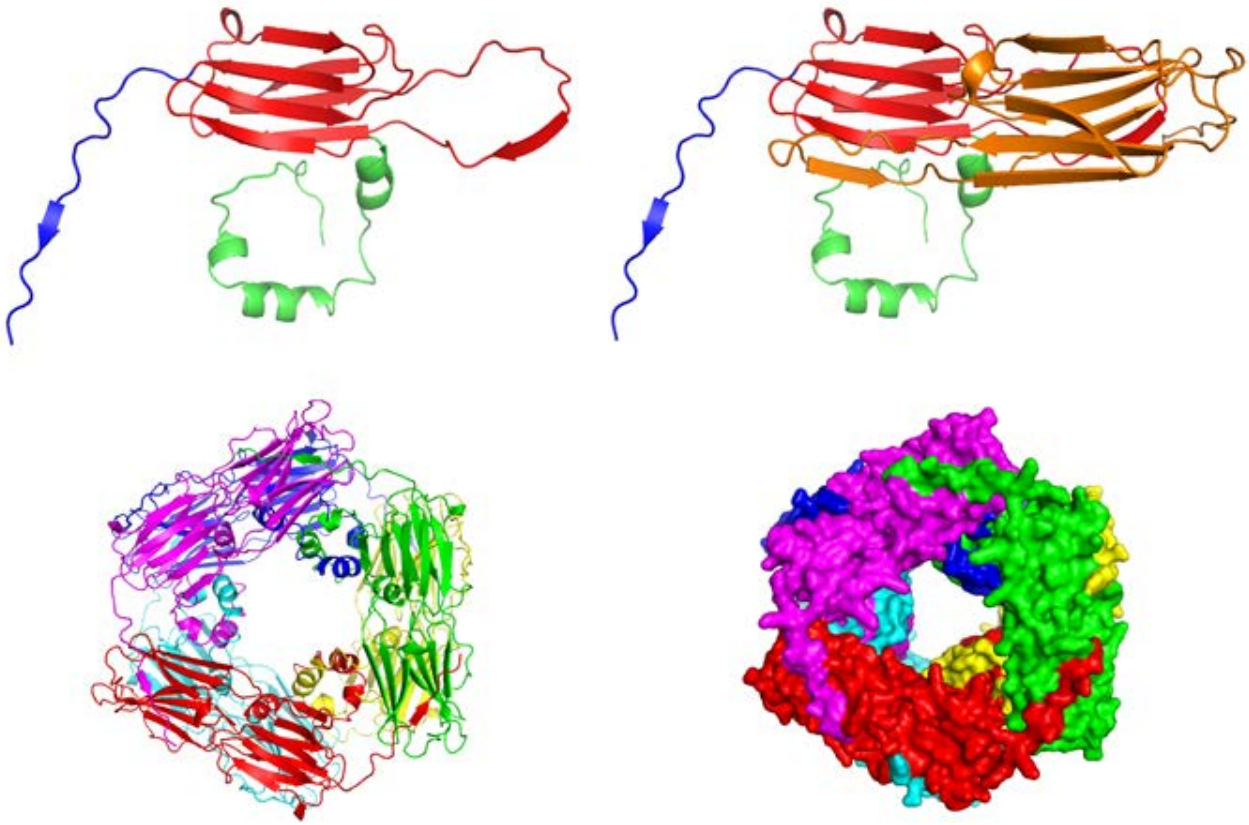

Figure 2. Schematic representation of monomers and oligomers formed by sHSPs. Upper left: Cartoon model of the monomer. Upper right: Cartoon model of the dimer which forms the substructure of the oligomer. Lower left: Cartoon model of the native dodecamer. Lower right: Surface model of the dodecamer (From: van Montfort et al. 2001).

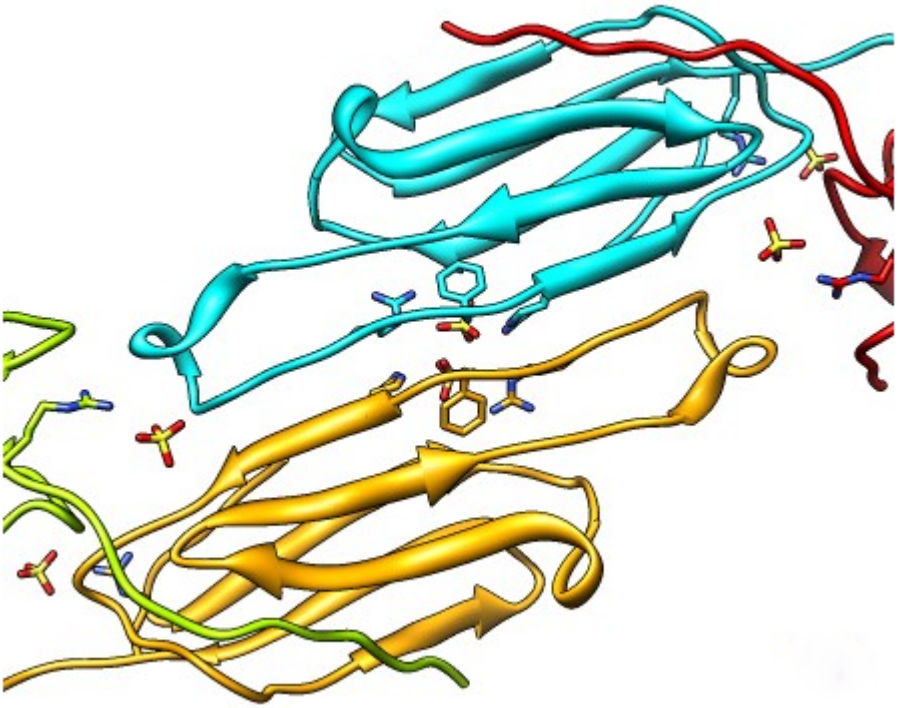

Figure 3. Schematic representation of side-by-side beta sheet dimer (From: https://www.cgl.ucsf.edu/chimera/data/acryst2011/acrystdemo.html).

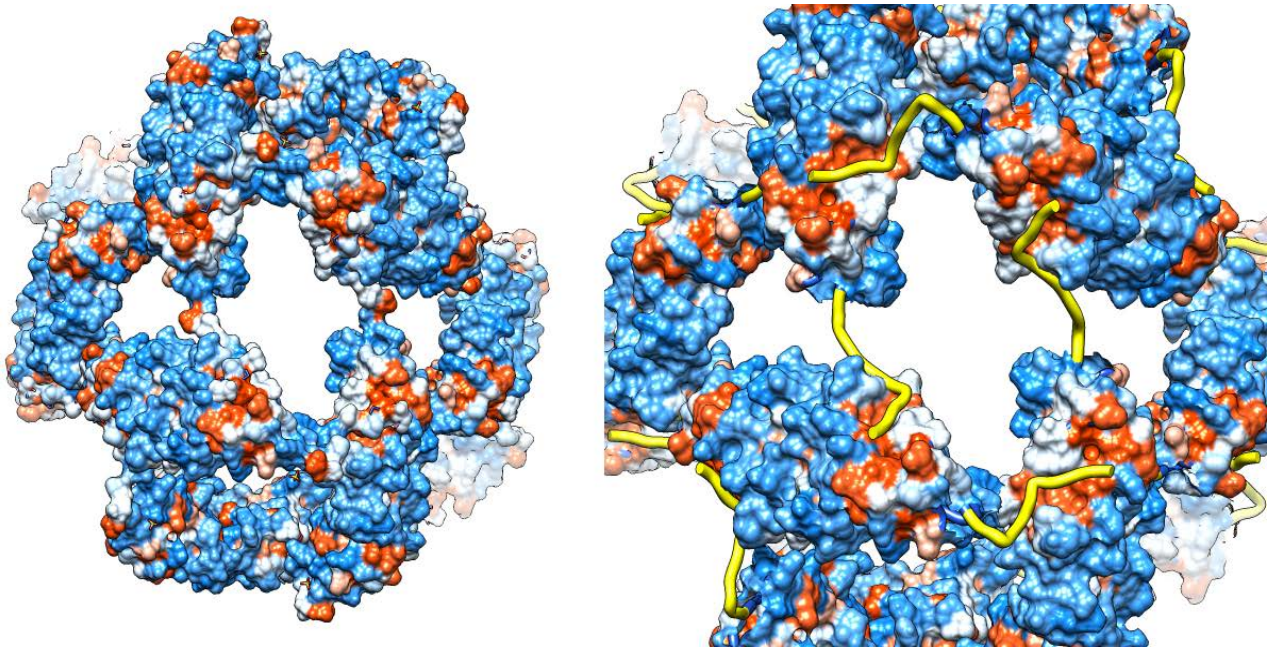

Figure 4. Mechanism of Chaperone Activity: A Hypothesis. Molecular surface with orange hydrophobic regions. C-terminal strands cover hydrophobic grooves. Literature says binding unfolded proteins requires oligomer to disassemble (From: https://www.cgl.ucsf.edu/chimera/data/acryst2011/acrystdemo.html).

The CTE makes inter-subunit contacts with the hydrophobic groove in the β-sandwich of the ACD (van Montfort et al. 2001a; Kim et al. 1998) and has a propensity to engage in alternate inter-subunit contacts (Pasta et al. 2004). The interactions established by conserved IXI/V motif are important in determining the oligomeric size and chaperone activity of sHSPs (de Jong et al 1998; Jehle et al 2010; Saji et al. 2008) (see Figures 1 and 4). Mutations in the IXI motif of plant and prokaryotic sHSPs or truncations spanning this region were shown to dissociate the oligomeric structure of the proteins and to result in loss of chaperone-like activity (Studer et al. 2002; Kirschner et al. 2000).

Some of the human HSPBs, such as HSPB6 and HSPB8, contain only a very short C-terminal tail and are lacking the IXI motif and the C-terminal fragment. Thus, the N- and C-termini, which are less conserved between sHSPs of all species and display different length are supposed to confer peculiar structural and functional properties to the various sHSPs.

As previously mentioned, the basic unit/building of sHSPs of all species is the dimer. sHSP dimers are composed by two monomers that are partially associated via their ACDs; dimers are capable of generating oligomers ranging from ca. 200 to 600 kDa (see Figures 2 and 3) (Lambert et al. 1999; Cobb and Petrash 2000). The various sHSP monomers can form both homo- and hetero-dimers as well as homo- and hetero-oligomeric complexes (van Montfort et al. 2001; Van Montfort et al. 2001a). The formation of large oligomers is to some extent dependent on the variable N- and C-terminal sequences; in particular the WDPF domain, located in the very N-terminal part, is important for the formation of large aggregates (Gusev et al. 2002). For mammalian HSPBs three different heterologous complexes were described in the literature (Sugiyama et al. 2000). These complexes simultaneously contained:

- HSPB5 and HSPB1
- HSPB1, HSPB5 and HSPB6
- HSPB1 and HSPB6

Thus, the various members of the HSPB family seem not to associate randomly; rather, preferences in the interactions between few members together exist (Sugiyama et al. 2000). However, once formed these mixed hetero-oligomers can rather easily exchange their components with each other (Bova et al. 2000). Association of sHSPs of all species into (large) hetero-oligomers likely contributes to confer different affinities for a given substrate and different functions (see later).

Concerning the expression profile, some members of the mammalian HSPB family are constitutively and ubiquitously expressed (e.g. HSPB1, HSPB5), while others are selectively expressed in a specific target tissue/organ (e.g. HSPB4, HSPB9, HSPB10; see Table 2). Moreover, the expression of sHPS of all origin can be induced in response to stress such as heat, oxidative stress or during tissue differentiation (e.g. mammalian HSPB2 and HSPB3 are induced during muscle differentiation, as we will discuss extensively in this thesis).

According to their expression profile, the mammalian HSPBs have been categorized as Class I or Class II (see Table 3) (Taylor and Benjamin 2005). The Class I of HSPBs is composed by HSPB1, HSPB5, HSPB6 and HSPB8 that are ubiquitously expressed and are predominantly heat-inducible suggesting that they exert functions both in resting cells (where they are constitutively expressed) and upon proteotoxic stress (when their expression is upregulated). The Class II of HSPBs includes HSPB2, HSPB3, HSPB7, HSPB4, HSPB9, and HSPB10, which are (generally) not stress-inducible and show tissue-restricted patterns of expression. In particular, Class IIm HSPBs are selectively expressed in striated muscle, while Class IIt HSPBs are only found in testis; this restricted expression profile points to specialized tissue-specific functions of these HSPBs (see Table 3).

Concerning the subcellular localization, the majority of mammalian HSPBs are mainly cytosolic, such as HSPB1, HSPB5 and HSPB8. In other species, sHSPs have been found to be associated with specific organelles and compartments. For example, plant sHSPs (which are up to 20 or more) are found in each organelle of plant cells, where they exert specific functions (Haslbeck and Vierling 2015). In *Drosophila melanogaster*, whose genome encodes for eleven sHSPs, some sHSPs are cytosolic, while Hsp22 is associated with the mitochondria and Hsp27 is exclusively expressed in the nucleus (Michaud et al. 2008). In contrast to Drosophila Hsp27, none of the mammalian HSPBs studied so far is expressed only inside the nucleus (Michaud et al. 2008). However, partial translocation into the nucleus of some HSPBs, such as e.g. HSPB1 and HSPB5, occurs upon stress (Marin-Vinader et al. 2006; den Engelsman et al. 2004).

Name	Subunit Mol. Mass (kDa)	pI	Tissue distribution	Stress-inducibility	Class	Functions
Hsp27 (HspB1)	22.8	6.4	Ubiquitous, high levels in heart, striated and smooth muscles	+	I	Chaperone activity, stabilization of cytoskeleton, anti-apoptotic and anti-oxidant function
HspB2 (MKBP)	20.2	4.8	Heart, skeletal and smooth muscle	-	II	Chaperones DMPK and enhances its kinase activity. Target protein-dependent chaperone activity, myofibrillar integrity, anti-apoptotic function, mitochondrial energetic, anti-apoptotic
HspB3	17.0	5.9	Heart, brain, skeletal and smooth muscle	-	II	Target protein-dependent chaperone activity, Maintaining myofibrillar integrity
αA-crystallin (HspB4)	19.9	6.2	Abundant in eye lens, skeletal muscle, liver, spleen, adipose tissue (low level)	-	II	Chaperone activity, genomic stability, eye lens refractive index
αB-crystallin (HspB5)	20.2	7.4	Ubiquitous, abundant in eye lens. High levels in heart and muscle	+	I	Chaperone activity, stabilization of cytoskeletal and nucleoskeletal matrix, cell cycle, cardioprotection, eye lens refractive index, regulation of muscle differentiation, anti-apoptotic function
Hsp20 (HspB6)	16.8	6.4	Ubiquitous, abundant in muscle	-	I	Smooth muscle relaxation, cardioprotection, chaperone activity, anti-apoptotic
HspB7(cardiovascular heat shock protein)	18.6	6.5	Heart and skeletal muscle. Adipose tissue (low level)	-	II	Chaperone activity, maintaining myofibrillar integrity,
Hsp22 (HspB8, E21G1, α-crystallin C)	21.6	4.7	Ubiquitous	+ (cell type dependent)	I	Chaperone activity, induction of autophagy
HspB9 (Hest shock protein beta-9, cancer/testis antigen 51 (CT51))	17.5	9.0	Testis	-	II	Role in cancer/testis antigen
HspB10 (Outer dense fibre of sperm tails, ODF27, ODFPG, RT7, ODFP, CT133)	28.3	8.4	Testis	-	II	Elastic cytoskeletal structure

Table 3. Nomenclature, distribution and functions of human sHSPBs (From: Bakthisaran et al. 2015).

The functions of sHSPs

Two main activities have been studied for sHSPs from various origins: the chaperone activity and the stabilization of the cytoskeleton.

Concerning the chaperone activity, it consists in the ability of specific proteins, called molecular chaperones to assist non-covalent folding/unfolding and the assembly or disassembly of other macromolecular substrates, thereby ensuring the maintenance of native protein conformation. The proteins transiently bound by the chaperones are referred to as substrates or clients. Chaperones transiently bind to hydrophobic residues exposed by the substrate during its folding or assembly process, but are excluded from the final stable conformation of their substrate/client (Hartl et al. 2011). Concerning the chaperone activity of sHSPs, it was initially attributed to the ACD for many, but not all, members of the sHSP families (Taylor et al. 2005). However, recent finding support that also the N- and C-termini are important for the chaperone function of sHSPs (Asthana et al. 2012). The chaperone activity of the ACD is temperature dependent; in fact a structural transition at 30-40°C leads to enhanced chaperone activity by increasing or favourably reorganizing the hydrophobic substrate-binding surfaces (Raman and Rao 1994; Datta and Rao 1999; Raman and Rao 1995;

Raman and Rao 1997; Smith et al. 1996; Das and Surewicz 1995). This chaperone activity has been initially studied using cell-free systems, where unfolded heat- or DTT-denatured substrates such as e.g. firefly luciferase or citrate synthase (CS) were co-incubated with a specific purified sHSP (Chowdary et al. 2004; Jakob et al. 1993). Co-incubation of the denatured substrate with the purified sHSP prevents irreversible substrate aggregation and, in some instances, allows the renaturation/refolding of the substrate, restoring its function. Of those human HSPB members tested in cell-free systems HSPB1, HSPB4, HSPB5 and HSPB8 were found to prevent irreversible aggregation of the denatured clients (Chowdary et al. 2004; Jakob et al. 1993). In cells, assisted refolding was first demonstrated for cells overexpressing HSPB1 (Bryantsev et al. 2007); later, also HSPB4 and HSPB5 overexpression was found to enhance the renaturation of heat-denatured firefly luciferase, whilst overexpression of the other members of the HSPB family did not (Vos et al. 2010). This already suggested that some human HSPB members may have different chaperone activity and functions.

The activity of sHSPs of various origins is governed by the dynamic association/dissociation of their oligomers and is also often regulated by their phosphorylation state (Landry et al. 1992; Lambert et al. 1999; Kato et al. 1998; Ito et al. 2001). Phosphorylation has been well-studied for few members of the HSPB family including HSPB1 and HSPB5, where it results in partial dissociation of the oligomers. Phosphorylation-driven dissociation of oligomers, in turn, modifies the chaperone activity and, consequently, the interaction of a specific phosphorylated HSPB with a target protein (Landry et al. 1992; Lambert et al. 1999; Kato et al. 1998; Ito et al. 2001).

As previously mentioned, in resting cells, sHSPs mainly exist in form of large homo- or hetero-oligomers, which are thought to represent the chaperone reservoir of the cells. Upon stress, these oligomers will dissociate (in some instance in a phosphorylation-dependent manner) to generate active dimers. Such a model is based on studies done on mammalian HSPB1 and HSPB5. In fact, HSPB1 exists in cells under resting conditions as large oligomers, consisting of 24 (or even more) monomers; upon stress, HSPB1 can be phosphorylated at three different sites; phosphorylation leads to its partial dissociation into tetramers. To achieve the complete dissociation of these tetramers into dimers, all three phosphorylatable sites of HSPB1 need to be simultaneously phosphorylated (Gusev et al. 2002). Also HSPB5 mainly exists, in resting mammalian cells, in form of large oligomers that (partly) dissociate upon phosphorylation; also for HSPB5 three different phosphorylation sites have been

documented (Ito et al. 2001). The use of mutant of HSPB1 or HSPB5 in which the phosphorylatable sites have been replaced to mimic the protein in its unphosphorylated or fully phosphorylated form has been extremely important to understand the role of phosphorylation on the oligomerization and chaperone function of these specific HSPBs (Lambert et al. 1999; Ito et al. 2001; Gusev et al. 2002; Chávez Zobel et al. 2005).

However, the activity of mammalian HSPBs is not only modulated by phosphorylation and oligomer dissociation. In fact, some HSPBs do not form oligomers, but rather exist in forms of dimers that can associate with other factors. For example, HSPB8 exists in mammalian cells in form of dimers that are stably and stoichiometrically complexed with BAG3, a co-chaperone of Hsc70/HSP70. This complex is composed of two molecules of HSPB8 (dimer) that bind tightly to one molecule of BAG3 (which is in turn bound to one molecule of Hsc70/HSP70) (Carra et al. 2008). The stability and activity of HSPB8 both depend on its association with BAG3 (Carra et al. 2008). Although HSPB8 has two phosphorylation sites (Gusev et al. 2002), these have not yet been characterized from the functional point of view and it is currently unknown whether they might modulate association to/dissociation from BAG3 of HSPB8.

Concerning the mode of action, dissociation of large oligomers, as it occurs in response to signal-induced phosphorylation of HSPB1, HSPB4 and HSPB5, favours the recognition of the substrate. (Shashidharamurthy et al. 2005; Mchaourab et al. 2002). Since sHSPs/HSPBs are ATP-independent chaperones, they are thought to mainly act as chaperone "holder" and therefore need to cooperate with other ATP-dependent chaperones and co-factors to exert their function. Thus, the substrate bound by the sHSPs/HSPBs would be maintained in a folding or degradation competent state by the sHSPs/HSPBs (based on *in vitro* assays). Interaction with Hsc70/HSP70 or with specific co-factors, such as e.g. DNAJ proteins or BAG3 (or other BAG proteins: BAG1-BAG6), would allow the transfer of the client hold by the sHSPs/HSPBs to the HSP70 machinery. This would use the ATP to process the client, which can be either refolded or degraded with the assistance of co-factors like DNAJ or BAG3 (or other BAG proteins; see Figure 5) (Mogk et al. 2003; Mogk et al. 2003a; Haslbeck et al. 2005; Cashikar et al. 2005; Kampinga et al. 1995). However, at least for yeast Hsp42, it has been demonstrated that it can be fully active as chaperone in an energy independent manner, demonstrating that the influence of ATP on the chaperone activity of sHSPs is still a remaining controversy (Haslbeck 2006).

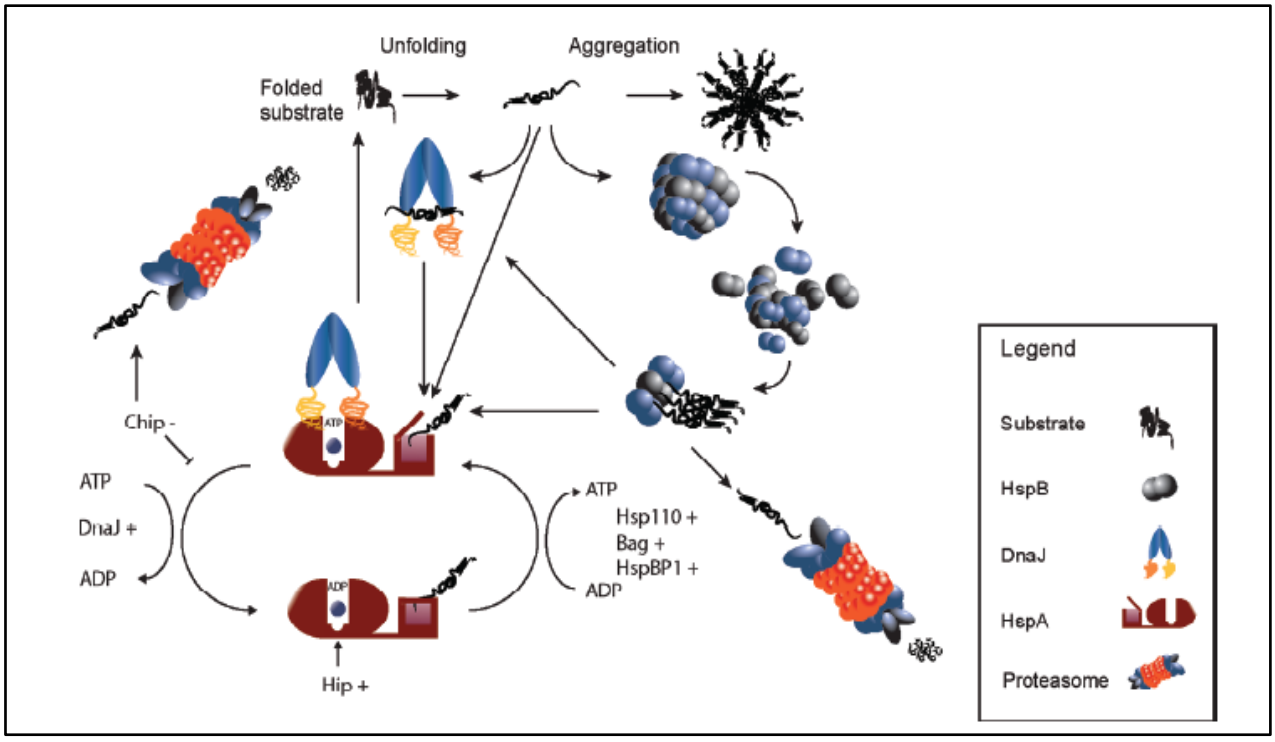

Figure 5. Schematic representation of protein processing clients by HSPB (From: Vos et al. 2008).

The second well-studied function of the mammalian HSPBs is their ability to interact with and/or modulate the structure and dynamics of the cytoskeleton. When exposed to stress, cells respond by drastically modifying their cytoskeletal network and by rapidly inducing the expression of selective HSPBs. Upon stress, microtubules undergo disassembly, intermediate filaments collapse toward the perinuclear region, and actin microfilaments are disorganized (Arrigo et al. 2007). Several HSPs were reported to interact with the different cytoskeletal components; for example, large HSPs, such as HSP90 and HSP70, bind mostly to the microtubule network and centrosome, while sHSPs/HSPBs seem to play an important role in maintaining the integrity of actin and of the intermediate filaments. For example, HSPB1, HSPB6 and HSPB5 have been shown to directly interact with intermediate filaments and actin microfilaments and to influence their stability and assembly/disassembly, especially upon proteotoxic stress (Lavoie et al. 1993; Lavoie et al. 1995; Liang and MacRae 1997; Iwaki et al. 1994; Nicholl and Quinlan 1994; Perng et al. 1999; Dreiza et al. 2005).

HSPB1 stabilizes microfilaments and prevents their depolymerisation induced by cytochalasin D and their aggregation induced by heat (Wang and Spector 1996); such function depends on the phosphorylation state of HSPB1, which, as previously mentioned, affects HSPB1 oligomerization. HSPB1 caps the plus end of the actin filament (F-actin), thereby inhibiting filament polymerization; this capping activity exerted by HSPB1 on F-actin protects

the plus end and favours the depolymerization of the minus end, allowing growth of the uncapped filaments (Lavoie et al. 1993, 1993a, 1995; Huot et al. 1996; Piotrowicz and Levin 1997; Piotrowicz et al. 1998). Also HSPB5 affects actin polymerization *in vitro* but to a lower extent as compared to HSPB1 (Mounier and Arrigo 2002). Recently, a role in cytoskeleton stabilization has been suggested also for HSPB9 (de Wit et al. 2004) and HSPB10 (Fontaine et al. 2003), which are specifically expressed in testis. For example, HSPB9 interacts with TCTEL1, a light chain component of cytoplasmic and flagellar dynein (de Wit et al., 2004).

Besides their chaperone function and their ability to stabilize the cytoskeleton upon stress (which has however been demonstrated so far for few members of the HSPB family), HSPBs are involved in other cellular processes such as cell growth, differentiation, apoptosis, tumorigenesis, and signal transduction. Among these functions, HSPB1 has been shown to protect against apoptosis induced by several agents, including e.g. actinomycin D, doxorubicin, cisplatin, the kinase C inhibitor staurosporine or the topoisomerase II inhibitor etoposide. Such protective effect occurs at different levels, both upstream and downstream of the mitochondria. For example, HSPB1 interferes with the activation of pro-caspase-9 and pro-caspase-3 and interacts/co-purifies with the apoptosome complex (Pandey et al. 2000; Garrido et al. 1999; Bruey et al. 2000). HSPB1 interacts directly with the mitochondria, thus inhibiting the release of the pro-apoptotic factors cytochrome c and Smac/Diablo (Chauhan et al. 2003). In the cytosol, HSPB1 can sequester cytochrome c, thus preventing the formation and/or function of the apoptosome (Bruey et al. 2000). In addition, HSPB1 interacts with the pro-apoptotic protein DAXX, which mediates Fas-induced apoptosis; this in turn prevents the interaction of DAXX with both Fas and the apoptotic signaling kinase 1 (Ask1), inhibiting the apoptotic cascade (Charette et al. 2000). Like for the protection of the cytoskeleton under stressful conditions, also the anti-apoptotic functions of HSPB1 seem to be modulated by its phosphorylation and its oligomeric status. For example, while the inhibitory effect at the level of pro-caspase-9 and pro-caspase-3 would be exerted by the large non phosphorylated oligomers of HSPB1, mainly small oligomers would bind to cytochrome c (Arrigo et al. 2007).

Recently, it has been demonstrated that HSPB1, also, protects to apoptosis induced by etoposide or Tumor Necrosis Factor α (TNF-α) in different cancer cell lines leading to an increase in the activity of the survival transcription factor nuclear factor kappa-light-chain-enhancer of activate B cells (NF-κB). NF-κB is involved in the expression of several anti-apoptotic proteins, such as Bcl-2, Bcl-xL and c-IAPs. HSPB1 acts on NF-κB through an increment of the ubiquitination and proteasomal degradation of the NF-κB inhibitor (I-κB),

which results in an increase in NF-κB activity and increased survival (Parcellier et al. 2003). Due to its anti-apoptotic activity, HSPB1 may exert tumorigenic activity (Garrido et al. 1998). In fact, many tumor cell lines constitutively express high levels of HSPB1, which may allow these cells to escape the immune system, favouring tumor growth and propagation (van Heijst et al. 2006). On the other hand, negative regulation or knock-down of HSPB1 may exert anti-tumorigenic effects. Indeed, HSPB1 auto-immune antibodies were found to improve the survival in patients with e.g. breast cancer (Conroy et al. 1998).

HSPB5, also, confers protection against a broad range of apoptosis-inducing agents, including TRAIL, TNF-α, chemotherapy and growth factor deprivation (Kamradt et al. 2002; 2005). These findings suggest that specific HSPBs may work in concert to inhibit apoptosis by acting on at different levels. While protective against apoptosis under specific conditions, deregulated expression of some sHPSs/HSPBs may contribute to confer resistance to tumor cells, thus favouring cancer propagation.

In addition, some HSPBs may participate in the development of several tissues, including e.g. epidermis (HSPB1) (Jantschitsch et al. 1998) or in the differentiation of e.g. skeletal myoblasts (HSPB2-HSPB3) (Maeda et al. 1995; Whiting et al. 1995 Lam et al. 1996; see later).

Mutations of HSPBs cause chaperonopathies

Mutations in several HSPBs have been identified as cause of several neurological, neuromuscular and muscular diseases. These mutations are located in the NTD, ACD, or CTE, further supporting that all the three domains of HSPBs are important for their structure and function. The diseases associated with mutations of HSPBs are referred to as "chaperonopathies" and include: cataract (HSPB4 and HSPB5), distal hereditary motor neuropathy (HSPB1, HSPB3 and HSPB8), distal myopathy with neuropathy (HSPB8), desmin-related myopathy and cardiomyopathy (HSPB5; see Table 4). We briefly list the mutations associated to disease and their location (for a detailed description see Boncoraglio et al. 2012 and Ghaoui et al. 2015). Some mutations affect highly conserved equivalent residues, called "hot spots". Such a "hot spot" residue is Arg140 (R140) of HSPB1 that corresponds to Arg120 (R120) in HSPB5, Arg116 (R116) in HSPB4 and Lys141 (K141) in HSPB8. These mutations affect either oligomerization, binding to partners and clients, and stability; in fact, often these mutant HSPBs tend to aggregate in the target tissue (Datskevich et al. 2012).

The residue R140 of HSPB1 is involved in the stabilization of the ACD of an isolated monomer (Ikeda et al. 2009) or in the stabilization of inter-subunit contacts between two monomers inside a dimer. The R120G mutation of HSPB5 is associated to desmin-related myopathy (DRM) (OMIM 601419; Vicart et al. 1998). It leads to significant changes of HSPB5 secondary, tertiary, and quaternary structure, and it decreases both the thermal stability and chaperone activity of HSPB5 (Kumar et al. 1999; Perng et al. 1999a; Bova et al. 1999; Chávez Zobel et al. 2003). This R120G mutant possesses higher affinity for the intermediate filaments formed by desmin and promotes their aggregation (Perng et al. 1999a). In R120G-induced myopathy the desmin aggregates colocalize with HSPB5. Desmin is important to maintain the overall structure, and the cytoskeletal organization of striated muscle cells and its mutation cause desmin-related myopathy (Vicart et al. 1996).

Concerning HSPB8, two mutations K141N and K141E have been associated with inherited distal myopathy (Irobi et al. 2004; Tang et al. 2005); both K141N and K141E decrease the interaction of HSPB8 with BAG3, which is essential for both HSPB8 stability and function (Carra et al. 2008; Carra et al. 2010; Shemetov and Gusev 2011).

Besides the mutations described in the "hot spot" conserved amino acid, other mutations located both in the N- and C-terminus have been identified and (often) lead to the same disease. Recently a new mutation of HSPB8 (c.151insC, p.P173SfsX43) has been associated with distal myopathy and motor neuropathy (Ghaoui et al. 2016), further supporting the importance of HSPB8 is the maintenance of both motor neuron and muscle cell function and viability. Amongst the mutations located in the N-terminus, we mention the following point mutations G34R, P39L, E41K, and G84R of HSPB1, all correlated with CMT2 (Houlden et al. 2008; James et al. 2008; Capponi et al. 2011). Other mutations found in the NCD of HSPB5 and responsible for autosomal dominant congenital nuclear cataract are the mutation, R11H, P20S, Ser21Alafsx24, R56W, and R69C, in the N-terminus. These mutations lead to the changes in secondary and tertiary structure, as well as, changes in hydropath and electrostatic potential, causing a change in thermo-dynamic stability of the protein and/or to the change in the binding of protein targets and protein partners (Chen et al. 2009).

Amongst the mutations located in the C-terminus of the various HSPBs are: the point mutations P182L, P182S and R188W of HSPB1 that all result in Charcot-Marie-Tooth type 2 (CMT2) disease (Houlden et al. 2008; Evgrafov et al. 2004); the mutations Q151X, G154S, R157H, A171T, 450delA and 464delCT of HSPB5 associated with myofibrillar myopathy,

cardiomyopathy (Pilotto et al. 2006; Inagaki et al. 2006), or lamellar cataract (Devi et al. 2008) (see Table 4).

In addition to point mutations, even deletions of amino acid residues in the CTE of HSPB1 are associated with CMT2, examples are: 476_477delCT or pSer158fsX200 and c.523T>C. Due to the absence of the conservative IXI motif and to the altered C-terminal sequence, these deletion mutants give rise to proteins with unusual quaternary structure, which interact differently with target proteins compared to wildtype (Datskevich et al. 2012).

Although not all mutations found so far have been characterized and it is not yet completely understood how they cause disease, generally the mutated HSPB proteins have lower chaperone activity than their wild type counterparts; this can lead to accumulation of denatured and aggregated proteins inside the cell, including aggregates containing the mutated HSPBs themselves. Nearly all the mutations identified so far lead to HSPB protein aggregation (Boncoraglio et al. 2012). Thus, the mutated HSPBs may exert a negative effect due to a gain-of-toxic function (GOF), which corresponds to an intrinsic acquired toxicity; or the mutation somehow lead to a loss-of-function (LOF) of the mutant protein, which cannot interact with and protect its natural clients. As a consequence, the clients of these mutant HSPBs aggregate, entrapping the mutant HSPBs alone or together with the wild-type HSPBs. This would lead to a loss of function of both the client and the HSPB itself. Alteration of the homo- or hetero-oligomerization of the mutated HSPB forms with their wildtype counterpart also occurs, thereby affecting also the activity of the wildtype HSPB (most of these diseases are autosomal dominant, thus both the wildtype and mutated proteins co-exist in the patient cells). While often GOF and LOF mechanisms can contribute to disease, in some cases a pure LOF mechanism can be at the basis of disease onset and pathogenesis. LOF occurs for mutations that cause the formation of a truncated HSPB protein that is either not expressed or not functional (see later: truncated HSPB3 mutant).

Protein	Mutation	Location	Disease and type of inheritance
HspB1	G34R	N-terminal domain	DHMN
	P39L	–"–	DHMN/CMT2 (AD)
	E41K	–"–	DHMN (AD)
	G84R	–"–	DHMN/CMT2 (AD)
	L99M	Crystallin domain	DHMN/CMT2 (AR)
	R127W	–"–	DHMN (AD)
	S135F/S135M	–"–	DHMN/CMT2 (AD)
	R136W/R136L	–"–	CMT2 (AD)
	R140G	–"–	DHMN/CMT2 (AD)
	K141Q	–"–	DHMN (AD)
	T151I	–"–	DHMN (AD)
	S156Y	–"–	Nonpathogenic
	T164A	–"–	CMT2 (AD)
	T180I	C-terminal domain	DHMN/CMT2 (AD)
	P182L/P182S	–"–	DHMN (AD)
	R188W	–"–	CMT2
	476_477delCT	–"–	PN (AD)
	pGln175X	–"–	CMT2
HspB3	R7S	N-terminal domain	MN
HspB4	W9X	–"–	Cataract (AR)
	R12C	–"–	Cataract (AD)
	R21L/R21W	–"–	Cataract (AD)
	R49C	–"–	Cataract (AD)
	R54C	–"–	Cataract (AD, AR)
	F71L	Crystallin domain	Age-related cataract
	G98R	–"–	Cataract (AD)
	R116C/R116H	–"–	Cataract (AD)
	c.350_352delGST or R117/H, Y118del	–"–	Cataract
HspB5	R11H	N-terminal domain	Cataract (AD)
	P20S	–"–	Cataract (AD)
	Ser21Alafsx24	–"–	MFM (AR)
	R56W	–"–	Cataract (AR)
	R69C	Crystallin domain	Cataract (AD)
	D109H	–"–	Cataract, MFM (AD)
	c.343delT or Ser115Profsx14	–"–	MFM (AR)
	R120G	–"–	DRM, cataract (AD)
	D140N	–"–	Cataract (AD)
	Q151X	C-terminal domain	MFM (AD)
	G154S	–"–	DM
	R157H	–"–	DCM (AD)
	A171T	–"–	Cataract (AD)
	450delA or K150fs_184X	–"–	Cataract (AD)
	464delCT or L155fs_163X	–"–	MFM (AD)
HspB6	P20L	N-terminal domain	Decrease in cardioprotective activity
HspB8	K141N/K141E	Crystallin domain	DHMN/DHMN and CMT2 (AD)

DHMN, distal hereditary motor neuropathy; DRM, desmin related myopathy; DCM, dilated cardiomyopathy; DM, distal myopathy; MFM, myofibrillar myopathy; MN, motor neuropathy; PN, peripheral neuropathy; CMT2, Charcot–Marie–Tooth disease of the second type. Type of inheritance: AD, autosomal dominant; AR, autosomal recessive.

Table 4. Mutations of human HSPBs and congenital disease associated (From: Datskevich et al 2012).

MKBP/HSPB2 and HSPL27/HSPB3

HSPB2, named with old classification MKBP (myotonic dystrophy protein kinase binding protein), contains 182 amino acid residues and has an estimated molecular mass of 20,295 kD. HSPB2 represents the most diverged member of the HSPB family, showing more than 30% overall sequence identity to each known human HSPBs (Caspers and Bhat 1995). The greatest similarity (42% or greater identity) occurs in the ACD that is important for all HSPB chaperone activity (Jakob et al. 1993; Rao et al. 1994).

HSPB3 is the smallest member of the HSPB family, encoded by a single exon and it contains 150 amino acids. HSPB3 has a monomeric mass of 17 kDa (Boelens et al. 1998). Concerning the primary structure, HSPB3 is the most deviating protein among the human HSPBs. From the structural point of view, HSPB3 lacks a long CTE, which is generally involved in the stabilization of oligomers. Thus, the five residues at the C-terminus of HSPB3 seem to be too short to form a bridge between adjacent ACD dimers. HSPB2 forms a stable complex with HSPB3 with a size of ca. 150 kDa (den Engelsman et al. 2009) and a stoichiometry of 3:1 HSPB2/HSPB3 (den Engelsman et al. 2009). The characterization of the complex was carried out by nano-electrospray-ionization mass spectrometry (nano-ESI MS) under conditions that preserve non-covalent interactions (Sobott et al. 2005). The absence of a long C-terminus in HSPB3 might be an important factor for the unique nature of this HSPB2/HSPB3 complex (den Engelsman et al. 2009). Overall, both HSPB2 and HSPB3 are amongst the less-studied members of the HSPB family.

HSPB2

HSPB2 interacts via its ACD with the myotonic dystrophy protein kinase (DMPK), the protein product of the gene responsible for myotonic dystrophy type 1 (DM1) (Sugiyama et al. 2000). HSBP2 binds specifically to the kinase domain of DMPK and this interaction is exclusive, since the other members of the HSPB family, abundant in skeletal muscle, such as HSPB5 and HSPB1, do not interact with DMPK (Sugiyama et al. 2000). The association of HSPB2 with DMPK has been shown to activate DMPK kinase activity and to protect the kinase from heat-induced inactivation (Suzuki et al. 1998).

Concerning the expression profile, HSPB2 is localized not only at the neuromuscular junction, where DMPK is concentrated (Maeda et al. 1995; Whiting et al. 1995), but also at the Z-band of myofibrils, where HSPB2 may contribute to the maintenance of myofibril integrity.

HSPB2 is also expressed at high level in the heart (Sugiyama et al. 2000). The majority of the studies concerning HSPB2 was focused so far on its role at the cardiac level. The first studies on HSPB2 have been conducted in double knock-out (DKO) mice lacking both HSPB5 and HSPB2 (Brady et al. 2001). The DKO is due to the fact that the genes encoding for HSPB2 and HSPB5 are adjacent and therefore it was not feasible to only knockout one single gene at the time when these transgenic mice were generated (Iwaki et al. 1997). The DKO mice do not present cardiac problems during the heart development, and surprisingly their hearts were histologically normal, even at older ages, suggesting that HSPB5 and HSPB2 are not essential for development and viability of cardiac cells. However DKO adult mice showed severe muscle cell degeneration. Since both HSPB5 and HSPB2 are expressed in skeletal muscle, it was not possible to ascribe the degenerative muscle phenotype specifically to HSPB2 (Brady et al. 2001). As previously described, HSPB2 exerts regulatory effects on DMPK, which plays an important role in maintaining muscle structure and function; thus, the absence of HSPB2 may be partly responsible for the effects observed in the DKO mice (Brady et al. 2001). In line, a similar late-onset progressive skeletal myopathy was observed in DMPK knockout mice (Jansen et al. 1996). Moreover, patients affected by myotonic dystrophy show an up-regulation of HSPB2, but not of the other HSPBs (HSPB5 and HSPB1), also expressed in the skeletal muscle; this up-regulation is thought to compensate for the reduced amount of DMPK (Brady et al. 2001).

In addition, due to its localization to the Z lines in skeletal muscle, HSPB2 may also play a more direct role in stabilizing the sarcomeric structure, although direct experimental evidence for such function are still lacking.

Concerning the functions of HSPB2 in cardiomyocytes, it has been demonstrated that HSPB2 is dispensable for cardiac function under normal/physiologic condition; instead, confounding results from independent groups were reported for cardiac responses to different stressful conditions (e.g. ischemia/reperfusion or pressure overload) (Golenhofen et al. 2006; Kadono et al. 2006; Morrison et al. 2004). In order to determine the specific requirements of HSPB2 in heart, Ishiwata et al. generated cardiac-specific HSPB2 deficient (HSPB2cKO) mice and examined the cardiac function under basal conditions and following cardiac pressure overload induced by transaortic constriction (TAC). Under normal conditions, HSPB2cKO did not exhibit any obvious cardiac anomaly; this is in agreement with the observations made in the DKO lacking both HSPB2 and HSPB5 mentioned before and demonstrates that HSPB2 is dispensable for cardiac function (Ishiwata et al. 2012). Although

these HSPB2cKO mice did not present alteration of the cardiac hypertrophic response to pressure overload in response to either mild or severe stress, they were characterized by a significant decrease of the respiration rate, of ATP production, as well as by alterations of the levels of transcripts of several metabolic and mitochondrial regulatory genes (Ishiwata et al. 2012). Such effect of HSPB2 on the mitochondrial function is consistent with previous findings from Nagawaga et al. who demonstrated that HSPB2 is associated with the outer membrane components of the mitochondria, where it contributes to the stress response (Nagawaga et al. 2001).

In parallel, to study the potential protective effects of high expression levels of HSPB2 upon myocardial ischemia reperfusion injury (I/R), Grose et al. generated a mouse model overexpressing HSPB2 specifically in cardiac cells (HSPB2cTg) (Grose et al 2015). These HSPB2cTg mice were characterized neither by early lethality nor age-related cardiomyopathy; instead, overexpression of HSPB2 protected cardiomyocytes from I/R, decreased infarct size after I/R and enhanced mitochondrial recovery with improved ATP levels at reperfusion. Combined with the finding that mice lacking HSPB2 cannot efficiently recover ATP levels following I/R stress, these results demonstrates that HSPB2 protects mitochondrial function during I/R (Grose et al 2015). Collectively these studies support that HSPB2 might participate in the following processes: 1) maintenance of (skeletal and cardiac) muscle structure; 2) cardioprotection under stress (ischemia) and 3) maintenance of ATP levels associate with consequent maintenance of mitochondrial function after stress.

It is currently unknown whether the functions ascribed to HSPB2 depend on HSPB2 itself or are influenced by the presence of endogenous HSPB3. In fact, the HSPB2-HSPB3 complex has been found both in skeletal and cardiac muscle cells (although the apparent molecular mass of the complex found in skeletal muscle is slightly different from the one found in cardiomyocytes (Suzuki et al. 1998).

HSPB3

In vitro studies aimed at characterizing the chaperone activity of HSPB3 have demonstrated that HSPB3 alone exhibits molecular chaperone-like activity in preventing the heat-induced aggregation of alcohol dehydrogenase (ADH). It exhibits moderate chaperone-like activity towards heat-induced aggregation of citrate synthase. However, it does not prevent the DTT-induced aggregation of insulin (Asthana et al. 2012). Thus, globally, HSPB3 seems to have a poor chaperone activity, restricted to specific target substrates.

Regarding the expression profile of HSPB3, it was well characterized in the mouse, where hspb3 messenger RNA (mRNA) is expressed in the gray matter of the spinal cord, including large cells in the ventral horn that are morphologically motor neurons (Allen Spinal Cord Atlas) (Lein et al. 2007). The expression of human HSPB3 mRNA is less well characterized than the mouse one; nevertheless, mRNA may be enriched in pituitary gland and nerve (Vos et al. 2009). HSPB3 mRNA is also found in adult smooth muscle and heart (Lam et al. 1996) and in several other fetal tissues, suggesting that it has not only a function in different types of muscle tissues, but it might be also involved in fetal development. Like HSPB2, the expression levels of HSPB3 are not upregulated upon heat-shock (Sugiyama et al. 2000). As previously mentioned, a mutation of HSPB3 has been documented: R7S. It is a missense mutation located in the N-terminal domain of HSPB3 that leads to a loss of a conserved arginine. The R7S mutation of HSPB3 was discovered in two siblings with an asymmetric axonal motor neuropathy (dHMN 2C) (Kolb et al. 2010). Electrophysiological studies revealed an axonal, predominantly motor, length-dependent neuropathy (Kolb et al. 2010). The association of HSPB3 with motor neuropathy points to a potential function of this protein in the maintenance of the viability of motor neurons, although no experimental findings are yet available concerning how the R7S mutation affects HSPB3 function and what is the exact function of HSPB3 on motor neurons. Recently, both HSPB2 and HSPB3 were found to be upregulated in a knock-in mouse model of spinal and bulbar muscular dystrophy, which further supports a role of these proteins in the maintenance of the neuromuscular system (Rusmini et al. 2015).

The relevance of HSPBs at the skeletal muscle level

Considering that muscles are frequently subjected to severe conditions caused by heat, oxidative and mechanical stresses, especially during exercise, the presence of HSPs is especially important in this particular tissue (Brooks et al. 1971). In fact, several HSPs, including HSP60, HSP70, and HSP90, have been shown to be induced after exhaustive exercise (Locke et al. 1990). In addition, the inducible isoform of HSP70 (HSPA1A) has been shown to be constitutively expressed in a certain type of skeletal muscle fibers (Locke et al. 1991), suggesting that muscle cells are chronically ready to respond to stress.

In the context of skeletal muscles, HSPB1 and HSPB5 are localized on specific sarcomeric structures of the skeletal or cardiac muscle myofibril, such as Z-bands or I-bands

(Bennardini et al. 1992; Lutsch et al. 1997; van de Klundert et al. 1998; Suzuki et al. 1998; Atomi et al. 1991). Here, HSPB1 and HSPB5 exert cytoprotective roles by stabilizing cytoskeletal structures such as actin stress fibers and intermediate filaments (Iwaki et al. 1994; Lavoie et al. 1995). The expression profile of several HSPBs changes during muscle differentiation (see next paragraph). In particular, during the initial phase of skeletal muscle differentiation the levels of HSPB1 remain unchanged, while HSPB5 is up-regulated, and HSPB6 levels gradually decrease. During the late phases of skeletal muscle differentiation, the expression of HSPB2 and HSPB3 is induced. The increase in HSPB5, HSPB2 and HSPB3 mRNA is the result of myogenic differentiation controlled by the myogenic regulatory factor MyoD, and is not due to stress stimulation. Combined with the finding that knockout of HSPB2 and HSPB5 do not affect skeletal muscle differentiation, but rather affect muscle fiber integrity and maintenance, the expression profile data suggest that specific HSPBs are required to assist proper muscle organization and viability, in a yet unidentified manner.

Skeletal muscle differentiation

The process by which the skeletal muscles originate is a highly coordinated and defined process called skeletal muscle differentiation. In adults, the vast majority of new skeletal muscle cells come from myogenic precursor cells called satellite cells, which require Pax3/Pax7 for their specification and self-renewal (Oustanina et al. 2004; Relaix et al. 2005). These adult stem cells are able to proliferate and produce myoblasts, which in turn are capable of withdrawing from the cell cycle, in response to extracellular cues, and then differentiate into postmitotic myocytes (early differentiation). The postmitotic myocytes, subsequently, fuse into multinucleated myotubes (late differentiation), which finally bundle to form mature muscle fibers (terminal differentiation) (Chargé and Rudnicki 2004). A number of transcription factors and structural proteins have been implicated in the transition from postmitotic myocytes into mature muscle fibers (Parker et al. 2003; Paulin and Li 2004). Primary myogenesis initiates in satellite cells via the spatial and temporal expression of myogenic regulatory factors (MRFs), that include MyoD and Myf5, which are already being expressed in proliferating myoblasts prior to the onset of muscle differentiation (Bergstrom et al. 2002; Biamonti et al. 1992; Bonne et al. 2000). The activity of these transcription factors is regulated by their association with histone deacetylase (HDAC), histone acetyltransferases, and the SWI/SNF chromatin remodeling complexes (McKinsey et al. 2001; Puri et al. 2001). MRFs are required for initial specification of skeletal myoblasts and operate in concert with myogenin, MRF4 and other transcriptional regulators, such as myocyte-specific enhancer factors (MEF2a and MEF2c), in a coordinated manner to regulate the transcription of muscle-specific genes, including those for myosin heavy chain (MyHC) and muscle creatine kinase (MCK) (Braun and Gautel 2011; Molkentin et al. 1995; Olson and Klein 1994); all together these factors orchestrate the terminal differentiation of satellite cells.

The differentiation of skeletal muscle *in vitro* is a well characterized developmental model. Indeed studies of the differentiation process performed on cultured myoblasts have revealed that muscle-differentiation-specific gene expression occurs in a stereotypic pattern. Within 24 hours of serum removal, proliferating myoblasts initiate the expression of myogenin. Subsequently, these cells express the cyclin-dependent kinase (Cdk) inhibitor p21 and permanently exit the cell cycle. The Cdk inhibitor p21 prevents the phosphorylation of the cell-cycle regulator retinoblastoma protein (pRb), which becomes competent to bind to and repress the activity of the E2F transcription factor (Dyson 1998; Macleod 1999). As a consequence, the synthesis of proteins required for entry into S phase and for apoptosis is

inhibited and there is an arrest in the G0 phase of the cell cycle (Nahle et al. 2002). Thus, cells entry into a postmitotic state, that is a prerequisite for differentiation.

Once the cells have become post-mitotic, approximately 36–48 hours after the onset of differentiation, the expression of myofibrillar proteins such as myosin heavy chain (MHC) and enzymatic genes such as muscle creatine kinase (MCK) begins; this is followed by the fusion of the cells into multinucleated myotubes (Novitch et al. 1999). In addition several structural and cell surface proteins play important roles in terminal differentiation. These include desmin, a muscle-specific intermediate filament protein that is one of the first proteins expressed upon satellite cell activation (Lazarides and Hubbard 1976), and M-cadherin, a cell surface adhesion protein that is a marker for satellite cells *in vivo*. Perturbation of M-cadherin expression *in vitro* delays the onset of differentiation (Zeschnigk et al. 1995; Kaufmann et al. 1999), while the exact function of desmin in myogenesis remains unclear (Li et al. 1994; Weitzer et al. 1995; Smythe et al. 2001).

The late differentiation results in myotube formation. Myotubes are formed through a two-step mechanism: primary myotubes are formed by fusion of lined-up myoblasts, whereas other committed cells are fused laterally to primary myotubes to form secondary myotubes. During this process, nuclei become regularly spaced and myonuclear domains are well defined in the cytoplasm. The mechanism regulating nuclear positioning in myotubes involves critical transcription factors, such as NFATc and FHL1 (Cowling et al. 2008), cytoskeleton constituents, including desmin and tubulins, and an increasing number of nuclear envelope proteins, such as nesprins, SUN1, and SUN2.3 (Worman and Gundersen 2006).

Although a complete understanding of the mechanisms governing skeletal muscle fusion is lacking, it is clear that dramatic reorganization of the cytoskeleton, as well as nuclear positioning, occurs during this dynamic process (Peckham 2008).

Importance of lamins in muscle differentiation and viability

Lamins (which includes A and B types) are nuclear type V intermediate filaments that form a complex meshwork, thin 10–20 nm, underneath the nuclear membrane (Dechat et al. 2010), regulating nuclear shape and mechanical stability. Mutations of A-type lamins and integral proteins of the nuclear envelope (NE), such as emerin and nesprin1/2, cause e.g. Emery-Dreifuss muscular dystrophy (EDMD), Limb-girdle muscular dystrophy, Dilated Cardiomyopathy and Charcot-Marie-Tooth disease type 2B1, globally referred to as

"laminopathies" (Capell and Collins 2006; De Sandre-Giovannoli et al. 2002; Bione et al. 1994; Maraldi et al. 2005). These findings support that alterations of nuclear function and stability is detrimental for the viability of many cell types, but especially for peripheral neurons and muscle cells (Capell and Collins 2006; De Sandre-Giovannoli et al. 2002; Bione et al. 1994).

In addition to their structural role, lamins A and C also take part in other nuclear functions, including gene transcription regulation. A-type lamins are associated with several transcription factors by direct and indirect interactions; these interactions can be mediated by several lamin-binding proteins including emerin, LAP2β and pRb (important components during myogenesis) and components of the RNA polymerase II (pol II) transcriptional complex (Kumaran et al. 2002; Shaklai et al. 2007; Spann et al. 2002). Mutation of lamins affects also their role in transcriptional regulation. In fact, patients with LMNA-associated muscular dystrophy showed dysregulation of specific miRNA, which have proven to be implicated in modulating myoblast differentiation, these results suggest the pathologic implication of altered pol II-mediated transcription in laminopathies (Sylvius et al. 2011). At the nucleoplasm level lamins also participate to modulate DNA replication and chromatin organization (Gerace and Burke 1988; Gant and Wilson 1997), thereby indirectly regulating cell proliferation/differentiation (Dechat et al. 2010). The effects of mutant lamin and e.g. emerin on muscle cell differentiation have been well-investigated in cell and mice models. For example, recent studies reported that overexpression of different EDMD mutations, such as R453W, W520S and H222P, inhibits the *in vitro* differentiation of C2C12 myoblasts (Favreau et al. 2004, Markiewicz et al. 2005, Arimura et al. 2005). Cells lacking lamins A and C showed a dramatically compromised differentiation potential. Furthermore, myoblasts with reduced lamin A/C or emerin also contain reduced levels of at least four proteins important for muscle cell differentiation and/or the maintenance of their differentiated state: MyoD, desmin, pRB, and M-cadherin (Zeschnigk et al. 1995; Kaufmann et al. 1999). All these studies highlight the importance of the integrity of the nuclear envelope for proper muscle differentiation and maintenance.

Through the LINC complex (linker of nucleoskeleton and cytoskeleton) lamins are connected to the cytoskeleton (Crisp et al. 2006). Like the cytoskeletal elements, lamin stability and organization can be compromised upon stress (e.g. oxidative stress, heat shock). On one hand, heat shock proteins including HSP70, HSPB1 and HSPB5 can interact with and stabilize cytoskeletal elements upon stress (Lavoie et al. 1993; 1995; Perng et al. 2004). On the other hand, disease-associated mutants of HSPB1 and HSPB5 destabilize intermediate

filaments, which contribute to disease progression (e.g. P182L-HSPB1, associated with CMT disrupts neurofilament assembly; (Houlden et al. 2008; Evgrafov et al. 2004). The interactions between the nuclear lamin and the cytoskeleton have important functional significance: they regulate the organization of microfilaments, intermediate filaments and microtubules, modulating mechanical stiffness and mechanotransduction, the process that allows the cells to translate mechanical stimuli into chemical signals, enabling cell adaptation to the physical environment (Jaalouk and Lammerding 2008). Proper mechanotransduction is particularly important for muscles, which are subjected to repetitive mechanical strain. Interestingly, mutations of lamins and NE proteins causing muscular dystrophy increase nuclear deformability and fragility to mechanical stress and impair the activation of mechanosensitive genes; this in turn renders muscle cells more vulnerable to repetitive strain, participating to disease (Zwerger et al. 2013). Thus, in addition to affecting nuclear stability, loss of A-type lamins and mutations linked to EDMD can also disrupt nucleo-cytoskeletal coupling, resulting in the loss of synaptic nuclei from neuromuscular junctions (Méjat et al. 2009), impaired nuclear movement and positioning (Folker et al. 2011) and disturbed cytoskeletal organization (Méjat and Misteli 2010). Altogether these findings support the importance of lamins and integral proteins of the NE in nuclear function and stability and their requirement for proper muscle cell differentiation and maintenance, especially upon stress conditions and highlight that modifications of any of these functions will result (directly or indirectly) in impairment of skeletal muscle cell viability.

AIM OF THE THESIS

Little is known about HSPB3 functions and how its R7S mutation leads to motor neuropathy type 2C (dHMN 2C). We identified in myopathic patients two yet unpublished HSPB3 mutations. One mutation affects the R116 residue of HSPB3, equivalent to the R120 and the K141 residues of HSPB5 and HSPB8, associated with myopathy and motor neuropathy, respectively. The second mutation causes a premature stop codon, generating an unstable peptide that is rapidly degraded after synthesis. We started to characterize in Hela cells the stability, subcellular localization and functions of HSPB2 and HSPB3 (wildtype/wt and mutants).

At the beginning we studied the stability of the HSPB3 mutants, their ability to bind to HSPB2 and to form the typical complex observed in differentiated muscle cells. Then, we analysed the subcellular distribution of HSPB2 and HSPB3 (wt and mutants) in several cell types. Surprisingly, unlike other HSPBs that are predominantly localized in the cytoplasm, HSPB2 and HSPB3 (wt and mutants) are both found in the cytoplasm and in the nucleus, where they form aggregates. The presence of these HSPB2-HSPB3 containing aggregates prompted us to investigate if they affect the nuclear shape and integrity, which may be relevant to neuro/muscular diseases. In fact, mutations in lamin A/C cause muscular disease. We evaluated the impact of HSPB2 and HSPB3 (wt and mutants) on the distribution of lamins (lamin A/C, lamin B), as well as prelamin A maturation and integral proteins of the nuclear envelope. Next, we evaluated whether by aggregating inside the nucleus and at the perinuclear region, HSPB2 and HSPB3 might affect nuclear functions such as RNA transcription and splicing.

In light of their expression profile, restricted mainly in differentiated myoblasts, we overexpressed HSPB2 and HSPB3 (wt and mutants) in human skeletal myoblasts and we investigated their effects on nuclear shape and function, as well as differentiation.

MATERIALS AND METHODS

Cell Culture

HeLa (human cervical cancer), *Lmna*$^{+/+}$, *Lmna*$^{-/-}$, LCO (mouse embryonic fibroblasts), NSC34 (Mouse Motor Neuron) and Hek293T (human embryonic kidney containing the SV40 Large T-antigen) cells were cultured in DMEM (ECB7501L; EuroClone, Milan, Italy) supplemented with 2mM L-glutamine (ECB3000D; EuroClone, Milan, Italy), 100 U/mL penicillin/streptomycin (ECB3001D; EuroClone, Milan, Italy) and 10% Fetal Bovine Serum (FBS) (F7524; Sigma-Aldrich, Milan, Italy) in a 37°C incubator with 5% CO_2. *Lmna*$^{+/+}$, *Lmna*$^{-/-}$, LCO MEFs were kindly provided by Dr. Lammerding (Cornell University).

Cycling LHCN-M2 (Zhu et al. 2007) cells were cultured in HAM's F12 (ECB7502L; EuroClone, Milan, Italy) supplemented with 2mM L-glutamine, 100 U/mL penicillin/streptomycin, 20% FBS (Gibco 10106-169; Invitrogen, USA) and 25 ng/mL of rh FGF-b/FGF-2 (11343625; ImmunoTool, Germany). Differentiated LHCN-M2 cells were cultured in DMEM supplemented with 2mM L-glutamine, 100 U/mL penicillin/streptomycin, 2% horse serum (Gibco 26050-088; Life Technologies, USA) and 30 µg/mL of Insulin (I1882; Sigma-Aldrich, Milan, Italy).

Transfection

HeLa, MEF and Hek293T cells were transfected using the calcium phosphate method (as previously described; Carra et al. 2005). 0.9 µg of plasmid DNA were mixed with 2.5 µL 2.5 M $CaCl_2$, the volume was adjusted to 50 µL with sterile H_2O. Then drop by drop 25 µL HBS 2X (50mM HEPES, 280mM NaCl, 1.5mM Na_2HPO_4) was added. Precipitates were allowed to form for 20 minutes, and then the solution was added to cells. Overnight after incubation, the medium was replaced and cells were either further incubated at 37°C with 5% CO_2 or treated or processed for western or immunofluorescence.

Lentiviral Production and Infection

The production of lentiviral particles was performed according to Wang and McManus 2009. Briefly, lentiviral particles were generated by co-transfection of Hek293T cells with the 3rd generation packaging systems (pMDlg/pRRE #12251; pRSV-Rev #12253; pMD2.G #12259; Addgene) and lentiviral vectors encoding for Human HSPB2 (EX-Q0523-Lv105-B; Tebu-bio; Italy) and Human myc-HSPB3 wt (EX-T1904-Lv107; Tebu-bio; Italy) or mutants (myc-HSPB3 R116P and myc-HSPB3 R7S). The 2nd generation packaging systems (pCMV-dR8.74 #22036; pMD2.VSVG #12259; Addgene) was used for the production of lentiviral particles expressing GFP (pLKO.1 GFP shRNA; Plasmid #30323; Addgene). The DNA mixture was transfected using the calcium phosphate method previously described. After transfection the cells were incubated at 37°C with 5% CO_2 for 48-96 hours and the supernatant was collected, filtered using 0,45 μm syringe filter (431220; Corning, NY), and then aliquoted and stored at -80°C. Alternatively, the supernatant containing the lentiviral particles was filtered directly into a Beckman Ultracentrifuge tube (Thinwall, Ultra-Clear™, 38.5 mL, 25 x 89 mm; 344058; Beckman Coulter, Kraember Blvd Brea, CA) and then ultracentrifuged into SW-28 rotor buckets for 2 hours and 30 minutes at 4°C at 19,000 rpm. The viral pellet was re-suspended with sterile DMEM. Finally the virus was left at 4°C o/n to complete re-suspension and then the virus was aliquoted and stored at -80°C. Cycling LHCN-M2 were transduced by adding the desired volume of virus, diluted into infection medium (HAM's F12, 2mM L-glutamine, 10% heat-inactivated FBS (30 minutes at 56°C), 25 ng/mL of rh FGF-b/FGF-2) supplemented with 8 μg/mL polybrene. 24 h post-transduction, the medium was replaced with fresh cycling medium, and left for 48 h prior to fixation. For experiments under differentiation conditions 24 h post-transduction, the medium was replaced with differentiation medium and left for ca. 3-5 days prior to fixation.

Mutagenesis

The pcDNA vectors encoding for myc-HSPB3 R7S, R116P and the truncated mutant A33AfsX50 were generated by mutagenesis by Jeanette Brunsting in collaboration with Prof. Carra. The lentiviral vector encoding for myc-HSPB3 R7S was obtained by mutagenesis using the lentiviral vector encoding for myc-HSPB3 purchased by Genecopeia (EX-T1904-Lv107). Mutagenesis was performed using Phusion Site-Directed Mutagenesis Kit (Thermo Scientific) according to the manufacturer's instructions. The primers used are listed below:

hspB3 R7S for	TCATTTTGAGCCACCTCATAG
hspB3 R7S rev	CTATGAGGTGGCTCAAAATG

Immunofluorescence Microscopy

Cells (HeLa, *Lmna*$^{+/+}$, *Lmna*$^{-/-}$, LCO and Hek293T) were grown on coverslip, coated with sterile poly-L-lysine. Cycling LHCN-M2 were grown on coverslip, coated with 0,1% of sterile gelatine. Differentiating LHCN-M2 cells were grown on plastic chamber slide (177445; Thermo Scientific™ Nunc™ Lab-Tek™; NY). After transfection/infection cells are washed with cold PBS 1x (ECB4004L; EuroClone, Milan, Italy) and fixed with 3.7% formaldehyde in PBS 1x for 9 minutes at room temperature, followed by permeabilization with cold acetone 100% for 5 minutes at -20°C. Alternatively, cells were fixed with ice-cold methanol for 10 minutes at -20°C. Coverslips or wells of chamber slide were blocked with PBS 1x containing 3% BSA and 0.1% Triton X-100 for 1 h and then incubated o/n with primary antibodies at 4°C. After 3 washes with PBS 1x cells were incubated with fluorescently labelled secondary antibodies for 1 h at room temperature and in dark conditions. Primary and secondary antibodies were diluted in PBS 1x containing 3% BSA and 0.1% Triton X-100. Primary and secondary antibodies used are listed below. Cells were then washed 3 times with PBS 1x and coverslips/chamber slide were mounted on glass microscope slides with mounting solution (PBS pH 7,4, Mowiol 20%, 1.4-diazabiciclico-[2,2,2]-ottano DABCO as antifading agent). Slides were stored at 4°C. Analysis of the cells was done by confocal imaging using a Leica SP2 AOBS system (Leica Microsystems) and a 63x oil-immersion lens. The primary antibodies used in this study are: mouse anti-HSPB2 (6), goat anti-Lamin B (M-20), rabbit anti-Lamin A/C (H-110), goat anti-Lamin A (C-20), all from Santa Cruz Biotechnology Inc. Rabbit anti-HSPB1 was an homemade antibody kindly provided by Prof. Jacques Landry (Landry et al. 1989). Rabbit

anti-Cleaved Caspase-3 (Asp175) was from Cell Signaling, while mouse anti-Flag M2 (F1804), rabbit anti-HSPB3 (11-25), mouse anti-V5 and mouse anti-SC35 were from Sigma-Aldrich (Milan, Italy). Rabbit anti-Prelamin A (ANT0045) was from DIATHEVA. Mouse anti-αB Crystallin (SMC-159A) was from StressMarq Biosciences Inc. (Canada). Mouse anti-c-myc (9E10) was kindly provided by Prof. Robert Tanguay, Canada. Rabbit pS10-H3 (06-570) was from Millipore. Mouse anti-Emerin and rabbit anti-SUN2 were kindly provided by Prof. Marmiroli Sandra and Dr. Jessika Bertacchini and were previously described (Mattioli et al. 2011).

All the Alexa-conjugated secondary antibodies were from Life Technologies: donkey-anti-goat-Alexa488, donkey-anti-mouse-Alexa594, donkey-anti-rabbit-Alexa594, goat-anti-rabbit-Alexa488 or 594 and goat-anti-mouse-Alexa488 or 595. DAPI (SC-3598 Santa Cruz Biotechnology Inc) was used to mark cellular nuclei.

EU Detection by Click Chemistry

The EU assay was performed basically as described by Jao and Salic 2008. Briefly, 48 h post-transfection/infection HeLa/LHCN-M2 cells were incubated at 37°C with 5% CO_2 with 200μM of EU (from 100mM stock in DMSO) for 6 h. After EU labelling, cells were fixed in 125mM Pipes, pH 6,8 / 10mM EGTA / 1mM magnesium chloride / 0.2% Triton X-100 / 3.7% formaldehyde for 30 minutes at room temperature and processed for Alexa Fluor 594 azide (A10270) staining (100mM Tris pH 8,5 / 1mM $CuSO_4$ / 10μM Alexa azide 594 / 100mM ascorbic acid) for 30 minutes at room temperature and in dark condition. After the azide staining, the cells were processed with DAPI. Where required, cells were blocked with blocking solution and processed for immunofluorescence as previously described. As control for the specificity of EU incorporation and staining, HeLa cells were incubated for 6 h with 1mM EU and 2μM actinomycin D, which inhibits RNA synthesis (Sigma).

Protein lysate preparation and western blot

Cells were lysed in Laemmli buffer (2%) and homogenized by sonication. Protein samples were boiled for 3 minutes at 100 °C and reduced with β-mercaptoetanol (final 3-5%). Protein samples were electrophoretically separated by SDS-PAGE under denaturing conditions (Laemmli et al. 1970) followed by blotting of the proteins onto a nitrocellulose membrane. Membranes were blocked with PBS-T (137mM NaCl, 2.7mM KCl, 10mM Sodium Phosphate dibasic, 2mM Potassium Phosphate monobasic, 0.1% Tween-20 Bio-Rad, pH 7,4) and 5% dried non-fat milk for 1 h at room temperature. Primary antibodies were applied o/n at 4°C in PBS-T containing 3% BSA and 0.02% Na-azide. HRP-conjugated secondary antibodies (GE Healtcare) were prepared in PBS-T and 3% dried non-fat milk and left for at least 1 h at room temperature. After antibody incubation, 3 washes (10 minutes each) with PBS-T were performed. Then chemiluminescence was induced using an ECL kit (Thermo Scientific).

The antibodies used for both western blotting and immunofluorescence are listed in the previous section. The following antibodies were used only for western blotting: rabbit anti-Desmin (H-76), mouse anti-Caspase-3 (31A1067), rabbit anti-Myogenin (M-225), rabbit anti-MyoD (M-318), mouse anti-PARP-1(F-2) and mouse anti-p53 (DO-1) all from Santa Cruz Biotechnology Inc. Mouse anti-Tubulin (T6074) was from Sigma-Aldrich (Milan, Italy).

Nuclear–Cytosol extraction

Cells were harvested with Buffer A (10mM HEPES pH 7,9, 10mM KCl, 0.1mM EDTA pH 8, 0.1mM EGTA pH 8, DTT 1mM, 0.15% NP40 and 1% complete). Sample was homogenized by passing 3-4 times through a needle 26G. After centrifugation at 12,000 rpm for 30 seconds at 4°C, the cytosolic fraction (the supernatant) was separated from the pellet. The pellet fraction was lysed with Buffer B (20mM HEPES pH 7,9, 400mM NaCl, 1mM EDTA, 1mM EGTA, 1mM DTT, 0.5% NP40 and 1% complete), sonicated and centrifuged to extract the nuclear fraction. SDS buffer 4x was added to both cytosolic and nuclear fractions, which were then reduced with β-mercaptoetanol and boiled for 3 minutes. Then the expression/localization of proteins were analysed by western blot. Anti–Tubulin and anti-Lamin B1 were used as loading control for the cytosolic and nuclear fractions, respectively.

SDS-soluble and -insoluble extraction

Cells were scraped, homogenized in 2% SDS sample buffer supplemented with 50mM dithiothreitol and heated for 10 minutes at 100°C. Cell lysate was immediately centrifuged for 20 minutes at room temperature. After centrifugation, two fractions, the supernatants (SDS-soluble fraction) and the SDS-insoluble pellet, were obtained. The SDS-insoluble pellets were incubated with 100% formic acid for 30 minutes at 37°C, lyophilized o/n, and finally re-suspended in 2% SDS sample buffer. Both SDS-soluble and SDS-insoluble fractions were processed for western blotting.

Co-immunoprecipitation (Co-IP)

Cells were lysed in IP lysis buffer (150mM NaCl 0.5% IGEPAL 1.5mM Mg_2Cl, 20mM TRIS-HCl pH 7,4, 3% glycerol, 1mM DTT, complete EDTA-free). After homogenization the cell lysates were centrifuged at 14,000 rpm for 15 minutes at 4°C. Small amount of supernatant was kept apart as INPUT fraction. The cell lysates were cleared with Mouse TrueBlot beads (88-7788-31; tebu-bio) at 4°C for 1 h. Beads complexed with specific antibodies (anti-Flag antibody) were added to the precleared lysates. After incubation for 1 h at 4°C, the immune complexes were centrifuged. SDS buffer 4x was added to both co-immunoprecipitated proteins and input fractions, which were then reduced with β-mercaptoetanol, boiled for 3 minutes and resolved on SDS-PAGE.

Ni-NTA precipitation of His-tagged proteins

The Ni-NTA was performed basically as described by Vos et al. 2010. Cells were washed with PBS 1x and harvested in lysis buffer (150mM NaCl, 50mM NaH_2PO_4, 10mM imidazole, 0.5% NP-40 (igepal), 1.5mM $MgCL_2$, 3% glycerol, 0.9mM DTT and protease inhibitors). Cells were lysed by passage through a 26G needle for 5 times, and centrifuged at 14,000 rpm for 15 minutes at 4°C. A small part of the supernatant was kept apart and mixed with 4x sample buffer (INPUT fraction). The rest of the supernatant was transferred to a new vial and Ni-NTA agarose beads (Qiagen) were added and incubated at 4°C for 1 h with slow agitation. The beads were washed several times with wash buffer (300mM NaCl, 50mM NaH_2PO_4, 20mM imidazole, 0.5% NP-40 (igepal), 1.5mM $MgCl_2$, 3% glycerol). Beads were boiled in ½ volume of lysis buffer, ½ volume of 4x sample buffer and β-mercaptoetanol. Beads and input were analysed by western blot.

Filter Trap Assay

The filter trap assay was performed basically as described by Carra et al. 2005. Briefly, cells were scraped in filter trap assay buffer (10mM Tris-HCl pH 8, 150mM NaCl, and 50mM dithiothreitol) supplemented with 2% SDS and homogenized by 3 passages through a 26G needle. Different dilutions of each sample were heated at 98 °C for 3 minutes and immediately applied with mild suction onto 0,22 μM cellulose acetate membrane pre-washed with filter trap assay buffer containing 0.1% SDS. The membrane was then washed 3 times with the same buffer and processed for western blot analysis as described earlier.

Sucrose gradient centrifugation

The sucrose gradient was performed basically as described by Vos et al. 2010. Cells were scraped in cold lysis buffer (150mM NaCl, 50mM NaH_2PO_4, 10mM imidazole, 0.5% NP-40, 1.5mM $MgCl_2$ and 3% glycerol), Cells were lysed by 5 passages through a 26G needle, followed by centrifugation at 14,000 rpm for 15 minutes. The cell lysate was loaded on top of a linear 15-45% (wt/wt) sucrose gradient (10mM Tris-HCl pH 8, 5mM EDTA, 50mM NaCl) and centrifuged for 2 h at 34,000 rpm in a Beckman Coulter SW 40 Ti rotor, Swinging Bucket. Individual fractions were ethanol-precipitated to remove sucrose and to concentrate the

proteins. Proteins were re-suspended in reducing SDS sample buffer and processed for western blot.

RNA extraction, RT-PCR and Real-Time PCR

Total RNA was isolated using Trizol reagent (15596-026; Life Technologies) according to the manufacturer's instructions. Subsequently 1 μg of extracted RNA was treated with DNase I (AM2222; Life Technologies) according to the manufacturer's instructions, prior to reverse transcription-PCR (RT-PCR). First-strand cDNA was generated using High Capacity cDNA Reverse Transcription Kit (Applied Biosystems) according to the manufacturer's instructions. In detail the 2x Reverse Transcription Master Mix (10x RT BUFFER; 25x dNTP Mix; 10x RT random primers; Multiscribe Reverse Transcriptase; Rnase inhibitor Nuclease free H_2O) was added to the DNase treated RNA. The samples were incubated at 25°C for 10 minutes followed by a step of 37°C for 120 minutes, and then 85°C for 5 minutes. The cDNA was stored at -20°C or used immediately for real-time PCR. Relative changes in transcription levels of hHSPB2, hHSPB3, hMgn and hHPRT were determined using CFX96 Touch Thermal cycler (Bio-Rad, Hercules, CA, USA) in combination with SYBR green master mix. The primers used are listed below.

The real-time PCR was performed in collaboration with Dr. Milena Nasi.

h HSPB2 For	CATGGTCCACAATGTATGGT
h HSPB2 Rev	ATTTGGGTTTATTCAGCTCCAC
h HSPB3 For	GACTAAGTGACATCGTATCGG
h HSPB3 Rev	ACAAACATTCTCGTAGTACCAG
h myogenin For	CACTCCCTCACCTCCATCGT
h myogenin Rev	CATCTGGGAAGGCCACAGA
h HPRT For	CGTCGTGATTAGCGATGATGA
h HPRT Rev	TCCAAATCCTCGGCATAATGA

The real-time PCR was performed as follow: one cycle of denaturation (95°C for 3 minutes) followed by 40 cycles of amplification (95°C for 10 seconds, 60°C for 30 seconds). Each reaction was monitored by the use of a negative control (no template). All the analyses were performed in triplicate. Data were analysed with Bio-rad CFX Manager 3.1 (Windows 7.0). We used HPRT as housekeeping gene.

Fluorescence-Activated Cell Sorting (FACS)

Cells were transfected with GFP alone or in combination with HSPB2 and/or myc-HSPB3. 48 h post-transfection cells were collected and sorted using eS3 sorter (Bio-rad, Hercules, CA) equipped with two lasers (488nm and 561nm). A minimum of 1 x 10^5 cells per sample were acquired. The GFP positive cells were processed for western blot. FACS experiments were conducted in collaboration with Dr Sara de Biasi.

Electron Microscopy (EM)

Cells were washed first with preheated PBS 1x and then with 0.1M cacodylate buffer. Samples were fixed with 2.5M glutaraldehyde for 1 h at room temperature. Post-fixation the samples were washed with 0.1M cacodylate buffer and left at 4°C in the same buffer. The electron microscopy was performed at Laboratory of Cell Biology and Electron Microscopy, Rizzoli Orthopedic Institute, Bologna, Italy by our collaborator Prof. Marmiroli Sandra.

Statistical analysis

Student's t-test was used for comparisons between two groups. One-way ANOVA followed by Bonferroni–Holm post-hoc test was used for comparisons between three or more groups. *P<0.05; **P<0.01; ***P<0.001.

RESULTS

Identification of HSPB3 mutants in patients affected by motor neuron disease and myopathy

Until now, only one pathogenic mutation has been reported in the HSPB3 gene, namely the R7S mutation that is located in the N-terminus of HSPB3 and caused in two sisters of age 58 and 51 years, distal hereditary motor neuropathy type 2C (dHMN type 2C) (Kolb et al. 2010). In light of the association of HSPB mutations with neuron/muscular diseases and considering the rather selective expression of HSPB2 and HSPB3 in differentiating skeletal muscles (Sugiyama et al. 2000), we sequenced the DNA of 400 patients affected by myopathy of unidentified origin in search for mutations in either the HSPB2 or HSPB3 gene. The patients have been enrolled in a study aimed at generating a national register for Facioscapulohumeral muscular dystrophy (FSHD), a study conducted by Prof. Rossella Tupler (University of Modena and Reggio Emilia) and that include not only patients affected by FSHD but also patients for whom a diagnosis of neuromuscular disease has been made, although the genetic causes are yet unknown. No mutations were found in the HSPB2 gene in the samples analyzed. Instead, we identified two mutations in the HSPB3 gene: p.R116P and p.A33AfsX50 (c.774_775het_insC) (see Figure 6C). Both mutations were not found in more than 400 normal alleles.

The R116P mutation was found in a 25-year-old woman and affects a key amino acid (hot-spot) in the ACD of HSPB3, which mutation in other members of the HSPB family also causes disease (it is equivalent to e.g. R120 in HSPB5, whose mutation into G causes MFM and to K141 in HSPB8, whose mutation into E or N causes dHMN; Carra et al. 2008; Carra et al. 2010; Shemetov and Gusev 2011; Ghaoui et al. 2016). The R116P mutation has been inherited genetically by the patient from the father. The father was also pauci-symptomatic and presented sciatic irregular pains, similar to his daughter with intermittent myalgia that was however associated to borderline creatine kinase (CK) elevation. The young woman presented weakness of upper limbs with pain and weakness in lower limbs. On cardiological visit she was found to have a “click on mitral valve”. The electromyography (EMG) showed slight neurogenic changes in lower limbs, compatible with an axonal neuropathy. However, the neurological exam showed peroneal muscle atrophy, winging scapulae and a decreased

dorsiflexion of tibial muscles. The saccadic movements were slow. The p.A33AfsX50 mutation was found in a 70-year-old man and disrupts the reading frame from amino acid 33 leading to a premature stop codon at amino acid 50. Concerning the A33AfsX50 mutation, this has not been found in the healthy brother of the proband. However, it was not possible to conclude whether the A33AfsX50 mutation has been genetically inherited by the parents of the proband or rather A33AfsX50 is a de novo mutation; in fact the parents were dead at the time when the diagnosis has been done to the patient.

Characterization of wildtype and mutant HSPB2 and HSPB3 proteins in different mammalian cell lines

As previously mentioned HSPB2 and HSPB3 form a complex, this is induced in differentiated skeletal muscle (Sugiyama et al. 2000). First, we confirmed that HSPB2 and HSPB3 are expressed and colocalize in human skeletal muscle tissue and that HSPB3 colocalizes at the z-disk with alpha-actinin (see Figure 6A and B), where also HSPB2 has been reported to be located (Sugiyama et al. 2000). Next, we performed electron microscopy studies on the muscle biopsy of the patient carrying the R116P mutation. Electron microscopic observation of the patient muscle biopsy revealed severe myofibillar disarray with loss of Z lines in several fibers, enlargements of SR cisternae and few lysosomes and sub-sarcolemmal glycogen accumulation, both in the intermyofibrillar and sub-sarcolemmal location (see Figure 6D). Plurisegmented nuclei, with marginated chromatin (see Figure 6E) and nuclear aggregation, were also observed (see Figure 6F).

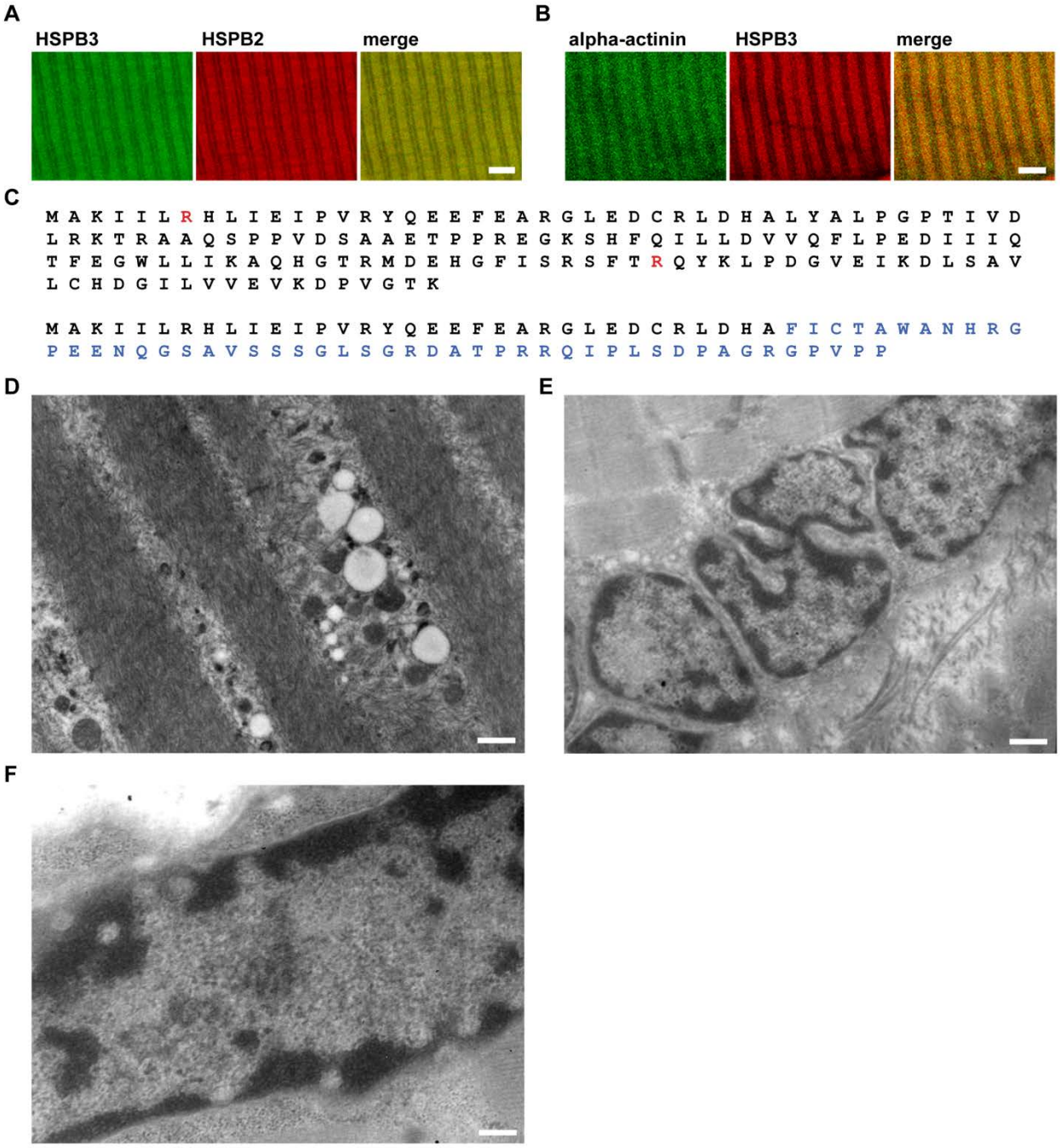

Figure 6. HSPB3 is expressed in human skeletal differentiated muscle and its mutation R116P affects muscle fiber organization and nuclear morphology. For a detailed description of nuclear changes see the main text.

Since little data are available concerning the subcellular distribution of HSPB2 and HSPB3 and virtually nothing has been yet published concerning stability and distribution of the R7S mutation of HSPB3 in mammalian cells we next characterized the expression, stability/oligomerization, aggregation propensity and subcellular distribution of HSPB2, HSPB3 and the three mutants R7S, R116P and A33AfsX50 in widely used mammalian cells such as Hela and Hek293T cells and in cultured immortalized human myoblasts that

represent “physiological” model (since HSPB2 and HSPB3 are mainly expressed in differentiated muscle cells). Another aspect that we addressed was the ability of HSPB3 mutants to form a complex with HSPB2.

Characterization of the biochemical properties and subcellular distribution of HSPB2 and HSPB3 (wt and mutants) in HeLa and Hek293T cells

Concerning the expression profile, first, we transfected HeLa cells with cDNAs encoding for HSPB2, myc-tagged HSPB3, R7S, R116P or A33AfsX50, alone or together. The truncated mutant A33AfsX50 of HSPB3 was undetectable both when transfected alone or with HSPB2. Due to the fact that A33AfsX50 is a truncated product, it is likely that it is recognized by the PQC system and rapidly degraded after synthesis. In order to test this hypothesis, we expressed A33AfsX50 with a myc-tag and we treated the cells overnight with the proteasome inhibitor bortezomib (100nM). The truncated mutant was barely detectable after overnight treatment with bortezomib, demonstrating its high instability and rapid targeting to degradation (see Figure 7A). Due to its short half-life, it was very difficult to characterize A33AfsX50; therefore, the work described in this dissertation is mainly based on the two other (stable) mutants of HSPB3, R7S and R116P. The expression profile of HSPB2, HSPB3 (wildtype/wt) and the two mutants R7S and R116P was similar, both in cells untreated or treated with bortezomib; this observation supports that these proteins are all stable and accumulate with time (see Figure 7A).

Concerning the ability of the two HSPB3 mutants to interact with HSPB2, unlike the R7S mutant, the R116P mutation completely abrogated HSPB3 association with HSPB2 (see Figure 7C). Instead, no significant change in the affinity for HSPB2 was measured when comparing HSPB3 wt and R7S (see Figure 7B).

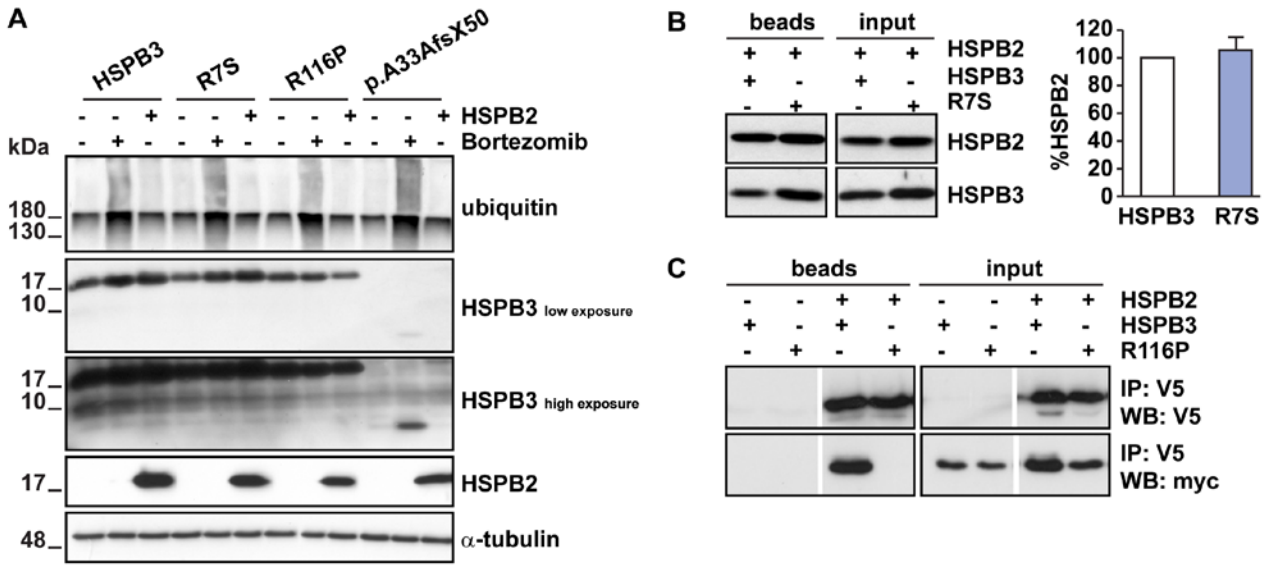

Figure 7. A: HeLa cells were transfected for 48 h with myc-HSPB3 (wt and mutants) alone or with HSPB2; cells were left untreated (-) or treated o/n with 100nM bortezomib. α-ubiquitin and α-tubulin were used as internal loading controls for proteasome inhibition and expression levels of proteins respectively. **B:** Hek293T cells were transfected for 24 h with his-HSPB2 and myc-HSPB3 or myc-R7S. Cell lysates were subjected to Ni-NTA. HSPB2 and HSPB3 levels were determined by western blot (beads and input fractions). **C:** Hek293T cells were transfected for 24 h with V5-HSPB2 and myc-HSPB3 or R116P. Cell lysates were subjected to CO-IP, using beads coated with the V5 antibody and V5-HSPB2 and myc levels were determined by western blot (beads and input fractions).

HSPBs form homo- and/or hetero-oligomers of different size and the oligomerization influences HSPB functions. After having assessed the stability of the wt and mutant HSPB2 and HSPB3 proteins, and how the HSPB3 mutants alter the complex formation, we investigated whether/how the HSPB3 mutant forms may affect oligomerization of HSPB3 and, indirectly, of HSPB2. For this purpose we used the technique of sucrose gradient ultracentrifugation that allows to separate protein and protein complexes, as well as organelles, on the basis of their molecular weight. We found that in HeLa cells both HSPB2 and HSPB3 proteins mainly sediment in the fractions containing low concentrations of sucrose, corresponding to low molecular weight proteins or small oligomers (see Figure 7D). These results suggest that HSPB2 and HSPB3 do not exist in form of high molecular weight complexes/oligomers but rather form a well-defined complex (in line with what reported by den Engelsman et al. 2009). Also, using this technique we did not observe any major difference in the sedimentation profile of HSPB3 wt as compared to mutant R7S or R116P. However, it is interesting to note that when expressed with HSPB2, the sedimentation profile of HSPB3 wt, which was mainly restricted to the first two fractions, is extended to fractions 3 and 4 (following the profile of HSPB2). Instead, the sedimentation profile of HSPB2 did not

significantly change when co-expressed with HSPB3 wt or the R7S or R116P mutants (see Figure 7D). All these observation underline that, the mutations of HSPB3 do not induce any profound variations in the size of HSPB3 oligomers or HSPB2 oligomers.

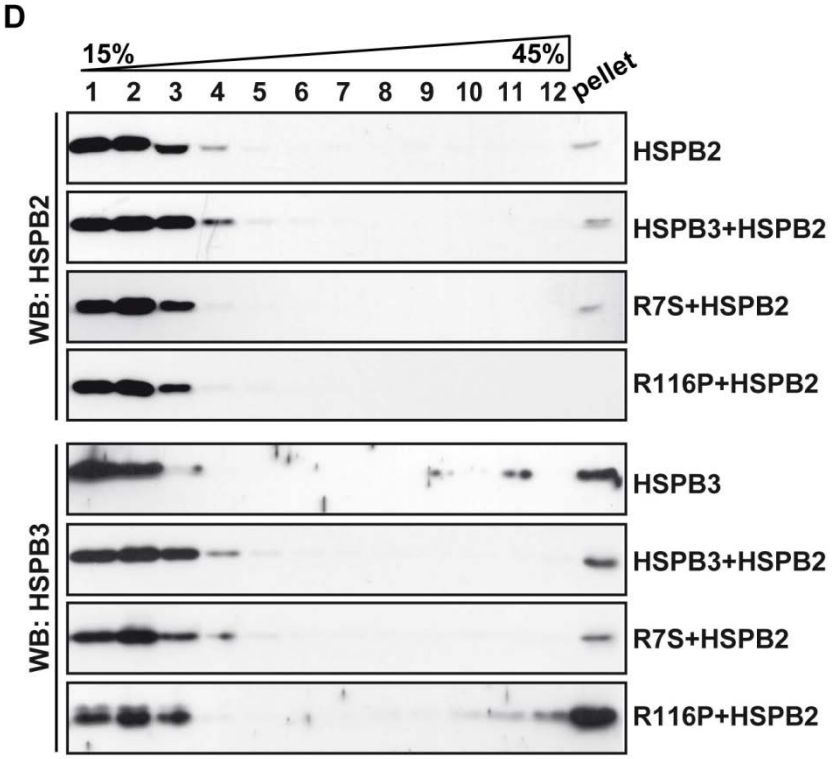

Figure 7. D HeLa cells were transfected with vectors encoding for HSPB2, myc-HSPB3 (wt and mutants) alone or in combination. The lysates were separated on a linear 15-45% sucrose gradient. Individual fractions from the sucrose gradients were subjected to western blot analysis to localize HSPB2/3. The lightest fractions are at the left. Pellet corresponds to the bottom of the gradients.

Concerning the subcellular distribution, we performed, in HeLa cells, the nuclear/cytosolic fractionation to evaluate by western blot the distribution of HSPB2 and HSPB3 (wt and mutants). The majority of HSPBs are mainly cytosolic, such as e.g. HSPB5 (used as positive control) (see Figure 8A); surprisingly, we found that, both HSPB2 and HSPB3 (wt and mutants) are distributed in the cytosol and in the nucleus. Interestingly, co-expression of HSPB2 with HSPB3 or R7S increased the nuclear/cytosol protein ratio as compared to HSPB3 or R7S expressed alone (see Figure 8B, compare lower and upper panel); this observation supports that when expressed together HSPB2 and HSPB3 are mainly localized in the cytosol, but tend to accumulate in the nucleus especially when expressed alone. Of note R7S is more enriched in the nuclear fraction as compared to HSPB3, both when expressed alone and with HSPB2. Concerning R116P, since it does not bind to HSPB2,

cytosolic/nuclear distribution of R116P was not affected by the co-expression of HSPB2 (see Figure 8B, compare lower and upper panel).

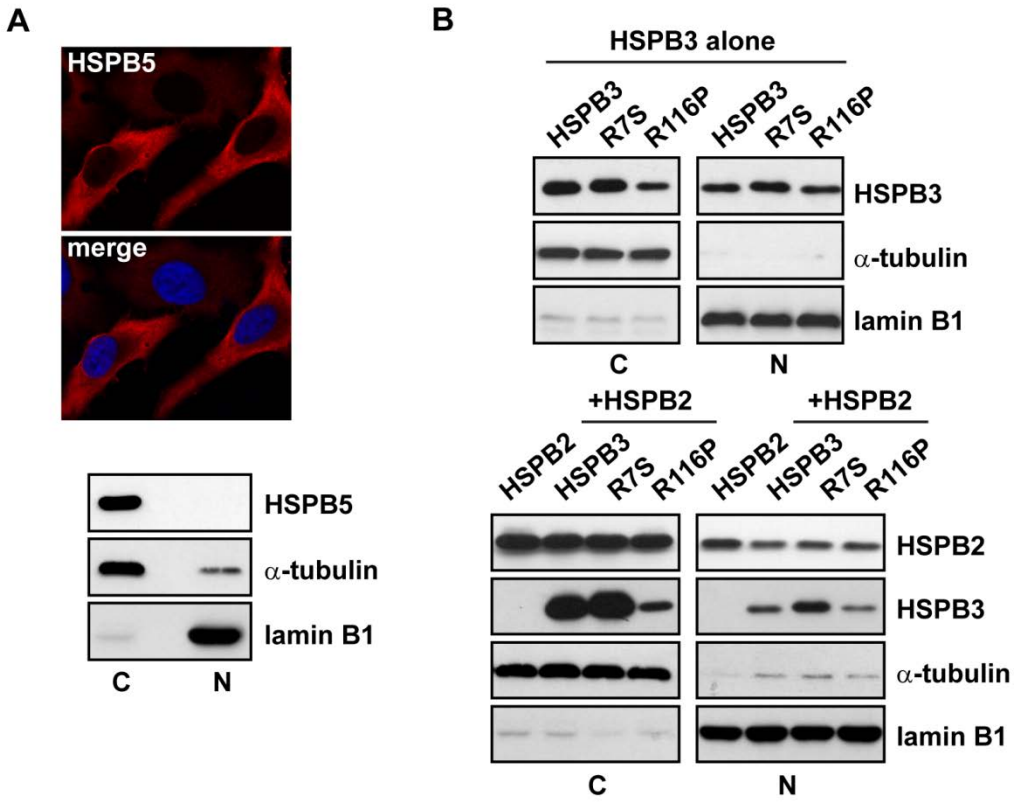

Figure 8. A: HeLa cells were transfected for 48 h with vectors encoding for HSPB5, used as control. **B:** Hek293T cells were transfected for 24 h with vectors encoding for HSPB2, myc-HSPB3, myc-R7S, myc-R116P, alone or in combination. Nuclear and cytoplasmic proteins were fractionated and expression of HSPB2, HSPB3 and HSPB5 was analysed in both fractions. α-tubulin and α-lamin B1 were used as internal loading controls for the cytoplasmic and nuclear fractions, respectively.

Then we studied the subcellular distribution of HSPB2, HSPB3 and its mutants by immunofluorescence. In line with our biochemical fractionation data, we found that HSPB2, HSPB3, R7S and R116P are present both in the cytosol and nucleus. Concerning HSPB2, in HeLa cells it forms large intranuclear (IN) aggregates/masses that displace the DNA. In some cells, the HSPB2 mass extrudes from the nucleus and causes the formation of a large nuclear-associated vacuole (see Figure 9A). HSPB3 is also enriched inside the nuclei, where it can form IN and perinuclear (PN) aggregates (see Figure 9B). Both R7S and R116P mutations enhance HSPB3 aggregation; interestingly, R7S increases the formation of a typical large PN aggregate, while R116P heavily aggregates inside the nucleus (see Figure 9B). We also verified that the PN aggregate formed by the R7S mutant is indeed accumulating at the perinuclear region of

the cell using dsRED as ER marker. This large aggregate in fact could likely accumulate in the space between the nuclear envelope and the ER or within the ER. Figure 9F shows that indeed the R7S aggregate that accumulates on one side of the nucleus is encaged/surrounded by dsRED, confirming its PN (and not IN) nature. Moreover, to further characterize the IN aggregates formed by HSPB2-HSPB3 and get insight on their impact on nuclear morphology we performed electron microscopy studies. Figure 9D shows the presence of a nuclear expansion surrounded by a membrane, but largely devoid of chromatin in HeLa cells expressing HSPB2 and HSPB3. This structure resembles the vacuole-like structure largely devoid of DNA observed by immunofluorescence in cells expressing HSPB2 alone or, at a lesser extent, HSPB2 and HSPB3 or R7S and is referred here to as nuclear bleb. Interestingly, the co-expression of HSPB3 or R7S with HSPB2 not only changed the nuclear/cytosol protein distribution of both chaperones, but it also significantly decreased the IN aggregation of both HSPB3 and HSPB2 (see Figure 9C and E). This is in line with our biochemical data demonstrating that the expression of both complex members increases the cytoplasmic pool and decreases the nuclear pool of proteins (see Figure 8B lower panel). Combined these data suggest that the IN aggregation of HSPB2/HSPB3 correlates with their IN levels. Consistent with the lack of binding of R116P to HSPB2 and the unaffected nuclear/cytoplasmic protein distribution of R116P expressed alone or with HSPB2 (see Figure 8B upper and lower panel), co-expression of R116P with HSPB2 did affect neither its aggregation propensity nor the one of HSPB2 (see Figure 9C and E).

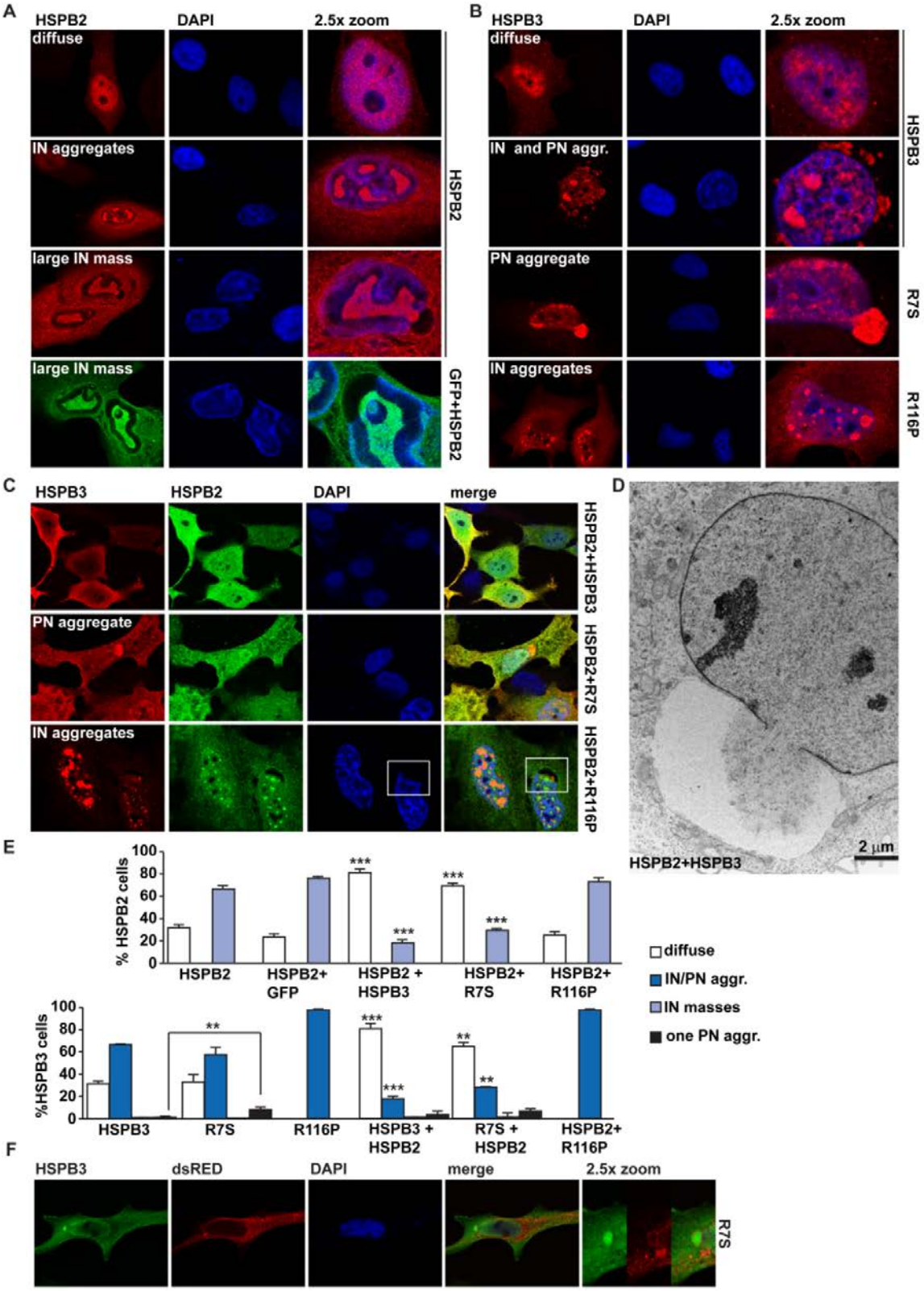

Figure 9. A-E: HeLa cells were transfected for 48 h with vectors encoding for HSPB2, myc-HSPB3, myc-R7S, myc-R116P, alone or in combination. When indicated, HSPB2 was co-transfected with a vector encoding for GFP. **A-C:** Aggregates formed by HSPB3 where classified as intranuclear (IN) or perinuclear (PN). Large intranuclear accumulations typical of cells overexpressing HSPB2 are referred to as IN masses. **D:** Electron microscopy image of HeLa cell transfected with HSPB2 and myc-HSPB3. **E:** Phenotype quantification of HSPB2 and HSPB3 alone or in combination. **F:** HeLa cells transfected with myc-R7S and dsRED and showing the PN nature of R7S PN aggregate.

Since for most our studies we used myc-tagged forms of HSPB3, we verified that the presence of the myc tag was not affecting HSPB3 subcellular distribution and aggregation (see Figure 10). We also confirmed the IN/PN accumulation and aggregation of HSPB3 and its mutants R7S or R116P using both antibody directed against the HSPB3 protein and the myc-tag (see Figure 10) and excluding artefacts due to "lack of specificity" of the primary antibody against HSPB3 used in our studies.

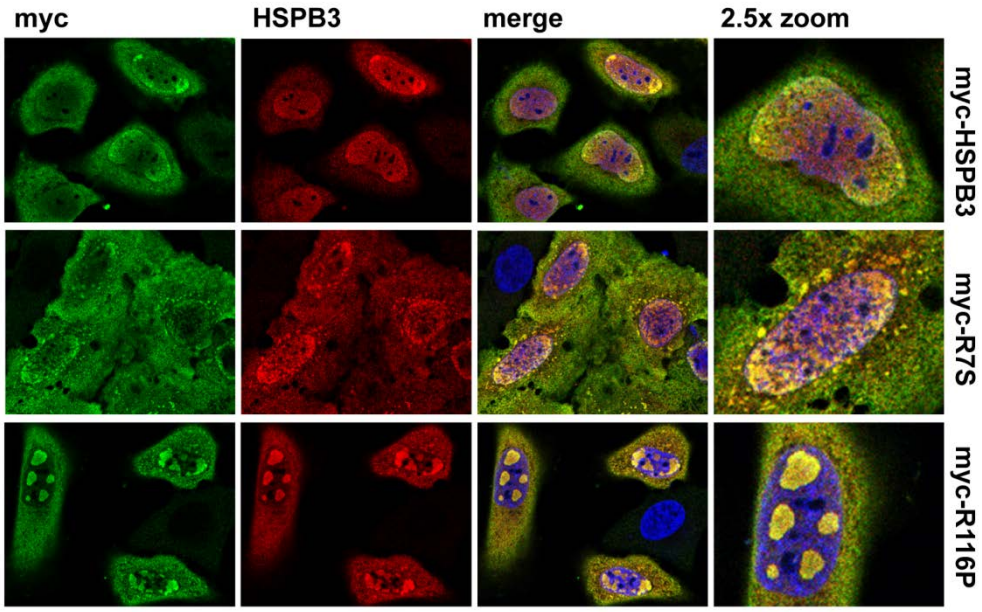

Figure 10. HeLa cells were transfected for 48 h with vectors encoding for, myc-HSPB3, myc-R7S, and myc-R116P. α-myc and α-HSPB3 were used to recognize overexpression proteins. Two antibodies recognize some structures classified as intranuclear (IN) or perinuclear (PN) aggregates. 2.5x magnification of the selected areas is shown.

We then asked whether the aggregates formed by HSPB2 and HSPB3 (wt or mutants) are amorphous or rather fibrillar-like SDS-insoluble, such as e.g. aggregates formed by exon 1 huntingtin with polyglutamine repeat expansion (HA-Htt43Q, used as a positive control). Using both filter trap assay (FTA; see Figure 11A and B) or re-solubilization mediated by treatment of SDS-insoluble proteins with formic-acid (see Figure 11C), we excluded that the IN and PN aggregates formed by HSPB3, R7S or R116P co-expressed with HSPB2 are SDS insoluble.

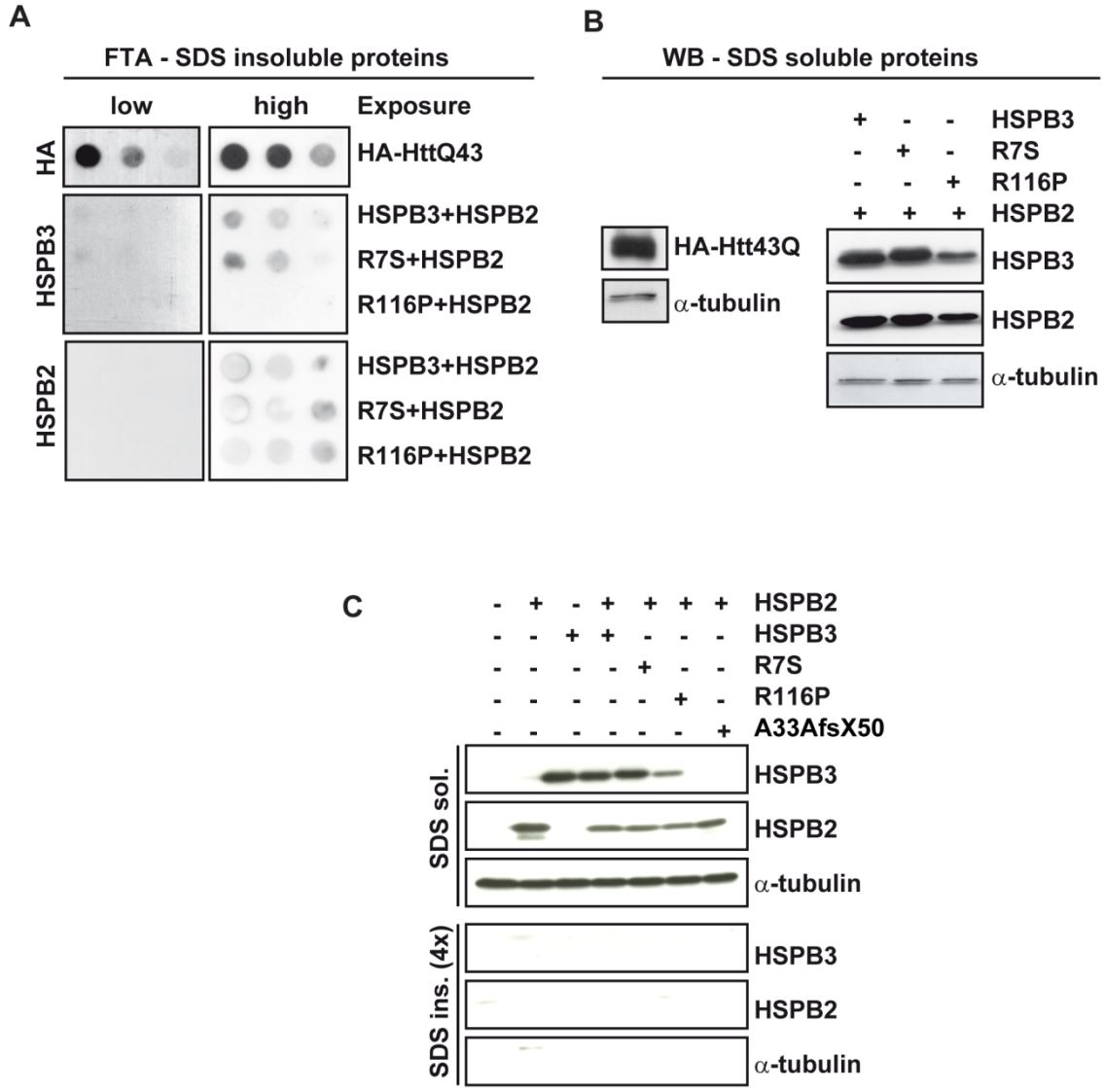

Figure 11. A: Cell lysates from HeLa cells transfected with HA-Htt43Q (used as positive control), HSPB2 or myc-HSPB3 (wt and mutants) were filtered through a cellulose acetate membrane that retains SDS-insoluble aggregated proteins. The membranes were processed for western blot with the indicated antibodies. **B:** An aliquot of the cell lysate has been subjected to SDS-PAGE followed by western blot to analyse the expression levels of the SDS-soluble proteins overexpressed. **C:** Cell lysates from cells transfected with HSPB2, myc-HSPB3(wt and mutants), alone or together, were prepared using a buffer containing 2% SDS. SDS-insoluble proteins were centrifuged and re-solubilized by treatment with formic acid (SDS ins.). All fractions were subjected to SDS-PAGE followed by western blot.

As previously mentioned, HSPB2 and HSPB3 are not endogenously expressed in HeLa and their expression is mainly restricted to differentiating myoblasts. This opens the possibility that the HSPB2/HSPB3 IN and PN aggregation observed and characterized may be partly an artefact due to the high expression levels of HSPB2 or HSPB3 in this specific cell line. For this reason, we next verified whether IN and PN accumulation and aggregation of HSPB2

and HSPB3 (wt, R7S and R116P) could be an artefact due to transient transfection. First, we overexpressed GFP, alone or with HSPB5 (used as control) or HSPB2. GFP alone or co-expressed with HSPB5 accumulates inside the nucleus, but did not form IN aggregates (see Figure 12A); in contrast upon co-expression of GFP with HSPB2, GFP was sequestered into the IN aggregates formed by HSPB2 (see Figure 12B). Next, we transfected HeLa cells with a cDNA encoding for HSPB7, whose expression, similarly to HSPB2 and HSPB3, is restricted to muscles (Krief et al. 1999). As additional controls, we used cDNAs encoding for two mutated forms of HSPB7 that contain a nuclear export and a nuclear localization signal, referred to as NES-HSPB7 or NLS-HSPB7, respectively (Vos et al. 2009). All forms of HSPB7 showed a diffuse staining. Neither expression of wt-HSPB7 and NES-HSPB7, nor forced accumulation within the nuclei of NLS-HSPB7 caused its IN aggregation (see Figure 12C). These results support that the IN aggregation observed in HeLa cells is specific to HSPB2 and HSPB3 and is not an artefact due to transient transfection in this cell type.

We next asked how mechanistically these small HSPs enter and exit the nucleus. NLS have been identified for drosophila Hsp27, which is exclusively distributed inside the nucleus of drosophila cells (Michaud et al. 2008). No NLS is predicted in HSPB2 and HSPB3 by computational methods (Brameier and Banzhaf 2007); this, however, does not fully exclude that a bipartite NLS sequence might be present in HSPB2 and/or HSPB3. We next studied whether HSPB2 and HSPB3 export might be dependent on CRM1/exportin 1. We treated HeLa cells overexpressing HSPB2 or HSPB3 with leptomycin B, an inhibitor of the CRM1/exportin 1; while this treatment caused the IN accumulation of endogenous p53, used as positive control, it did not affect the nuclear/cytoplasmic distribution of HSPB2 and HSPB3 (see Figure 12D). This result demonstrates that the export of HSPB2 and HSPB3 is not CRM1/exportin 1-dependent.

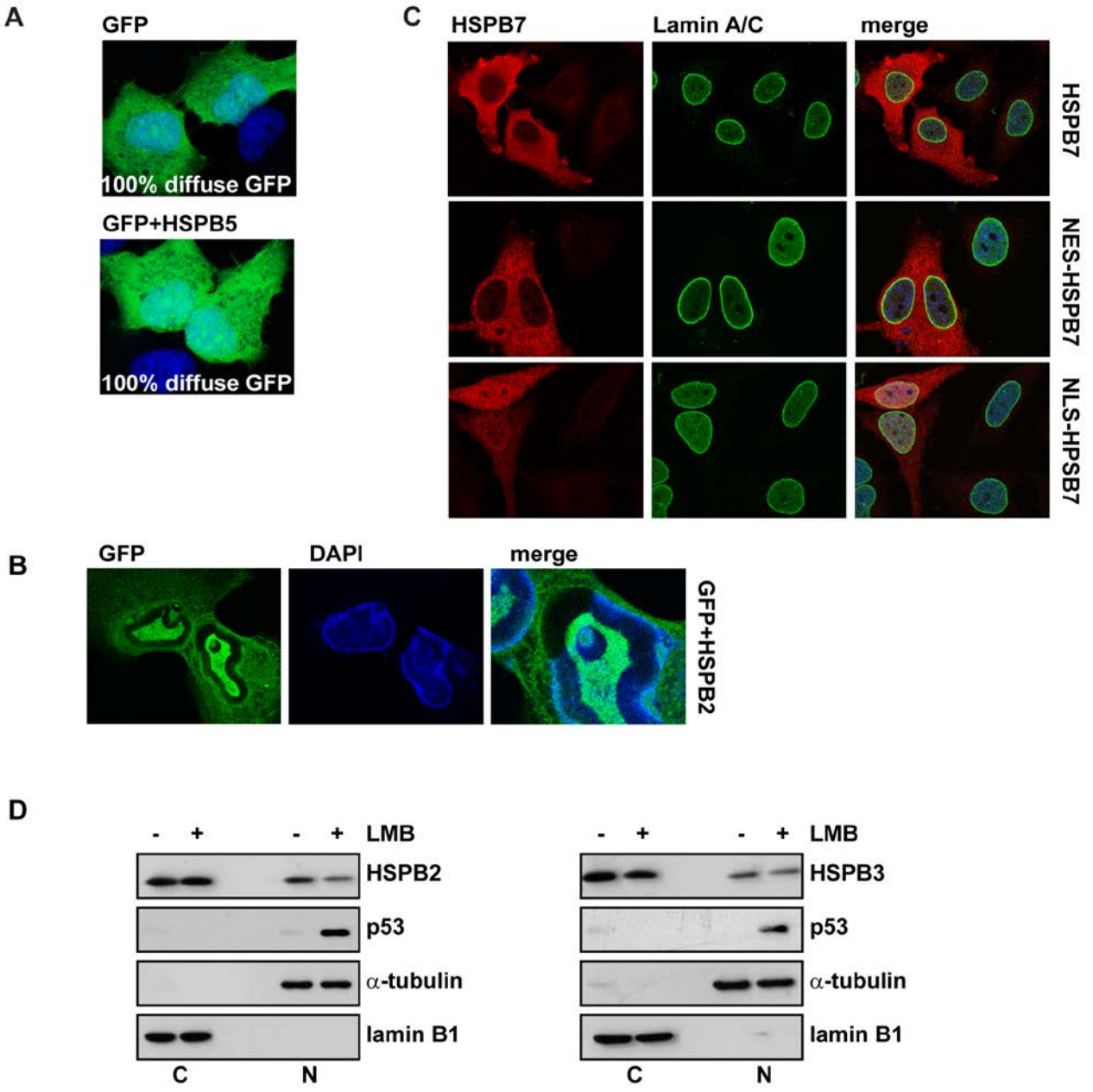

Figure 12. A-C: HeLa cells were transfected for 48 h with vectors encoding for, GFP alone or with HSPB5 or HSPB2 and with vectors encoding for V5-HSPB7, V5-NLS-HSPB7 or V5-NES-HSPB7. Cells were fixed and labelled for protein localization. **D:** HeLa cells were transfected with myc-HSPB3 and HSPB2. 24 h post transfection were left untreated (-) or treated o/n with leptomycin B (50nM). Nuclear and cytoplasmic proteins were fractionated and expression of HSPB2 and HSPB3 was analysed in both fractions. α-tubulin and α-lamin B1 were used as internal loading controls for the cytoplasmic and nuclear fractions, respectively.

Characterization of the subcellular distribution of HSPB2 and HSPB3 (wt and mutants) in human myoblasts

According to the literature, HSPB2 and HSPB3 are not expressed in dividing myoblasts but are induced during differentiation. These studies were done in murine myoblasts (C2C12 cells) (Sugiyama et al. 2000). In these C2C12 cells, HSPB2 was induced at early time-points (around 1-2 days after the induction of differentiation), while HSPB3 was induced only 4 days after differentiation (Sugiyama et al. 2000). We thus first investigated the expression profile and subcellular localization of endogenous HSPB2 and HSPB3 in human myoblasts (LHCN-M2 cells) (Zhu et al. 2007). In line with the data obtained in murine myoblasts, we found that HSPB2 and HSPB3 mRNA and proteins are not expressed in cycling human myoblasts, while being induced in differentiating myoblasts (see Figure 13). By real time-PCR, we measured the induction of the mRNA levels of HSPB2 and HSPB3; we used as positive control, to monitor skeletal muscle cell differentiation, the mRNA of myogenin (myogenic factor 4, MYOG), which is a muscle-specific transcription factor that belongs to the MyoD family of proteins and that participates in skeletal muscle development (Bergstrom et al. 2002; Biamonti et al. 1992; Bonne et al. 2000; McKinsey et al. 2001; Puri et al. 2001). Figure 13A shows that HSPB2, HSPB3 and MYOG are all induced during LHCN-M2 cell differentiation. We then verified that also the HSPB2 and HSPB3 proteins were present in the protein extracts of differentiated LHCN-M2 cells. By immunofluorescence we observed that HSPB2 and HSPB3 are not present in cycling LHCN-M2 cells, while being induced after 7 days of differentiation. At this time-point, both HSPB2 and HSPB3 are widely expressed in differentiated myoblasts, in the cytoplasm and nucleus (see Figure 13B). Then we verified HSPB2 and HSPB3 expression by western blot. Myogenin and desmin, a muscle-specific type III intermediate filament essential for the tensile strength and integrity of myofibrils, were used as positive controls to monitor skeletal muscle cell differentiation. HSPB2, HSPB3 and desmin proteins were not detected in cycling human myoblasts, while being all upregulated 5 to 10 days after differentiation (see Figure 13C).

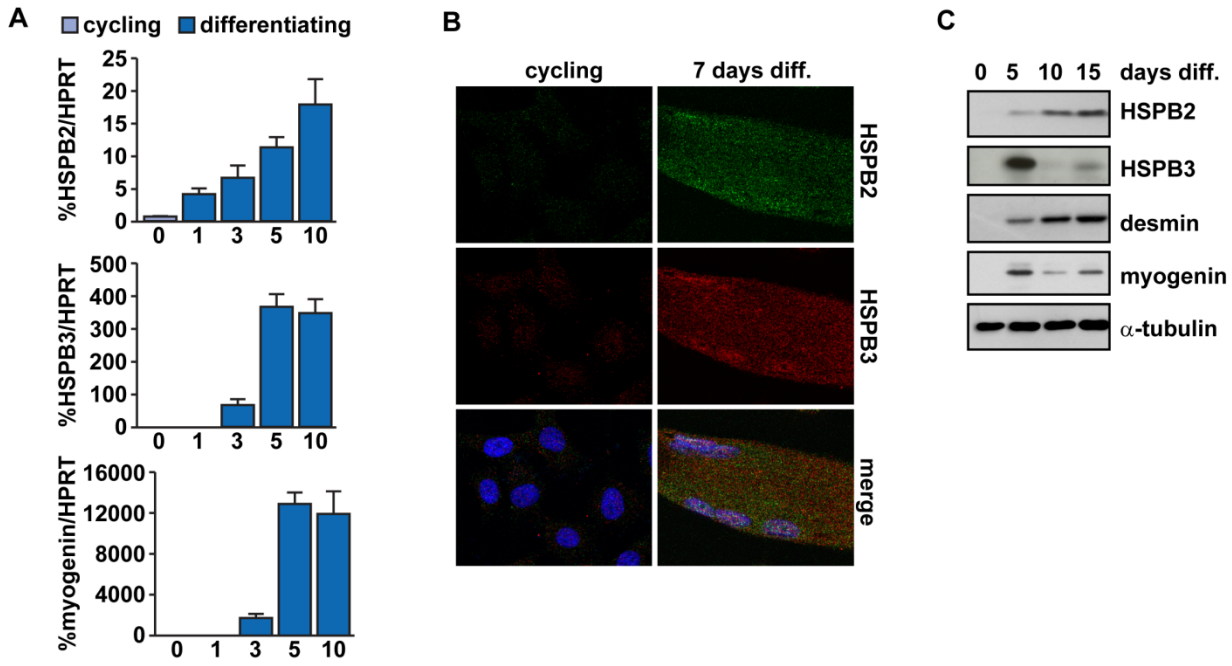

Figure 13. A: LHCN-M2 cells undifferentiated or differentiated for 1-10 days were analysed by real time-PCR to detect mRNA levels of endogenous HSPB2 and HSPB3. **B:** LHCN-M2 cells undifferentiated (cycling) or differentiated for 7 days (diff. days 7) were fixed and labelled with α-HSPB2 and α-HSPB3 to study the subcellular localization of endogenous HSPB2 and HSPB3. **C:** The total extracts of LHCN-M2 cells undifferentiated (0) or differentiated for 5-15 days were analysed by western blot to detect the endogenous levels of HSPB2 and HSPB3, α-desmin was used as loading control for the differentiation process.

We then studied the aggregation propensities of overexpressed HSPB2 and HSPB3 in LHCN-M2 cells that were grown under proliferating (cycling) or differentiating conditions. LHCN-M2 cells were difficult to transfect with classical methods of transfection such as e.g. calcium phosphate, lipofection; however, expression of exogenous proteins can be successfully obtained by infecting both cycling and differentiated LHCN-M2 cells with lentiviral vectors encoding for the protein of interest. Thus, in order to characterize the subcellular localization and aggregation propensities of HSPB2, HSPB3 and the two mutants R7S and R116P in human skeletal myoblasts, we used lentiviral vectors encoding for these proteins. While the lentiviral vectors encoding for HSPB2, myc-HSPB3 wt and myc-R116P were purchased at Genecopeia, the myc-R7S mutant was generated by us by mutagenesis using the lentiviral vector encoding for myc-HSPB3 wt as template (see section of materials and methods for detailed description of the mutagenesis reaction). As control we used a lentiviral vector expressing GFP (pLKO.1-GFP-shRNA). Although the presence of a fluorescent tag is extremely useful to quantify by e.g. FACS the % of infected cells, in light of the importance of both N- and C-terminal regions of HSPBs for the modulation of their stability and oligomerization, we avoided to insert large fluorescent tag on these proteins. We instead,

used the myc-tag for HSPB3 and no tag for HSPB2 and we relied on immunofluorescence for the calculation of viral titer and the % of infection. First, we infected cycling LHCN-M2 cells with the described vectors, obtaining efficiency around ca. 50% for HSPB2 and around ca. 30% for HSPB3. The % of infection with the lentiviral vector encoding for GFP was calculated both via immunofluorescence and FACS and reached around ca. 80-90%, which confirmed to us that both methods are good to determine the efficiency of infection (data not shown).

Concerning the sub-cellular distribution HSPB2 and HSPB3 were enriched in the nucleus of LHCN-M2 cells, where they formed IN aggregates (see Figure 14A and B). R7S could form, in few cells, the typical PN aggregate observed in HeLa cells (see Figure 14B). R116P aggregated inside the nucleus of cycling LHCN-M2 cells, similarly to what found in HeLa cells (see Figure 14B). In general the aggregation propensities of HSPB2 and HSPB3 (wt and mutants) were lower in LHCN-M2 cells as compared to HeLa cells. Moreover, although we frequently found large IN aggregates of HSPB2 in LHCN-M2 cells, these were generally always inside the nucleus and not extruding into the cytoplasm with formation of a vacuole-like structure as often observed in HeLa cells. Thus, although some differences were observed, the aggregation properties of HSPB2 and HSPB3 found in HeLa cells were mostly recapitulated in cycling LHCN-M2 cells.

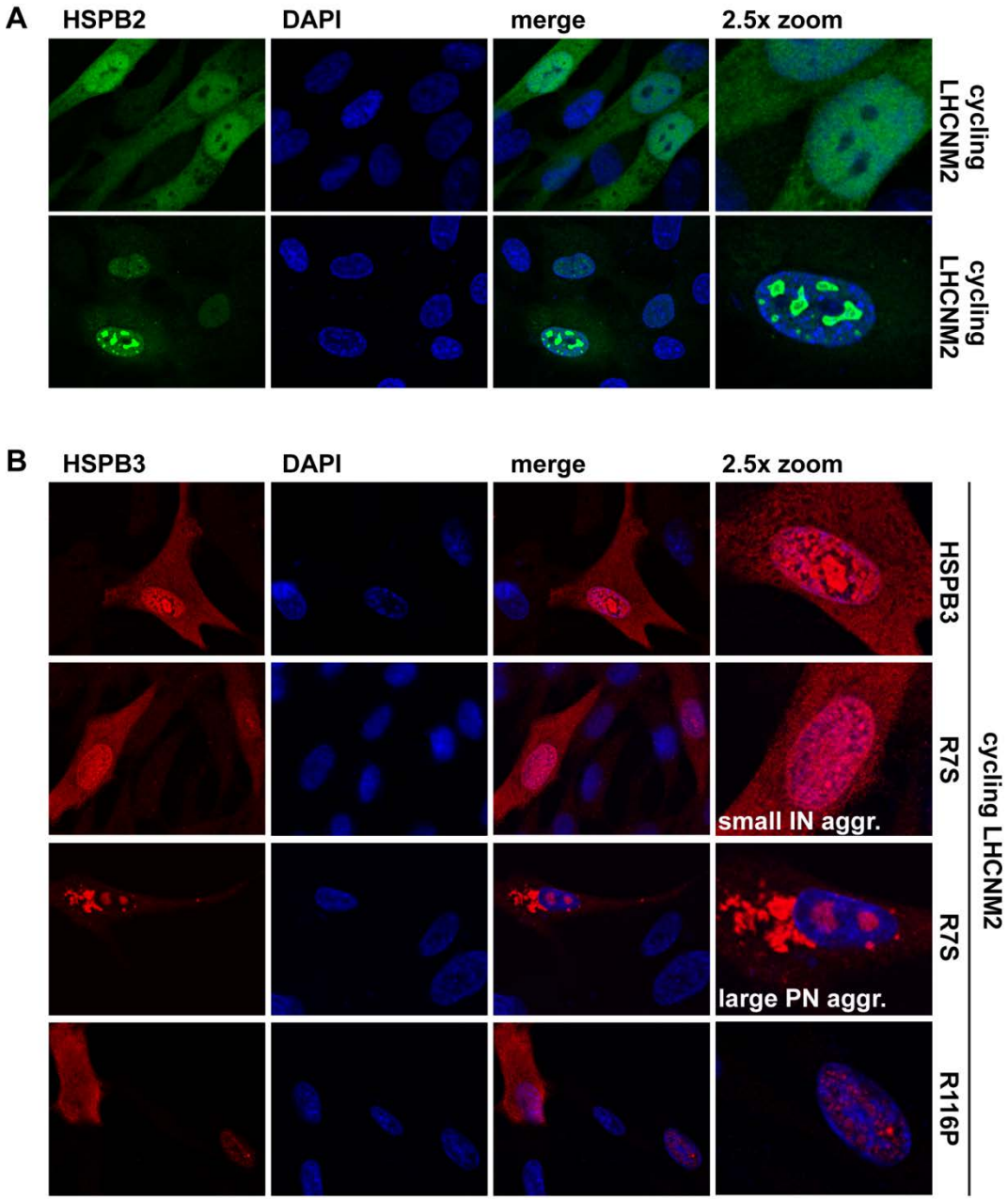

Figure 14. A-B: Cycling LHCN-M2 cells were infected with lentiviral vectors encoding for HSPB2, myc-HSPB3, myc-R7S, myc-R116P. Cells were fixed and labelled with α-HSPB2 and α-HSPB3 to study their subcellular localization. Aggregates formed by HSPB3 where classified as intranuclear (IN) or perinuclear (PN). 2.5x magnification of the selected areas is shown.

We then asked whether the aggregation propensities of HSPB2, HSPB3 (wt and mutants) in human myoblasts could depend on their differentiation state or rather is a consequence of their accumulation at high level and thus would occur in both cycling and differentiated LHCN-M2 cells. We then infected LHCN-M2 cells with the vectors encoding for HSPB2 and HSPB3 and, immediately after infection, we incubated the cells with a differentiating medium. Cells were fixed 48 h post-infection. We found no difference in the

aggregation propensities of HSPB2 and HSPB3 between cycling and differentiated human myoblasts, since also under these conditions IN HSPB2 aggregates and IN and PN HSPB3 aggregates were visible (see Figure 15A and B).

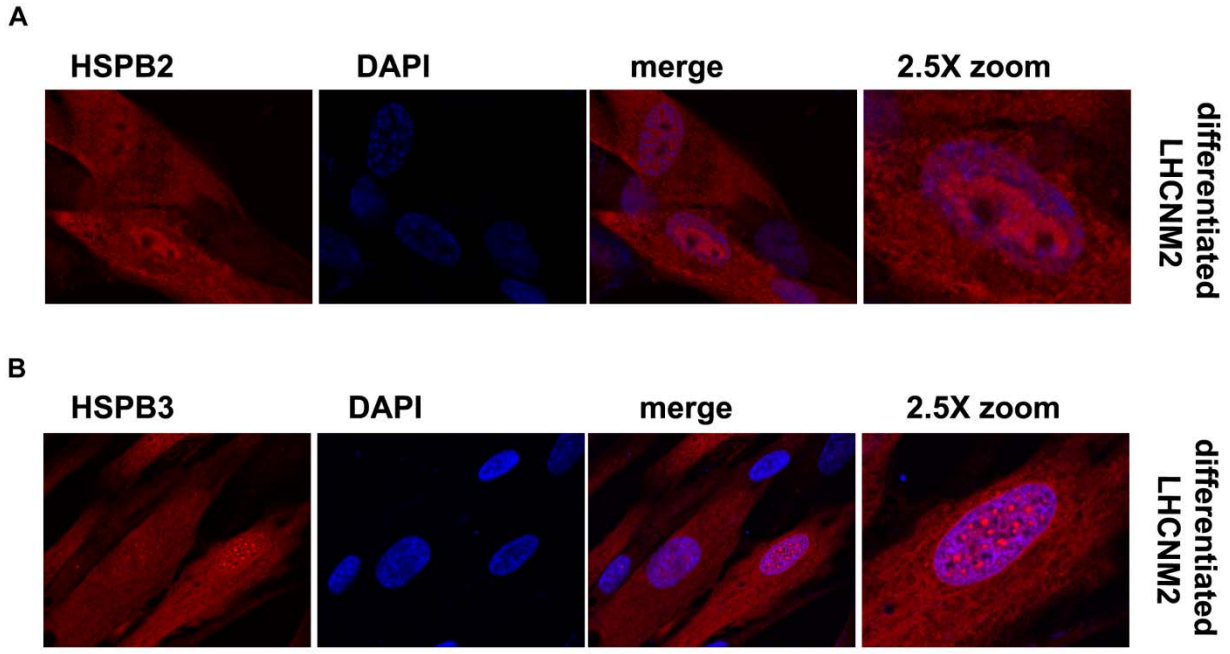

Figure 15. A-B: Cycling LHCN-M2 cells were infected with lentiviral vectors encoding for HSPB2 or myc-HSPB3 and left to differentiate for 2 days. Cells were fixed and labelled with α-HSPB2 and α-HSPB3 to study the subcellular localization of these proteins.

Subcellular distribution of HSPB2 and HSPB3, wt and mutants in Hek293T cells

Our results show that the aggregation propensities of HSPB2 and HSPB3 do not depend on the cell type, neither on whether human cultured myoblasts are cycling or differentiated. Rather, aggregation of HSPB2 and HSPB3 seems to be an intrinsic property of these small HSPBs when they are expressed at high levels. Hek293T cells are known to be easily transfected as compared to HeLa or LHCN-M2 cells, with high expression levels of the overexpressed proteins. Thus, we investigated the expression profile and the sub-cellular localization of HSPB2 and HSPB3 (wt and mutants) in Hek293T cells. The immunofluorescence data show that, also in this cell line, HSPB2 and HSPB3 (wt and mutants) tend to aggregate inside/near the nucleus (see Figure 16); this further confirms that the IN

aggregation of HSPB2/HSPB3 is not cell type specific. Moreover the aggregation propensity of HSPB2 and HSPB3 in Hek293T was higher as compared to HeLa and LHCN-M2 cells, likely due to their higher expression levels. All together our observations corroborate the interpretation that the IN aggregation of HSPB2/HSPB3 correlates with their IN levels. For this reason we restricted our immunofluorescence studies in HeLa and LHCN-M2 cells.

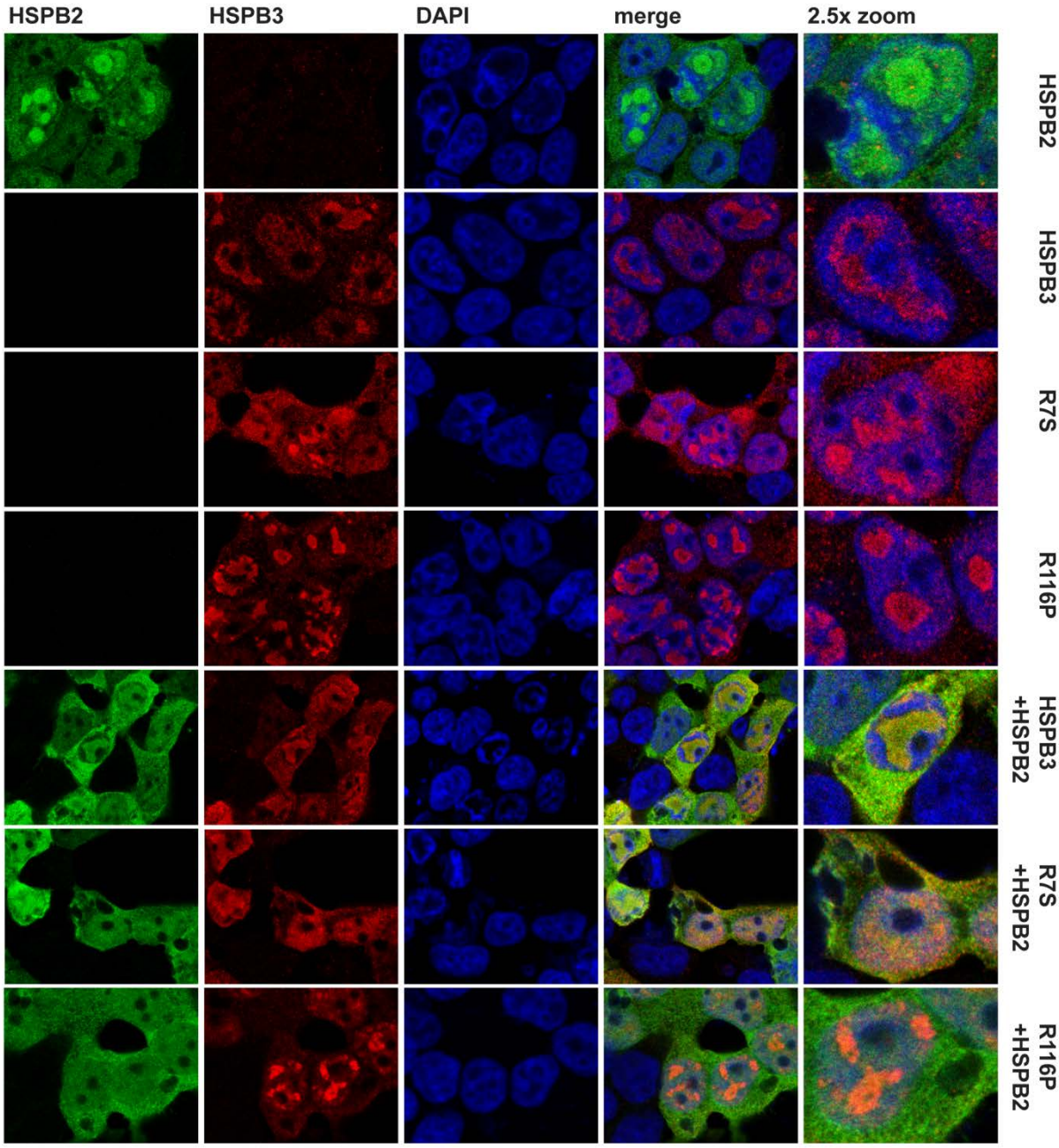

Figure 16. Hek293T cells were transfected for 24 h with vectors encoding for HSPB2, myc-HSPB3, myc-R7S, myc-R116P, alone or in combination to study their sub-cellular localization.

HSPB2 and HSPB3 affect nuclear morphology

Both our immunofluorescence and electronic microscopy data demonstrate that, independent on the cell type, upon overexpression HSPB2 and HSPB3, both wt and mutants, accumulate inside the nucleus and at the perinuclear region, affecting nuclear morphology.

The nucleus is separated from the cytoplasm by the nuclear envelope (NE), which is composed by the outer membrane (ONM) and the inner membrane (INM). Nuclear lamins form a meshwork underneath the NE that serve to maintain the nuclear architecture. Two major classes of lamins have been identified: the A-type (A, A D10 and C) and B-type (B1 and B2) lamins, whose purpose is to provide support to the nucleus and an anchor for the chromatin. The two major isoforms of A-type lamins are lamin A and lamin C that are encoded by a single gene and generate through alternative splicing (Moir et al. 1995; Stuurman et al. 1998). Lamin A and C share the same precursor, prelamin A, which trough different maturation steps generates the mature form of lamin A. Lamins B1 and B2, the two major B-type lamins originate from the LMNB1 and LMNB2 genes, respectively (Dechat et al. 2010). Thus, we investigated whether HSPB2 and HSPB3 (wt and mutants), by aggregating might affect the distribution of nuclear lamins and integral proteins associated with the NE, such as emerin and SUN2.

First, we analysed the distribution of lamin A/C in HeLa cells overexpressing HSPB2 and HSPB3 (wt and mutants), using an antibody that recognizes both lamin A and C. We found that aggregating HSPB2 sequesters endogenous lamin A/C (see Figure 17A). We previously show that when co-expressed with HSPB2, GFP is sequestered into HSPB2 IN aggregates. Thus, to avoid artefacts due to HSPB2 and lamin A/C antibodies, which might cross-react, we co-transfected HeLa cells with a cDNA encoding for flag-tagged lamin A together with GFP alone (used as control) or with HSPB2 and we visualized the distribution of overexpressed lamin A with a flag-specific antibody (see Figure 17B). In cells overexpressing GFP and flag-lamin A, the lamin A shows a weak IN diffuse staining with a major enrichment at the nuclear rim (as expected) (see Figure 17B lower panel). Instead, in cells co-expressing flag-lamin A, GFP and HSPB2, GFP and flag-lamin A were co-aggregating with HSPB2 (see Figure 17B upper panel). In parallel, we used another antibody specific for endogenous lamin A that cannot recognize lamin C (see Figure 17C); the use of this additional antibody allowed us to further demonstrate that endogenous lamin A is sequestered into the IN aggregates formed by HSPB2. We then investigated the effects of HSPB3 on the subcellular distribution of endogenous and overexpressed lamin A/C. Concerning HSPB3, upon overexpression in HeLa

cells, neither HSPB3 wt nor R7S and R116P affected the IN distribution of lamin A/C. However, we observed some aggregates of lamin A/C adjacent to perinuclear aggregates of HSPB3 and R7S (see Figure 17D and E). Moreover, perinuclear aggregates of lamin A/C, combined with altered distribution of lamin A/C at the nuclear rim were observed in cells co-expressing HSPB2 with HSPB3 wt or R7S (see Figure 17E). Instead, in cells co-transfected with R116P and HSPB2 we found IN aggregates of R116P that were negative to lamin A/C and IN aggregates containing R116P, lamin A/C and HSPB2 (see Figure 17E). Thus, while HSPB2 sequesters lamin A/C inside IN aggregates, overexpression of HSPB3 and R7S leads to partial aggregation of lamin A/C at the perinuclear region of the cells, with no major co-localization between HSPB3 and lamin A/C aggregates. This suggests that upon overexpression of HSPB3 wt and R7S (alone or combined with HSPB2) a pool of lamin A/C is not properly internalized into the nucleus, but rather tends to accumulate in the perinuclear region of the cells. (see Figure 17E).

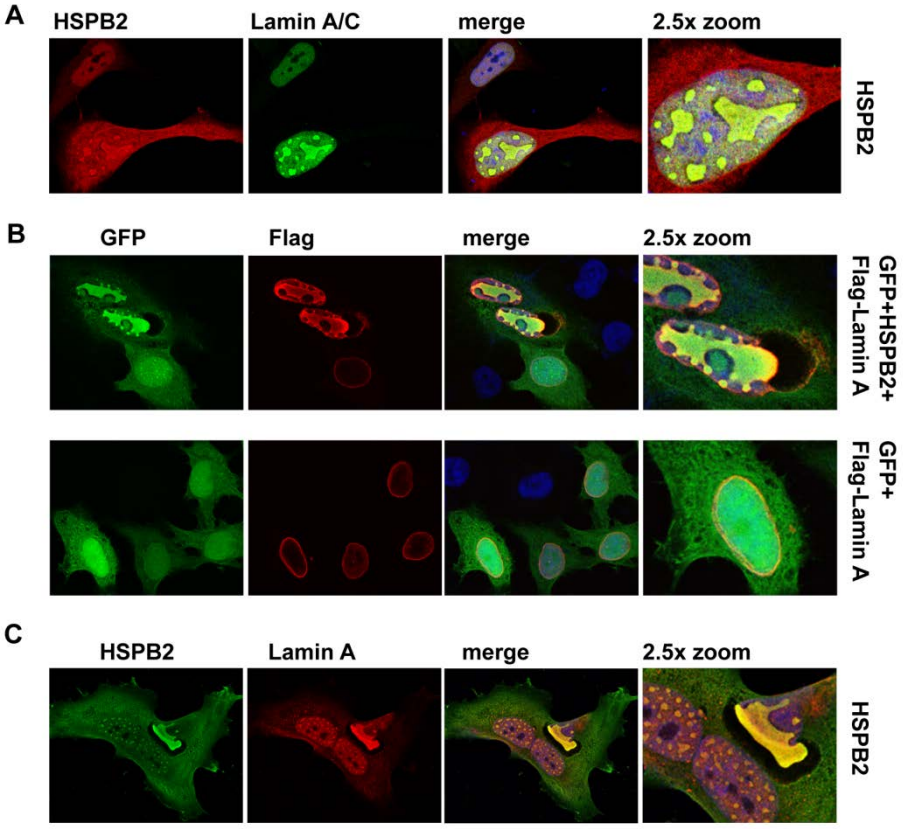

Figure 17. A: HeLa cells were transfected for 48 h with HSPB2. Cells were fixed and labelled with α-HSPB2 and α-lamin A/C. **B**: HeLa cells were transfected for 48 h with flag-lamin A and GFP alone or with HSPB2. Cells were fixed and labelled with α-flag. **C**: HeLa cells were transfected for 48 h with HSPB2. Cells were fixed and labelled with α-HSPB2 and α-lamin A.

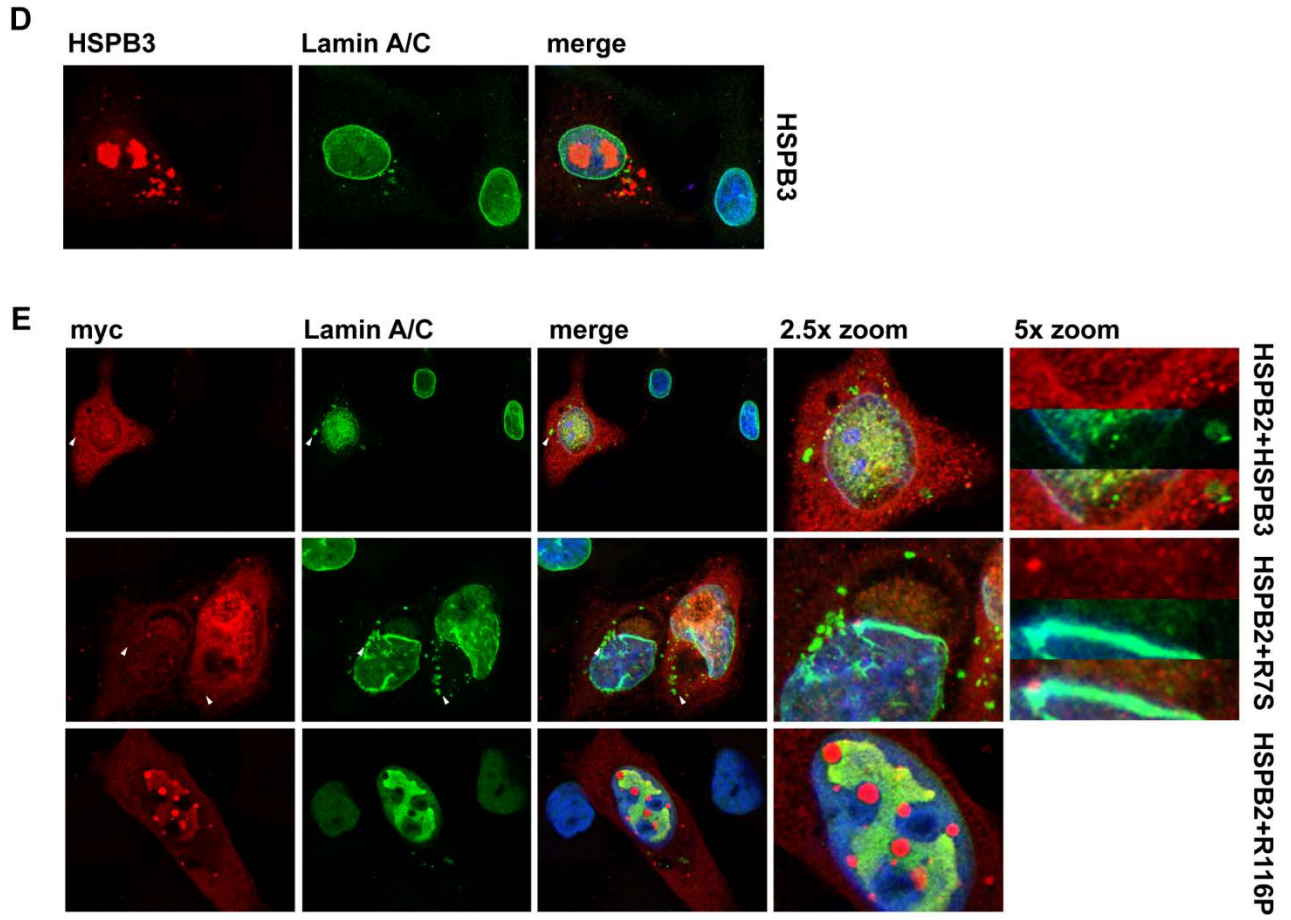

Figure 17. D: HeLa cells were transfected for 48 h with myc-HSPB3. Cells were fixed and labelled with α-HSPB3 and α-lamin A/C. **E**: HeLa cells were transfected for 48 h with HSPB2, myc-HSPB3, myc-R7S or myc-R116P in combination. Cells were fixed and labelled with α-myc and α-lamin A/C. 2.5x and 5x magnifications of the selected areas are shown.

To further study the impact of HSPB3 on lamin A/C distribution, we co-transfected HeLa cells with the cDNA encoding for myc-HSPB3 and flag-tagged lamin A. In control HeLa cells flag-lamin A is mainly distributed inside the nucleus and accumulates at the NE. Surprisingly, HSPB3 significantly decreased the IN accumulation of flag-lamin A, which instead accumulated at the perinuclear region of the cells (see Figure 18). Also the subcellular localization of HSPB3 was changed upon co-expression with flag-lamin A. In fact, in presence of flag-lamin A, HSPB3 also accumulated at the perinuclear region of the cells, where it partially aggregated. Curiously, little or no colocalization of HSPB3 with flag-lamin A was observed. Mutant R7S also led to the redistribution of flag-lamin A and HSPB3 itself into the cytosol, with their accumulation at the perinuclear region (data not shown).

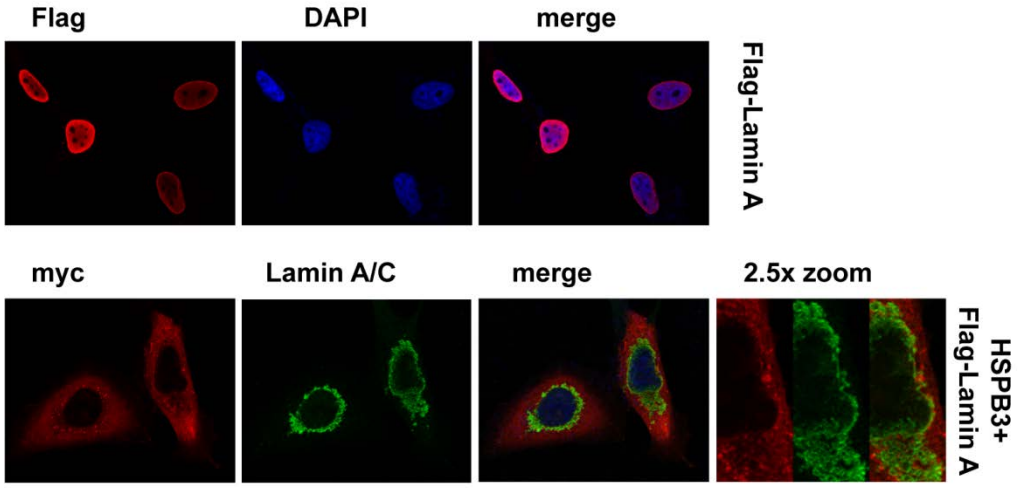

Figure 18. HeLa cells were transfected for 48 h with flag-lamin A alone or with myc-HSPB3. Cells were fixed and labelled with α-flag or α-myc and α-Lamin A/C.

On the basis of the data concerning the alteration of lamin A/C distribution caused by HSPB2/HSPB3 in HeLa cells, and, since, HSPB2 and HSPB3 also in cycling and differentiated LHCN-M2 cell, are enriched in the nucleus where they formed IN and PN aggregates, similarly to what found in HeLa cells, we evaluated whether the overexpression of HSPB2 and HSPB3 may affect lamin A/C also in cycling and differentiated myoblast

Concerning the distribution of endogenous lamin A/C, in cycling myoblasts similarly to what found in HeLa cells, the IN aggregates of HSPB2 sequestered lamin A/C, thereby altering its distribution (see Figure 19A). Instead, HSPB3 and the mutants R7S and R116P did not seem to alter the IN distribution of endogenous lamin A/C (see Figure 19C and E). Similarly to cycling human myoblasts, also in differentiated myoblasts the HSPB2 IN aggregates sequestered endogenous lamin A/C (see Figure 19B). Concerning HSPB3, it did not affect mature lamin A/C distribution, even when it formed IN aggregates (see Figure 19D). Thus, human cycling and differentiated myoblasts recapitulate mostly the tendency of HSPB2 to aggregate and sequester endogenous lamin A/C.

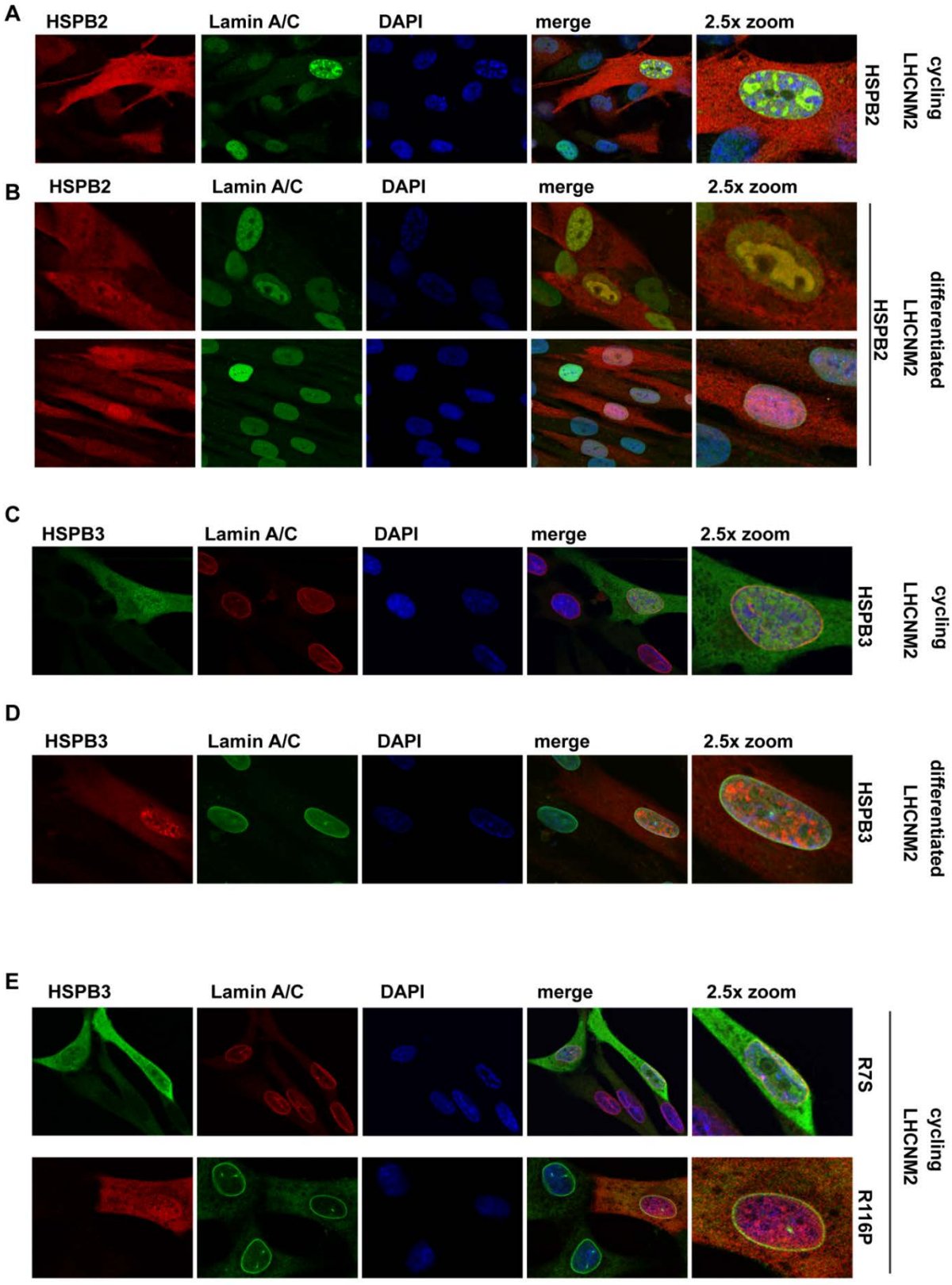

Figure 19. A, C, E: Cycling LHCN-M2 cells were infected with lentiviral vectors encoding for HSPB2, myc-HSPB3, myc-R7S and myc-R116P. Cells were fixed and labelled with α-HSPB2 or α-HSPB3 and α-lamin A/C. **B, D:** Cycling LHCN-M2 cells were infected with lentiviral vectors encoding for HSPB2, and myc-HSPB3, and left to differentiate for 48 h. Cells were fixed and labelled with α-HSPB2 or α-HSPB3 and α-lamin A/C.

HSPB2 and HSPB3 (wt and mutants) affect prelamin A processing and subcellular distribution in HeLa cells

The flag-lamin A cDNA employed in this study encodes for a precursor of lamin A, prelamin A. Prelamin A undergoes sequential post-translational modifications to generate mature lamin A that include also farnesylation (Sinensky et al. 1994). In most cell types, such as e.g. HeLa cells, the levels of prelamin A are undetectable and prelamin A accumulates only after treatment of the cells with specific farnesyltransferase inhibitors (FTI), which inhibits the addition of the farnesyl group to the prelamin A (the first processing step), or with Mevinolin (lovastatin), which causes an accumulation of full-length prelamin A.

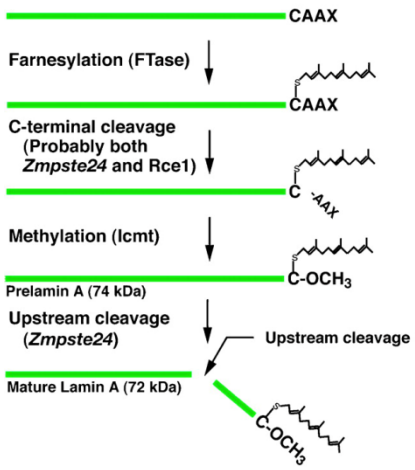

Figure 20. Schematic representation of the post translational modifications that prelamin A undergoes to produce mature lamin A.

To detect prelamin A both in untransfected HeLa cells or upon overexpression of flag-prelamin A (referred to as flag-lamin A), we used a specific antibody that recognizes both prelamin A and farnesylated prelamin A. We confirm here that HeLa cells have undetectable levels of prelamin A, even upon overexpression of flag-prelamin A, unless the cells are treated overnight with FTI or with Mevinolin. Upon treatment in HeLa cells with both drugs, we observed an accumulation of prelamin A at the nuclear rim and inside the nucleus (as expected)(see Figure 21A).To distinguish between flag-tag prelamin A, flag-tag mature lamin A and endogenous prelamin A we used an antibody specific for prelamin A, which recognizes both endogenous prelamin A and the flag-tag protein. Thus we transfected HeLa cells with HSPB2 myc-HSPB3 and HSPB1 (used as control) and we investigated their effect on endogenous prelamin A. Both HSPB2 and HSPB3 caused an accumulation of endogenous

prelamin A similar to the one observed in HeLa cells treated with FTI (see Figure 21A and B). Moreover, HSPB2 sequestered endogenous prelamin A into its typical IN aggregates. Instead, in cells overexpressing HSPB3 we observed accumulation of prelamin A both inside the nucleus and at the perinuclear region of the cells. Overexpression of HSPB1 had no effect on prelamin A distribution (see Figure 21C), thereby further supporting the specificity of the effects observed upon exogenous expression of HSPB2 or HSPB3.

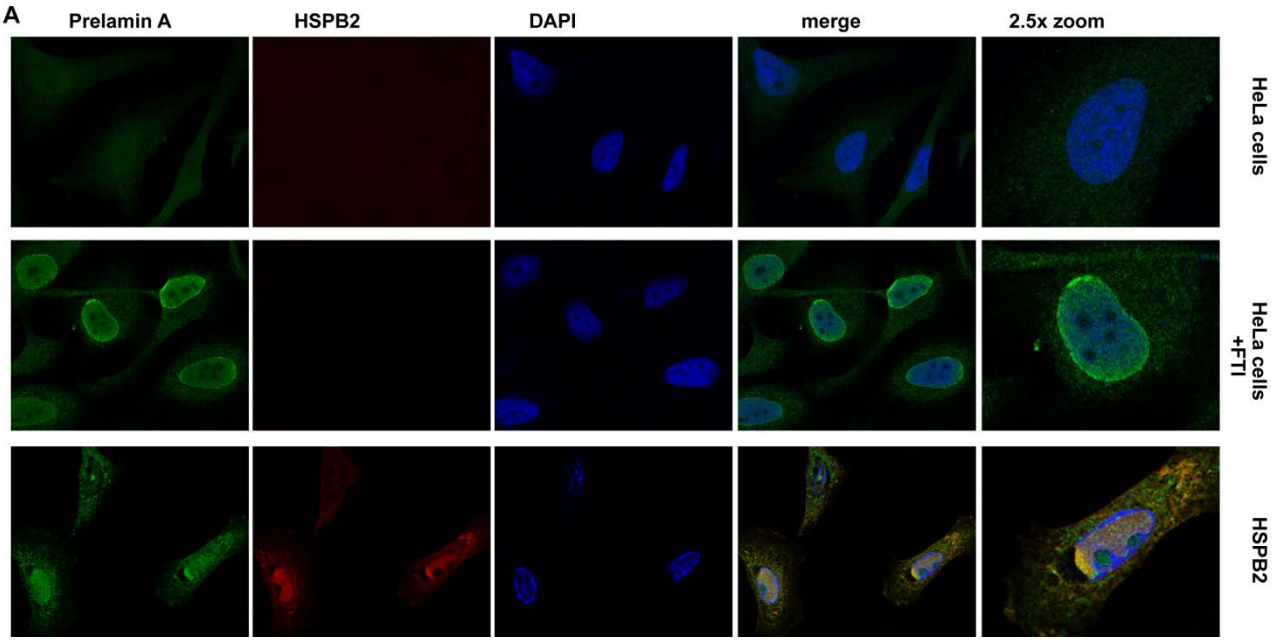

Figure 21. A: HeLa cells were transfected for 48 h with HSPB2. Where indicated cells left untreated or treated o/n with FTI. Cells were fixed and labelled with α-HSPB2 and α-prelamin A.

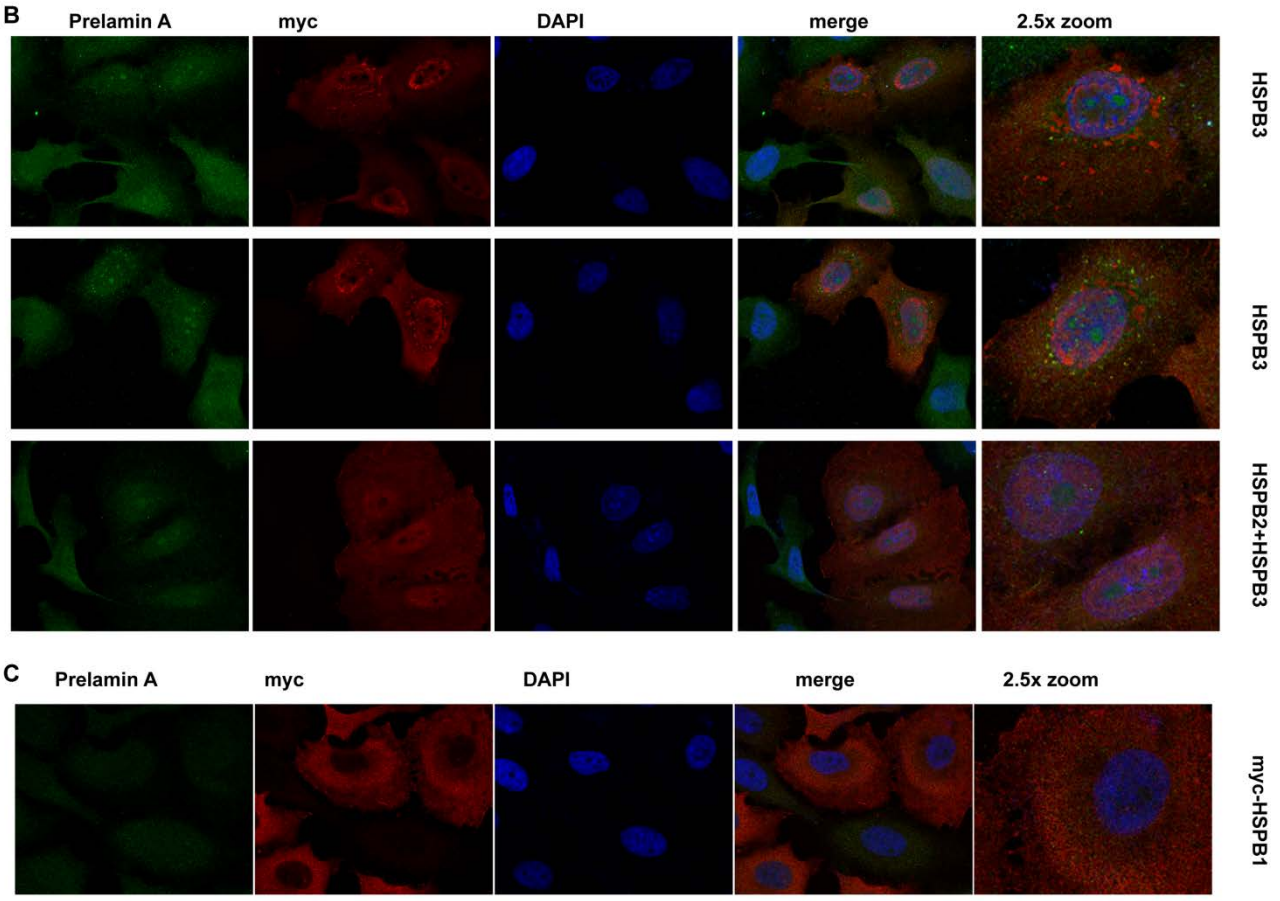

Figure 21. B: HeLa cells were transfected for 48 h with myc-HSPB3 alone or in combination with HSPB2; as control, cells were transfected with myc-HSPB1 (**C**). Cells were fixed and labelled with α-myc and α-prelamin A to study the localization and distribution of both endogenous prelamin A and the overexpressed HSPBs.

Then we co-transfected the cDNA, encoding for flag-tagged lamin A (in order to increase the starting level of prelamin A) together with HSPB2. Overexpression of HSPB2 with flag-prelamin A caused a redistribution of prelamin A; in particular, we observed both accumulation of prelamin A at the perinuclear region of the cells and sequestration of prelamin A by HSPB2 into IN aggregates (see Figure 22B). Concerning HSPB3, its co-expression with flag-prelamin A resulted in the accumulation of prelamin A mainly at the perinuclear region of the cells, although some IN aggregation of prelamin A was also found (see Figure 22C). Similarly to mature flag-lamin A, also prelamin A that accumulated in the perinuclear region of the cell did not co-localize with HSPB3 aggregates (see Figure 22C). Combined these results support that when expressed alone, HSPB2 and HSPB3 accumulate in the IN and PN regions of the cells with significant consequences on the distribution of both prelamin A and mature lamin A. In line, co-expression of HSPB2 and HSPB3 with flag-prelamin A significantly decreased the mislocalization and aggregation of prelamin A (see

Figure 22D). Such milder effect on prelamin A distribution is probably due to the fact that, upon co-transfection, HSPB2 and HSPB3 would mainly interact together, thereby co-stabilizing each other's.

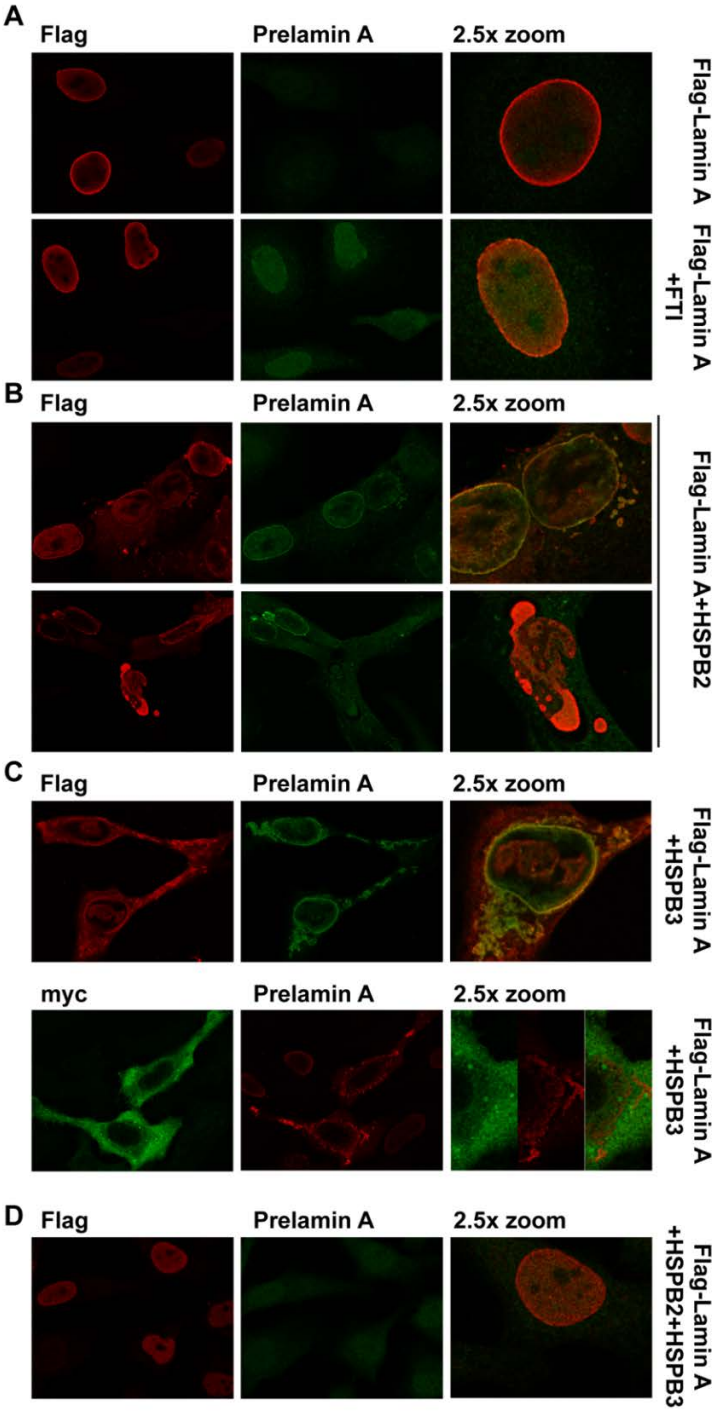

Figure 22. A: HeLa cells were transfected for 48 h with flag-lamin A and left untreated or, where indicated, treated o/n with FTI. Cells were transfected for 48 h with flag-lamin A with HSPB2 (**B**), or myc-HSPB3 (**C**) or the complex (**D**). Cells were fixed and labelled with α-flag and α-prelamin A and where indicated with α-myc to study the localization/distribution of both proteins.

Besides the mislocalization of prelamin A, our immunofluorescence results strongly suggested that the total levels of prelamin A were higher in HeLa cells overexpressing HSPB2 and, especially, HSPB3, an aspect that we verified by western blot. As previously anticipated the levels of endogenous prelamin A are undetectable in HeLa cells, unless its maturation is inhibited using e.g. FTI or mevinolin, which both cause a mild accumulation of prelamin A (see Figure 23, lanes 1-3). A similar scenario occurs also in HeLa cells that are transfected with the cDNAs encoding for GFP (used as control) and flag-prelamin A (see Figure 23, lanes 4-6). Co-transfection of flag-prelamin A with HSPB2 mimicked the effect of FTI or mevinolin and led to accumulation of prelamin A, while also stabilizing mature flag-lamin A (see Figure 23, lane 7). HSPB3 has an even stronger effect and caused a significant accumulation of both mature flag-lamin A and unprocessed/farnesylated prelamin A (see Figure 23, lane 8). Co-expression of HSPB2 and HSPB3 with flag-lamin A still led to a significant accumulation of mature flag-lamin A, as compared to GFP; however, the effect on prelamin A was much milder as compared to the effect exerted by HSPB3 alone. As additional control, we co-expressed flag-lamin A with myc-tagged HSPB1, which does not accumulate in the nucleus of HeLa cells and does not affect the distribution of lamin A/C or prelamin A (see Figure 21C). The levels of flag mature lamin A were similar between cells co-expressing flag-lamin A and myc-HSPB1, HSPB2 or myc-HSPB3; however, although expressed at much higher levels as compared to myc-HSPB3, myc-HSPB1 had no effect on prelamin A maturation, since prelamin A was undetectable by western blot (see Figure 23, compare lane 10 with lane 8). This observation excludes that the accumulation of prelamin A by HSPB2 and, in particular, by HSPB3 would be a consequence of higher expression levels of flag-lamin A and points to specific functions of HSPB2 and HSPB3 on prelamin A and mature lamin A turnover and distribution. Consistent with our immunofluorescence results, co-expression of HSPB2, myc-HSPB3 and flag-prelamin A only mildly affected prelamin A processing (see Figure 23, compare lane 7, 8 and 9). Thus, the increase in the total levels of prelamin A correlates with its accumulation in the perinuclear region of the cells, which mainly occurs in cells overexpressing wt HSPB3.

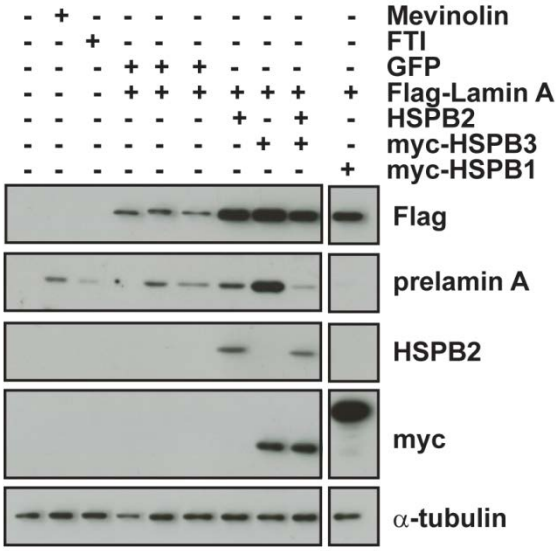

Figure 23. HeLa cells were transfected for 48 h with flag-lamin A and GFP (used as control), HSPB2, myc-HSPB3, alone or in combination. As additional control, cells were transfected with flag-lamin A and myc-HSPB1. To induce the accumulation of prelamin A, where indicated (+) cells were treated with mevinolin or FTI. Total protein extract were prepared 48 h post-transfection and samples were processed for western blot using flag, prelamin A, HSPB2 and myc antibodies. α-tubulin was used as loading control.

Considering that HSPB2 and HSPB3 affect in HeLa cells the subcellular localization of prelamin A, we next studied the effects of HSPB2 and HSPB3 on endogenous prelamin A in cycling myoblasts. Prelamin A participates in the initiation of the myogenic program and both changes in its expression levels and subcellular localization are important for this process (Capanni et al. 2008). Prelamin A is expressed at low levels in proliferating myoblasts and its expression progressively decreases during myoblasts differentiation (Capanni et al. 2008). In line with Capanni's findings, we found very low levels of prelamin A in human cycling myoblasts (see Figure 24A upper panel), as well as in LHCN-M2 cells infected with lentiviral particles expressing GFP, used as control to exclude that the infection per se alters prelamin A distribution (see Figure 24C). Thus, we treated the cells with the inhibitors mevinolin and/or FTI that led, as expected, to an accumulation of prelamin A inside the nucleus (see Figure 24A). Intriguingly, cycling LHCN-M2 cells overexpressing HSPB2 showed IN accumulations of prelamin A; round IN foci absent in control cells were decorating the nuclei of HSPB2 infected cells. When IN aggregates of HSPB2 were present, these sequestered prelamin A (see Figure 24A), similarly to what found in HeLa cells. Concerning HSPB3, it also caused the IN accumulation of prelamin A in cycling human myoblasts, sequestering into its IN aggregates (see Figure 24B). Concerning R7S HSPB3, it also causes the IN accumulation of prelamin A, even when R7S does not form PN aggregates and supporting that accumulation of prelamin A

is independent on the presence of R7S aggregates. When R7S formed IN aggregates, these sequestered and co-localized with endogenous prelamin A.

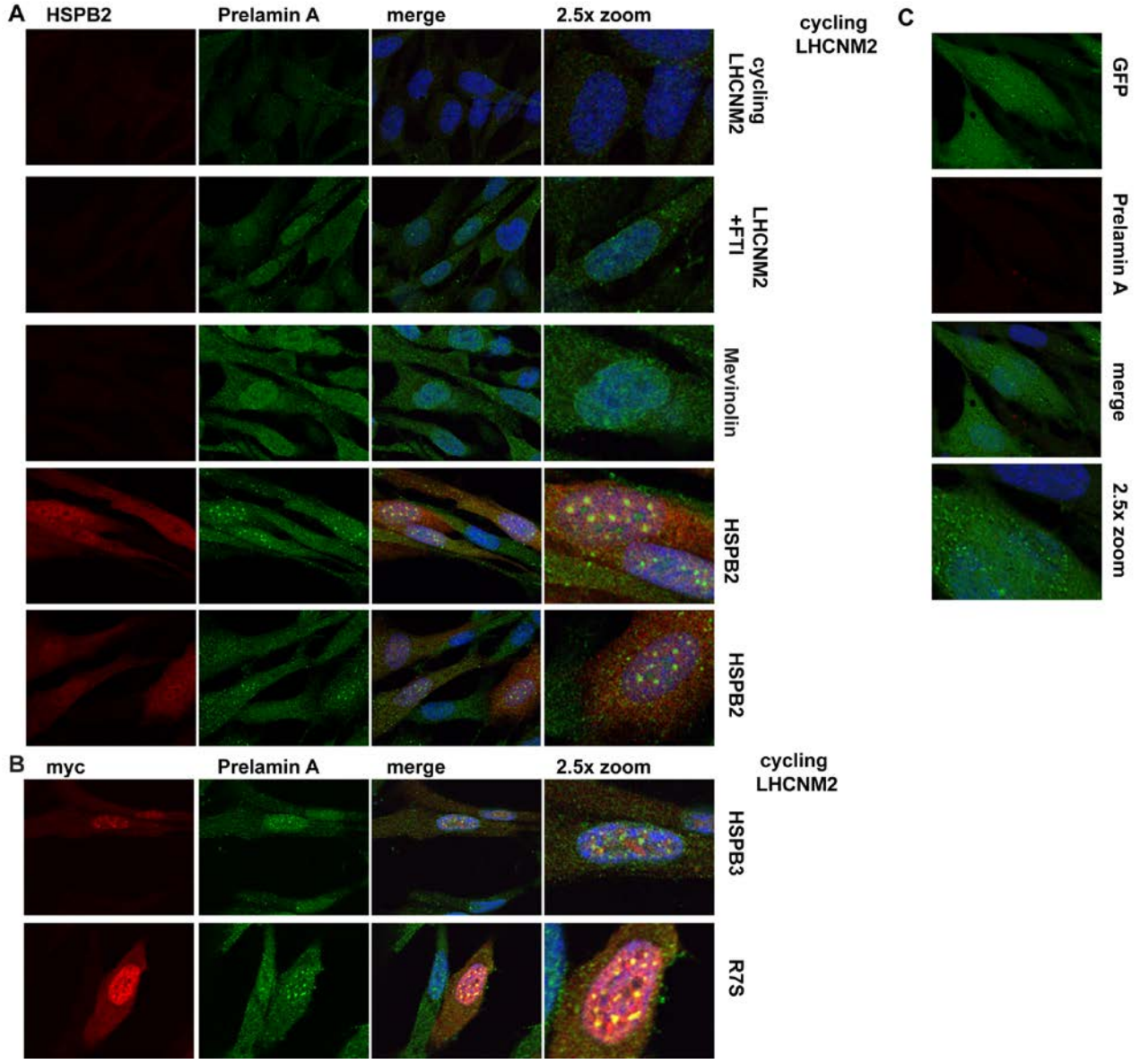

Figure 24. A-C: Cycling LHCN-M2 cells were infected with lentiviral vectors encoding for GFP (**C**), HSPB2 (**A**) and myc-HSPB3 or myc-R7S (**B**). Cells were left untreated or treated with FTI and mevinolin. Cells were fixed 48 h post-infection and labelled for α-HSPB2, α-myc and α-prelamin A.

Next, we investigated whether the overexpression of HSPB2 and HSPB3, affects the distribution of prelamin A also in differentiated human myoblasts. We found that also in differentiated myoblasts (ca. 5 days), both HSPB2 and HSPB3 cause the accumulation of prelamin A and affect its localization as compared to control cells (mock-infected and GFP-infected differentiated LHCN-M2 cells) (see Figure 25A and B). Also when HSPB2/HSPB3 are

expressed at low levels, showing a diffuse staining, they could alter the localization of prelamin A, which accumulates into IN foci (see Figure 25C and D). Combined these results demonstrate that high levels of HSPB2 or HSPB3 result in a redistribution of prelamin A both in cycling and differentiated myoblasts, independent on whether HSPB2 and HSPB3 form themselves visible aggregates.

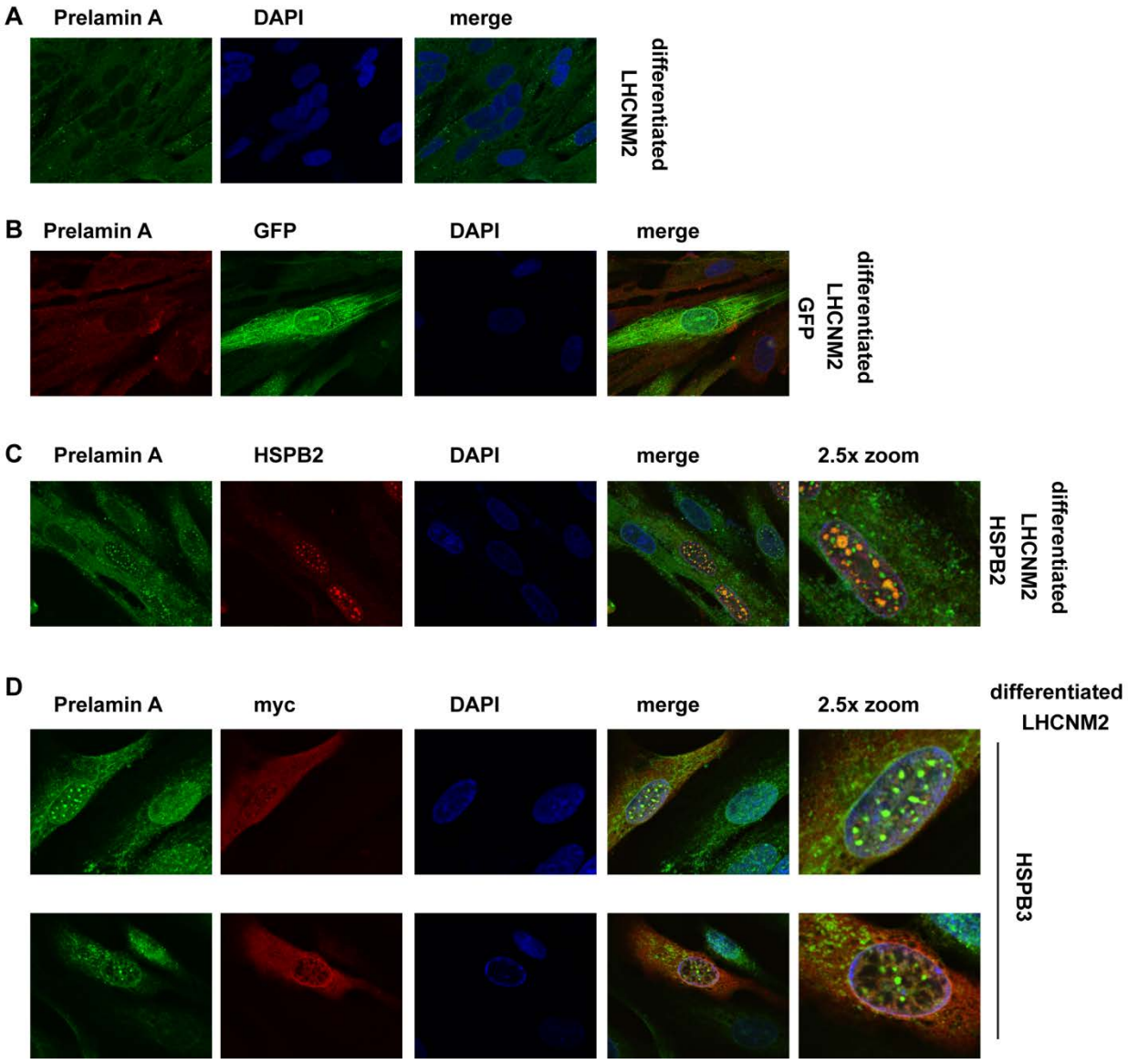

Figure 25. A-D: Cycling LHCN-M2 were mock-infected (**A**) or infected with GFP (**B**) (both used as controls), or with lentiviral vectors encoding for HSPB2 (**C**) or myc-HSPB3 (**D**). 24 h post infection the differentiation process was induced. 5 days after differentiation, the cells were fixed and labelled for α-HSPB2, α-myc and α-prelamin A.

HSPB2 binds to lamin A and HSPB3 negatively regulates such interaction

The immunofluorescence data support that HSPB2 either sequesters indirectly lamin A/C (and prelamin A) into its IN aggregates or directly binds to it. We thus tested by co-immunoprecipitation whether HSPB2 directly interacts with lamin A.

Interestingly, when overexpressed alone HSPB2 binds, although weakly, to lamin A (see Figure 26A). Instead, HSPB3 did not interact with lamin A and when co-expressed with HSPB2, it strongly competed with lamin A for binding to HSPB2 (see Figure 26A). Consistent with our co-immunoprecipitation results, HSPB3 did not colocalize with lamin A/C, even when forming large IN aggregates (see Figure 17D). Thus, co-expression of HSPB3 (wt or R7S) with HSPB2 significantly decreases HSPB2 IN aggregation (see Figure 9C and E), thereby avoiding that HSPB2 interacts with and sequesters lamin A/C into large IN aggregates (see Figure 26B and 17E). As expected, co-expression of HSPB2 with R116P, which does not bind to HSPB2, still leads to IN co-aggregation of lamin A/C with HSPB2. Consistently, cells expressing HSPB2 and R116P still show IN aggregates of HSPB2 that sequester lamin A/C (see Figure 17E). Combined these observations support that HSPB3 (and the R7S, but not the R116P mutant) negatively regulates the interaction of HSPB2 with lamin A/C. Concerning prelamin A, we could not detect any direct association of HSPB2 or HSPB3 with prelamin A (data not shown).

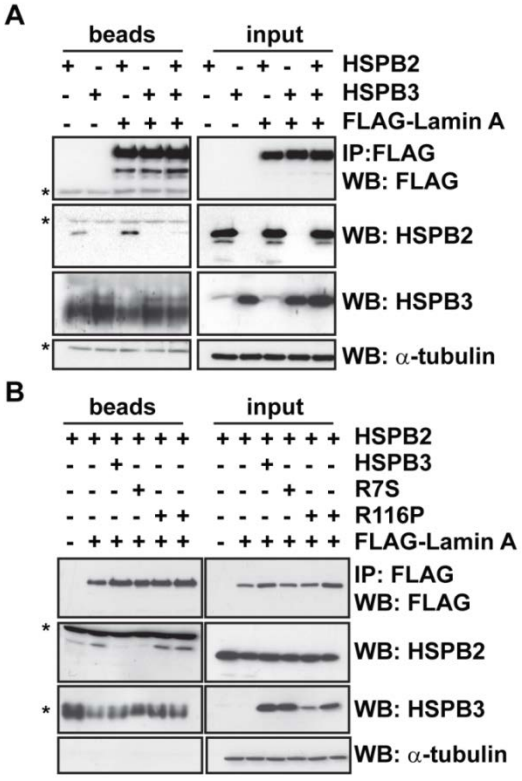

Figure 26. A-B: Hek293T cells were transfected for 24 h with flag-tagged lamin A, HSPB2, HSPB3 wt and mutants (alone or combined). Cell lysates were subjected to CO-IP, using FLAG coated-beads; myc and flag levels were determined by western blot on both beads and input fractions. Non-specific bands are marked (*).

In light of the direct binding of lamin A to HSPB2, we asked whether its IN aggregation is an intrinsic property of HSPB2 or whether it is enhanced by or depends on the presence of lamin A/C. We thus overexpressed HSPB2 in mouse embryonic fibroblasts from lamin A/C wt mice (*Lmna*$^{+/+}$), lamin A/C knockout mice (*Lmna*$^{-/-}$) or mice expressing only lamin C (LCO) (see Figure 27B). Figure 27A shows that the absence of lamin A (LCO) and lamin A/C (*Lmna*$^{-/-}$) significantly decreases, but does not abrogate, IN aggregation of HSPB2, as showed in the quantification of HSPB2 aggregation. This result supports that HSPB2 IN aggregation is an intrinsic property of HSPB2 itself that is accelerated by the interaction with or sequestration of lamin A/C.

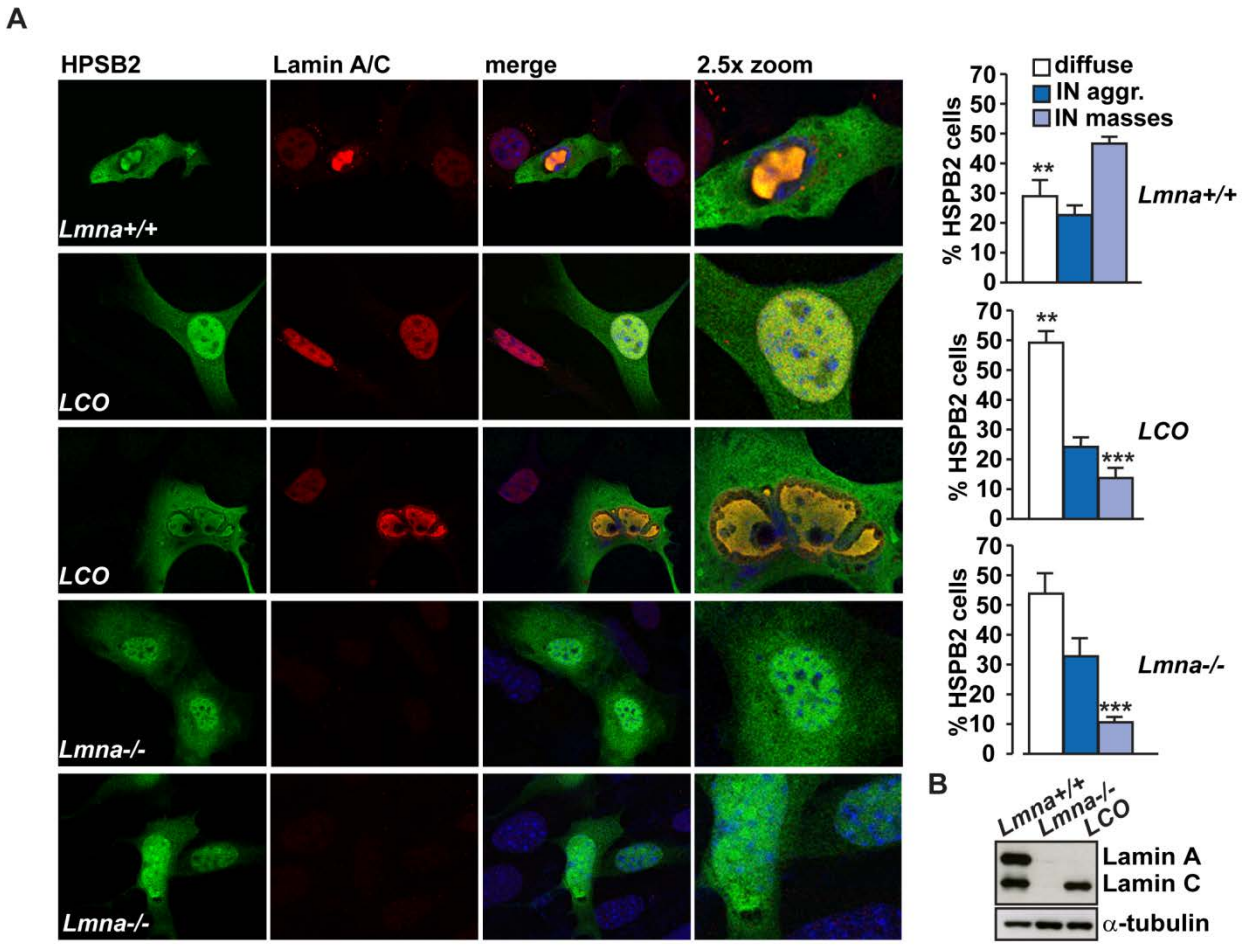

Figure 27. A-B: *Lmna*$^{+/+}$, *Lmna*$^{-/-}$ and LCO MEFs were transfected for 48 h with HSPB2. Cells were fixed and labelled with α-HSPB2 and α-Lamin A/C (**A**) or processed for western blot (**B**). Quantification of HSPB2's IN aggregation is reported. Error bar, S.E.M.

HSPB2 and HSPB3 affect the recruitment of emerin and SUN2 at the nuclear envelope.

It has been demonstrated that lamin A/C regulates the proper localization of integral proteins of the INM such ad e.g. emerin or SUN2. In fact, in lamin A/C knockout mice, emerin is located mainly in the ER in most tissues (Sullivan et al. 1999). Moreover, alterations of lamin A expression cause mislocalize emerin to the ER, where it accumulates in granular structures (Vaughan et al. 2001). In light of our results showing that HSPB2 dramatically changes lamin A/C distribution, we asked whether HSPB2 (and HSPB3, wt and mutants) could also affect the localization of integral proteins of the NE. For this purpose, we investigated the subcellular localization of emerin and SUN2. Interestingly, HeLa cells expressing HSPB2 and characterized by the presence of large IN aggregates of HSPB2 extruding from the nucleus showed a significantly altered distribution of emerin. Emerin did not colocalize with HSPB2, but rather aggregated in the PN region (see Figure 28A). Similarly, emerin distribution was affected in cells overexpressing HSPB3, R7S or R116P (see Figure 28B).

The distribution of SUN2 was also dramatically affected by the presence of the aggregates typical of HSPB2 or R7S, expressed alone or together, with an almost complete loss of signal, as compared to untrasfected cells (see Figure 28C and D). Collectively these data demonstrate that upon overexpression in HeLa cells, HSPB2 and HSPB3 (wt and mutants) alter the distribution of endogenous lamin A/C and also affect the localization at the NE of emerin and SUN2. Lamin A is not only required for proper localization of emerin and SUN2 at the INM, but also for the maintenance of NE integrity (Sullivan et al. 1999). Combined with the formation of nuclear bleb and PN aggregates, our results strongly suggest that the integrity of the NE can be partially disrupted by high levels of HSPB2 and HSPB3.

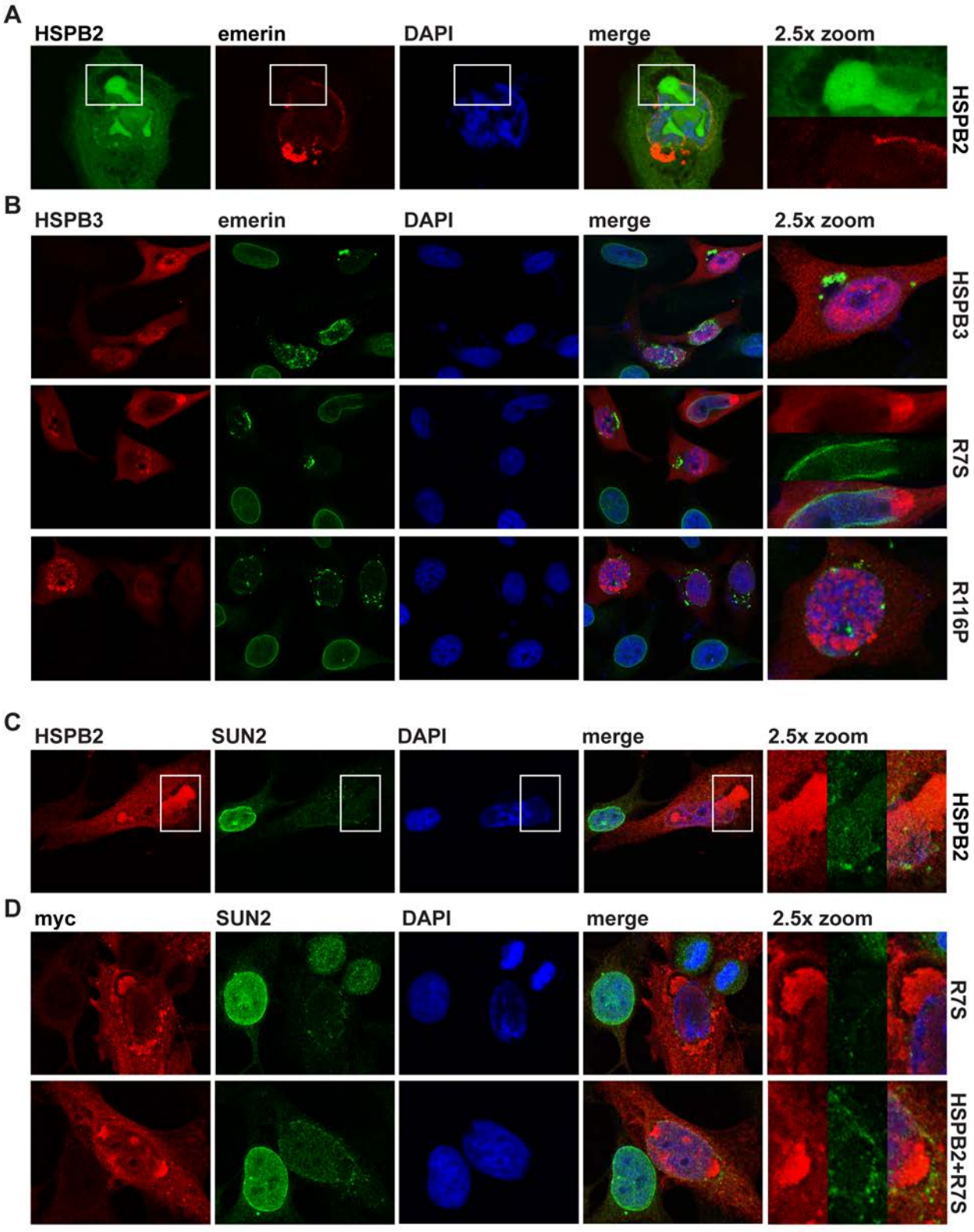

Figure 28. A-D: HeLa cells were transfected for 48 h with HSPB2, myc-HSPB3, myc-R7S, myc-R116P, alone or in combination. Cells were fixed and labelled for α-emerin and α-SUN2 to study the localization/distribution of these two integral proteins of NE in cells overexpressing the indicated HSPBs. 2.5x magnification of the selected area is reported.

HSPB2 and HSPB3 (wt and mutants) affect lamin B1 distribution

To further study the effect of HSPB2 and HSPB3 on the integrity and morphology of the nuclei, we subsequently analysed the distribution of lamin B1 in presence of IN/PN aggregates. Thus, we overexpressed, in HeLa cells, the GFP protein alone or with HSPB5, or HSPB5 alone (used as controls). Overexpression of GFP alone or combined with HSPB5, as well as overexpression of HSPB5 alone do not affect the distribution of lamin B1 (see Figure 29A and B). In contrast, co-transfection of HSPB2 with GFP slightly altered the distribution of lamin B1 (see Figure 29A lower panel). In particular, the lamin B1 meshwork appeared truncated in concomitance with HSPB2 masses extruding from the nucleus (see Figure 29 A lower panel and C).

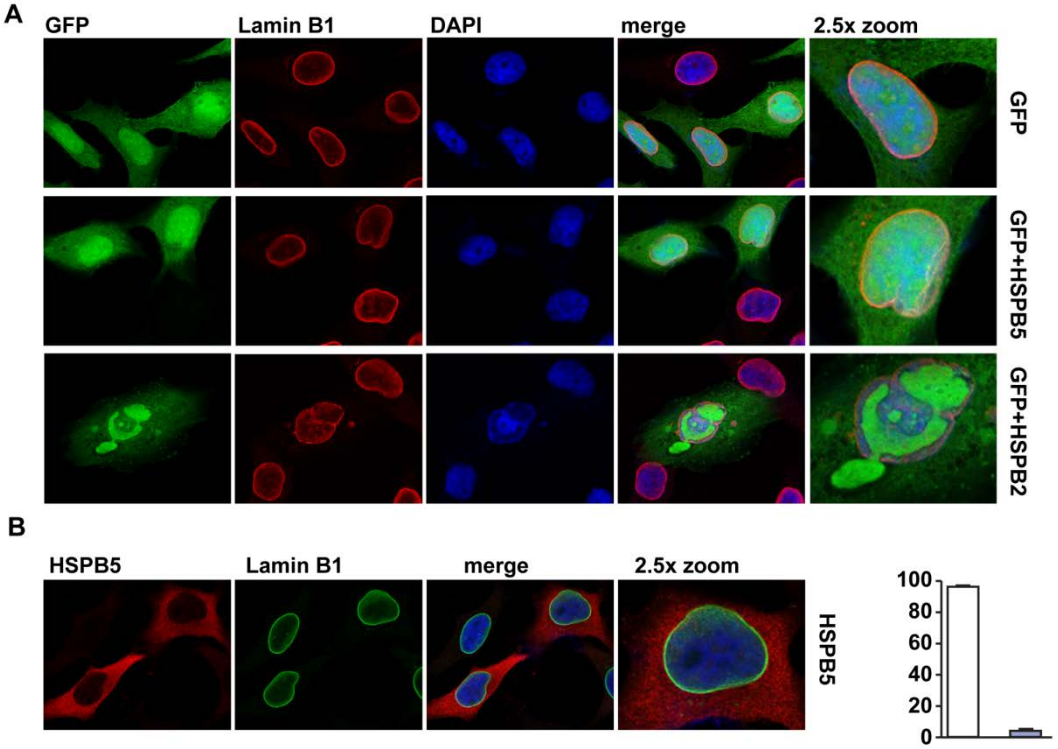

Figure 29. A: HeLa cells were transfected for 48 h with a vector encoding for GFP alone or in combination with HSPB5 and HSPB2. Cells were fixed and labelled with α-lamin B1. **B:** HeLa cells were transfected for 48 h with vectors encoding for HSPB5. Cells were fixed and labelled with α-HSPB5 and α-lamin B1.

Similarly, the integrity of lamin B1 meshwork was affected by the presence of HSPB3 PN aggregates, a phenotype that was significantly enhanced by the R7S mutant (see Figure 29D). R116P mainly formed IN aggregates that generally did not affect lamin B1 meshwork integrity, unless these aggregates were adjacent to it (which was a very rare event; see Figure

29D). Thus, when transfected R116P alone significantly increased the % of cells with intact lamin B1, as compared to both HSPB3 and R7S (see Figure 29E, where the lamin B1 was quantified and classified as: intact, truncated and/or damaged lamin B1). Concerning the effects of the complex on lamin B1 distribution, we observed an additive effect on lamin B1 integrity. In fact, although stabilizing each other's, HSPB2 and HSPB3 (wt or R7S) still significantly affected lamin B1 integrity.

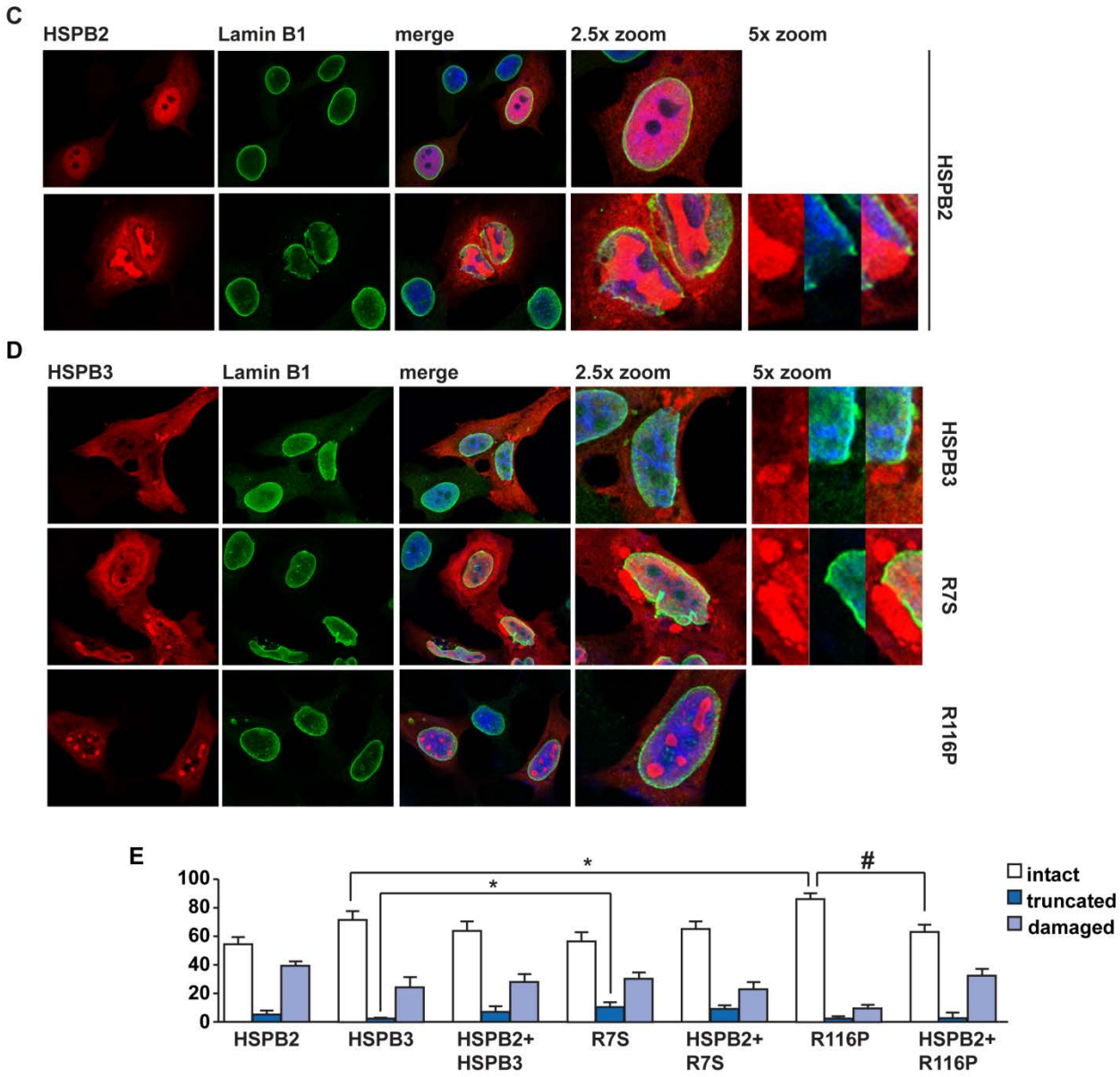

Figure 29. C, D: HeLa cells were transfected for 48 h with vectors encoding for HSPB2, myc-HSPB3, myc-R7S or myc-R116P alone or combined with HSPB2 (**E**). Cells were fixed and labelled with α-HSPB2 α-HSPB3 and α-lamin B1. 2.5x and 5x magnifications of the selected areas with nuclear envelope damage are shown. **E**: Quantitation of lamin B1 is reported. Error bar, S.E.M.

Next, we investigated whether/how HSPB2 and HSPB3 affect the distribution of lamin B1 in cycling myoblasts. We infected LHCN-M2 with lentiviral vectors encoding for HSPB2 and myc-HSPB3. Figure 30 shows the most characteristic phenotype of HSPB2 and R7S. Large IN HSPB2 masses extruding into the cytoplasm were not present in LHCN-M2 cells and, in line with the observation made in HeLa cells, also in cycling myoblasts HSPB2 did not co-aggregate with lamin B1 (see Figure 30A). A mild effect of R7S on lamin B1 was observed in presence of R7S PN aggregates (see Figure 30B).

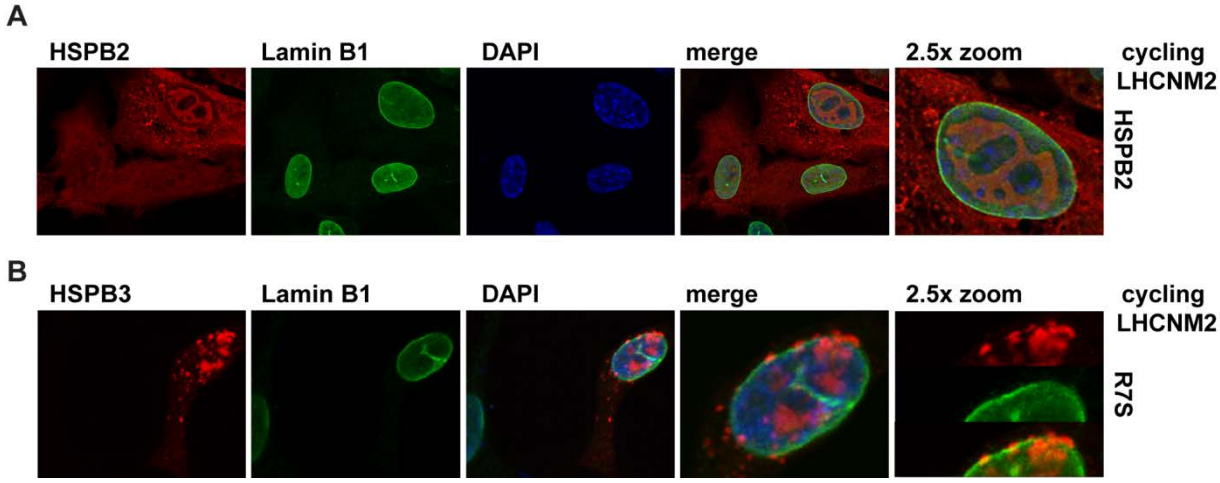

Figure 30. A, B: Cycling LHCN-M2 cells were infected with lentiviral vector encoding for HSPB2 and myc-R7S. Cells were fixed and labelled with α-HSPB2 or α-HSPB3 and α-lamin B1.

In summary, our results demonstrate that when expressed at high levels HSPB2 and HSPB3 accumulate in the nucleus and at the perinuclear region of the cells, where they affect the distribution of lamins and alter the integrity of the NE, with a predominant effect on prelamin A and mature lamin A/C and milder effects on lamin B1.

Overexpression of HSPB2 and HSPB3 affects nuclear functions in mammalian cells

Lamins A/C interacts with components of the RNA polymerase II (pol II) transcriptional complex and affects spatial organization of RNA splicing factors (Kumaran et al. 2002; Shaklai et al. 2007; Spann et al. 2002). Moreover, overexpression of lamin A/C and silencing of lamin B1 significantly inhibit pol II-mediated RNA transcription in HeLa cells, causing speckles round-up (Kumaran and Spector 2008; Shimi et al. 2008; Tang et al. 2008). Nuclear speckles are dynamic compartments involved in the storage of splicing factors that reorganize into spherical and larger foci when pol II is inhibited. Thus the analysis of speckle shape and number can indicate whether RNA transcription mediated by the RNA pol II is affected.

We observed that HSPB2 and HSPB3 alter the maturation of prelamin A and lead to an accumulation of both prelamin A and mature lamin A; moreover, HSPB2 sequesters endogenous lamin A/C inside large IN aggregates, affecting its nucleoplasmic distribution. In light of these results and considering that overexpression of lamin A is sufficient to cause speckle round-up and inhibit RNA pol II mediated transcription, we asked whether the overexpression of HSPB2 and HSPB3 could also affect, indirectly, speckle dynamics. First we analysed the effect of HSPB2 and HSPB3 (wt and mutants) on nuclear speckles using a mouse antibody against SC35, a well-known marker of speckles (Spector and Lamond, 2011). The antibody against HSPB2 used in this study is of mouse origin, like the antibody against SC35. Thus, considering that when co-expressed with GFP, HSPB2 leads to the formation of IN aggregates that sequester GFP, we co-transfected cells with GFP and HSPB2 and we monitored in the green-positive cells the shape and number of speckles labelled with the anti-SC35 antibody. Expression of GFP alone was used as control. As additional control we also used HSPB1 (see Figure 31C) and the co-expression of GFP with HSPB5. In control cells speckles look like irregularly shaped IN foci; however, upon treatment of the cells with actinomycin D (actD), an inhibitor of pol II, they become round and larger in size (Jao and Salic 2008). Speckles appeared as irregularly shaped IN foci in resting HeLa cells, as well as in cells overexpressing HSPB1, GFP or GFP and HSPB5, all used as controls (see Figure 31A and C).

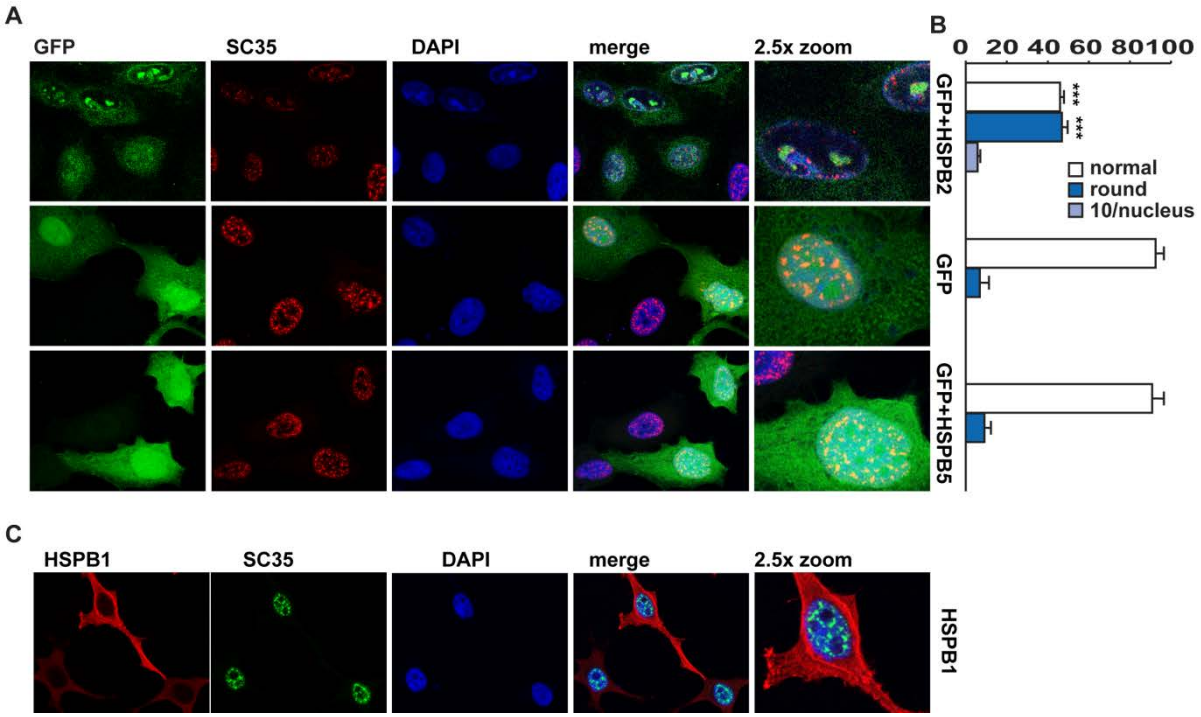

Figure 31. A: HeLa cells were transfected for 48 h with a vector encoding for GFP alone or combined with HSPB2 or HSPB5, used as control. **B:** Quantification of speckle shape/number from **A**. Error bar, S.E.M. **C:** HeLa cells were transfected for 48 h with a vector encoding for HSPB1. 2.5x magnifications of the selected areas are shown.

When HeLa cells were treated with actD, all speckles became round and larger in size (see Figure 32A). Overexpression of HSPB2 and HSPB3 both significantly increased the % of cells with round speckles (see Figure 31A upper panel and 32A). Speckle round-up was also strongly induced by overexpression of the mutants R7S or R116P. We quantified the following phenotypes: cells with normal/irregularly shaped speckles; cells with round speckles (more than 10 speckles/cell); cells with few and large speckles (less than 10 speckles/cell). Although in HeLa cells the effect of HSPB3 was already very severe, with nearly 80% of the cells showing altered speckle morphology/number, the R7S mutant significantly decreased the % of cells with normal, irregularly shaped speckles (see Figure 32B). Co-expression of HSPB3 with HSPB2 lead to an additive effect and further exacerbated the alteration of speckle morphology/number, as compared to the effect of the single proteins (see Figure 32B). Expression of R7S, alone or with HSPB2 led to a dramatic redistribution of speckles, which were found within the PN aggregate typical of R7S expressing cells (see Figure 32A). Instead, co-expression of R116P with HSPB2 had no additive effect on speckle morphology as compared to R116P alone and consistent with the lack of binding of R116P to HSPB2 (see Figure 32B). Importantly, round-up speckles were found also in cells with a diffuse HSPB2 or HSPB3 IN staining, as well as in cells with low expression levels of these proteins. Combined

these result suggest that the alteration of speckle morphology and number is not a mere consequence of HSPB2 or HSPB3 -wt and mutants- IN aggregation, but rather it represents an early event in response to accumulation of HSPB2 and HSPB3.

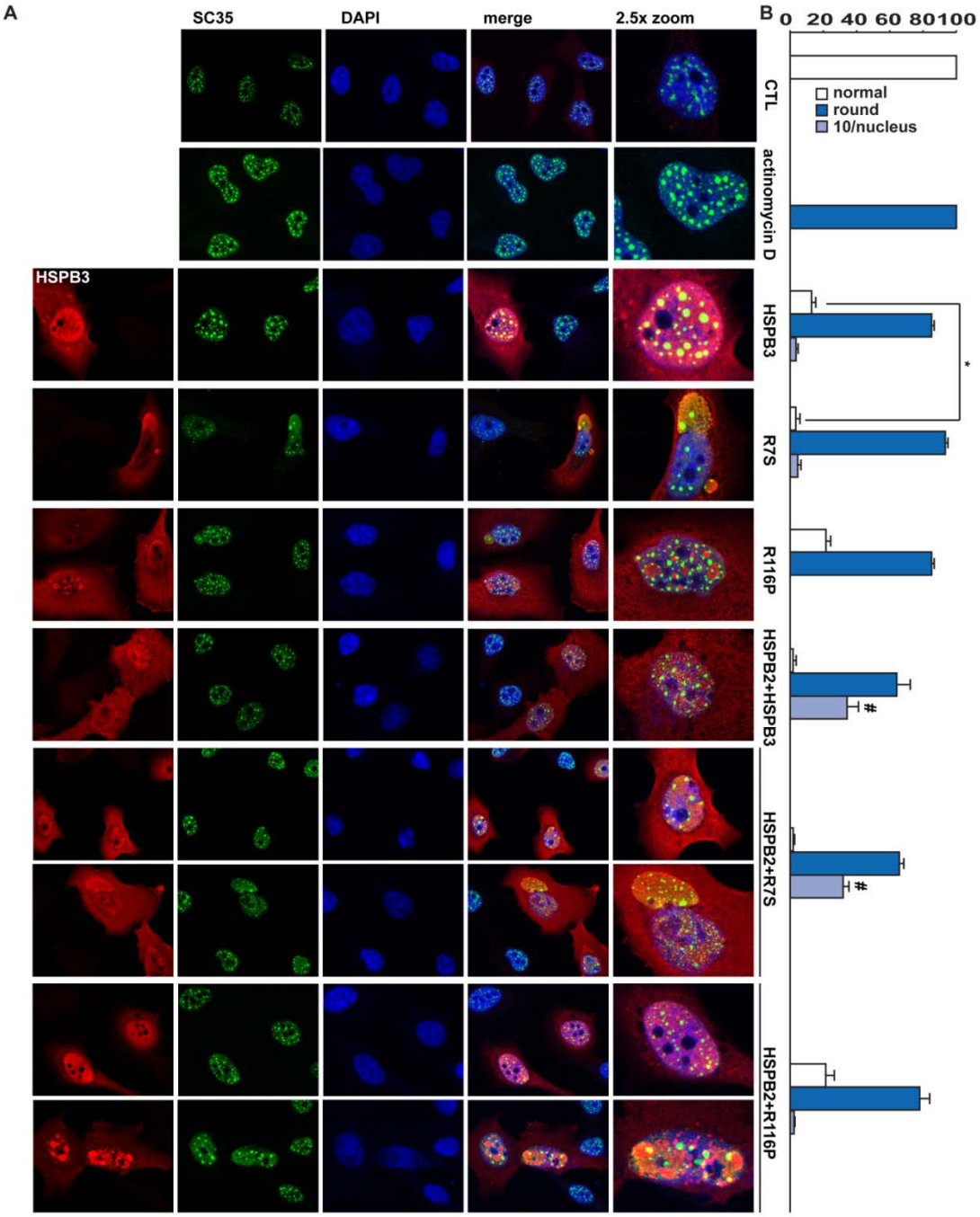

Figure 32. A: HeLa cells were transfected for 48 h with empty vector (CTL) and/or vectors encoding for myc-HSPB3, myc-R7S or myc-R116P alone or combined with HSPB2. Cells were treated with actinomycin D where indicated, fixed and labelled with α-SC35 and, where indicated, for α-HSPB3. 2.5x magnifications of the selected areas are shown. **B:** Quantitation of speckle shape/number from **A**. Error bar, S.E.M.

We then investigated whether overexpression of HSPB2 and HSPB3 also affected speckle shape and number in cycling and differentiated human myoblasts. Our findings demonstrating that sequestration of lamin A/C, alteration of prelamin A and IN aggregation of HSPB2 and HSPB3 occur in both cell types and, in the case of myoblasts, independently on their differentiated or proliferating status, strongly suggest that HSPB2 and HSPB3 would lead to speckle round-up also in human myoblasts. Considering that IN aggregates/masses of HSPB2 sequester endogenous lamin A/C, we monitored HSPB2 overexpression indirectly by looking at the distribution of endogenous lamin A/C and we considered as HSPB2 overexpressing cells the ones that showed aggregated lamin A/C. In these cells (HSPB2 positive population), we investigated speckle shape and number, using our monoclonal SC35 antibody. We infected cycling LHCN-M2 and then we either fixed the cells 48 h post-infection or 5 days after differentiation. To exclude that the infection with lentiviral particles could per se alter speckles shape/distribution, we infected LHCN-M2 cells with GFP particles. We found that LHCN-M2 cells overexpressing GFP did not show changes in speckle shape/number as compared to mock-infected myoblasts (see Figure 33A and B). In contrast, we observed a severe speckle round-up both in cycling and differentiated LHCN-M2 cells overexpressing HSPB2 or HSPB3 wt (see Figure 33C and D).

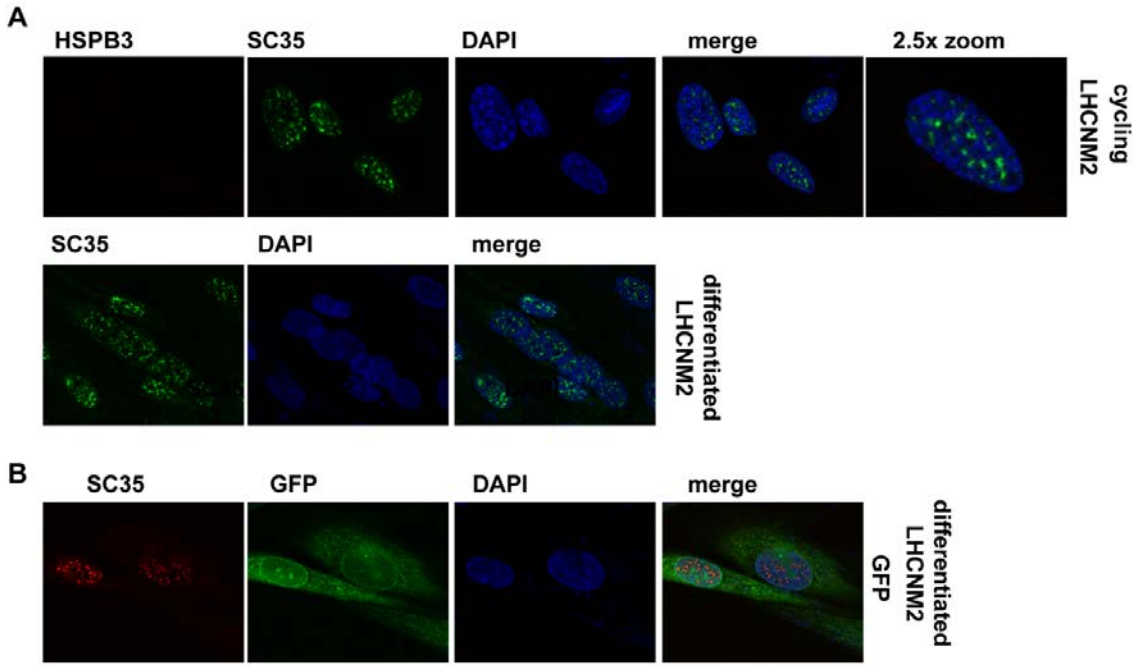

Figure 33. Cycling LHCN-M2 cells were infected with mock (**A**) or lentiviral vector encoding for GFP (**B**) (used as control). LHCN-M2 infected cells were cultured under cycling conditions for 48 h or under differentiating conditions for 5 days. Cells were then fixed and labelled with α-SC35.

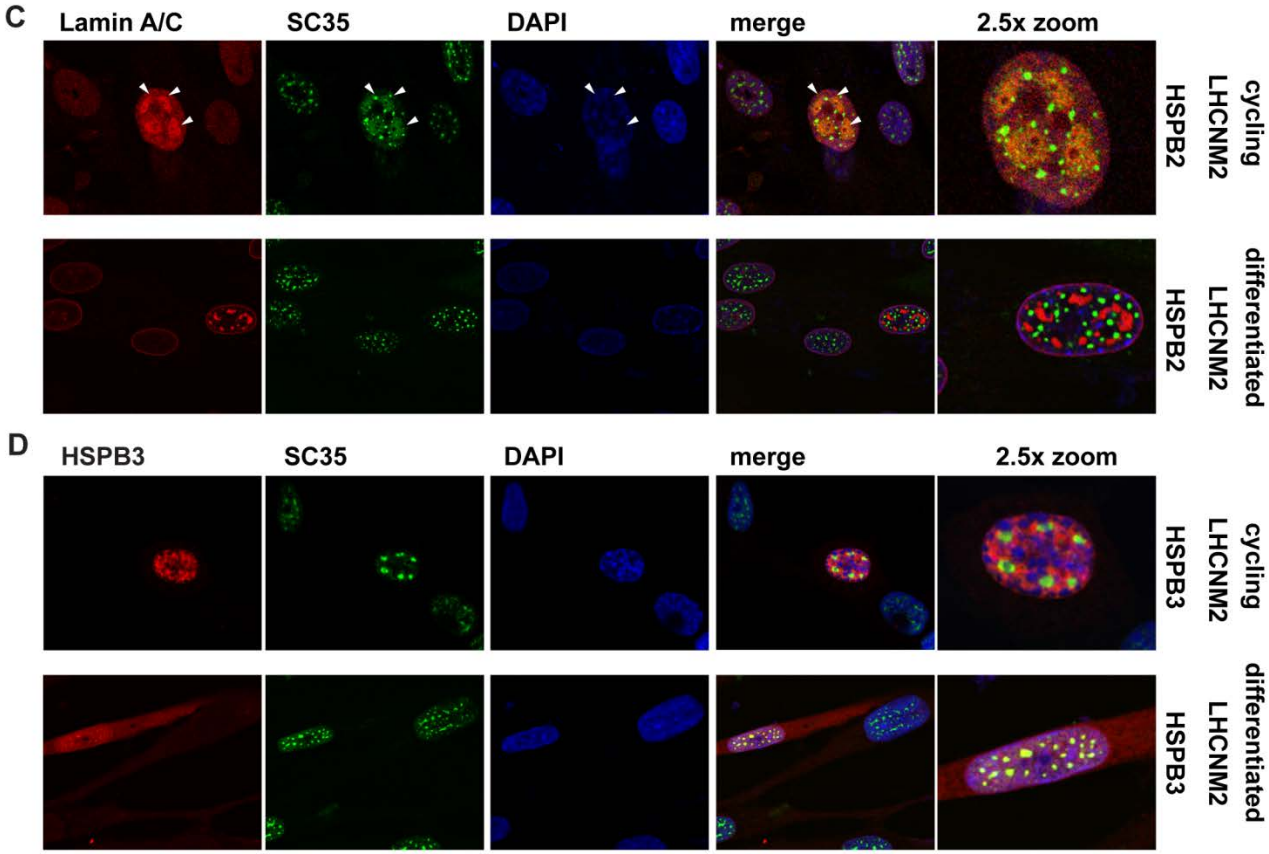

Figure 33. Cycling LHCN-M2 cells were infected with HSPB2 (**C**) and myc-HSPB3 lentiviral particles (**D**). 24 h post-infection, LHCN-M2 cells were cultured under cycling conditions for 48 h or under differentiating conditions for 5 days. Cells were then fixed and labelled with α-SC35 and, where indicated, for α-HSPB3 and α-Lamin A/C. 2.5x magnifications of the selected areas are shown.

While in HeLa cells we never observed co-localization of HSPB2 or HSPB3 with speckles, in LHCN-M2 cells we found some colocalization of overexpressed HSPB3 and R7S (data not shown) with SC35-speckles. HSPB1 and HSPB5 (that we used as controls in the speckles pattern analysis) are associated in a phosphorylation-dependent manner with nuclear speckles (Bryantsev et al. 2007; den Engelsman et al. 2004). This suggests that some HSPBs can be recruited at speckles upon specific stress to exert yet unknown functions. We thus verified whether, in HeLa cells, HSPB2 and HSPB3 (wt and mutants) could associate with speckles upon stress condition. We overexpressed HSPB2 or HSPB3 and we treated the cells with arsenite, which induces the translocation of HSPB1 into the nucleus and leads to its redistribution into nuclear speckles (Bryantsev et al. 2007). Also upon treatment with arsenite, HSPB2 and HSPB3 were not recruited into speckles, which were identified both by using the antibody specific for endogenous SC35 (data not shown), or by co-expression of the speckle marker YFP-ASF/SF2 (see Figure 34). In contrast, HSPB1 could colocalize with

overexpressed YFP-ASF/SF2 upon arsenite treatment. Thus, while upon overexpression HSPB1 and HSPB5 per se do not alter speckle shape/number but can be recruited at speckles, HSPB2 and HSPB3 indirectly lead to speckle round-up, without any direct association with this IN compartment, at least in HeLa cells.

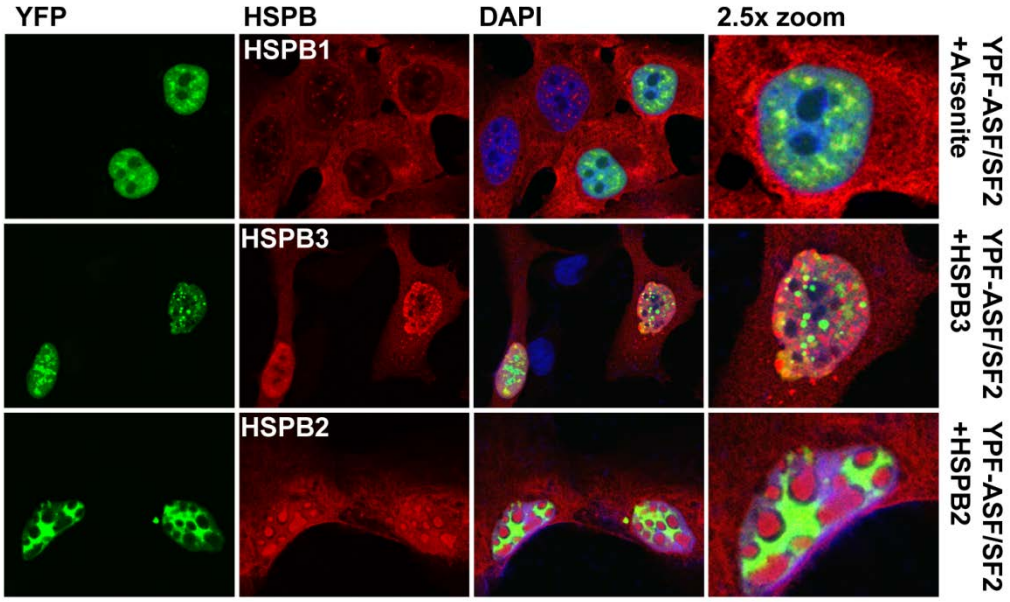

Figure 34. HeLa cells were transfected with YPF-ASF/SF2 and HSPB2 and HSPB3. 1 h prior to fixation cells were treated with arsenite 0,5mM. Cells were labelled with α-HSPB2 and α-HSPB3 and for endogenous HSPB1.

HSPB2 and HSPB3 affect the RNA pol II-mediated transcription

As said earlier the inhibition of pol II-mediated RNA transcription causes speckles round-up (Kumaran and Spector 2008; Shimi et al. 2008; Tang et al. 2008). Based on these findigns, we asked whether HSPB2 and HSPB3 could inhibit RNA transcription, which, in turn, would lead to speckle round-up. We thus measured RNA synthesis in cells expressing HSPB2 and/or HSPB3 using the uridine analog 5-ethynyluridine (EU), which is incorporated into newly transcribed RNAs and is detected using click chemistry (Jao and Salic 2008). As expected, in HeLa cells, incorporation of EU into nascent RNAs was completely abrogated by incubation of the cells with the pol II inhibitor actD (used as positive control) (see Figure 35C). Overexpression of HSPB5 or NLS-HSPB7 did not significantly affect EU incorporation as compared to control HeLa cells (see Figure 35A). Consistent with the round-up speckle phenotype observed, overexpression of HSPB2, HSPB3 (wt, R7S or R116P), alone or in combination, significantly decreased the incorporation of EU in the nucleoplasm. These

results support that RNA transcription is inhibited by HSPB2, HSPB3, R7S and R116P (see Figure 35A and B). HSPB2 had a very strong inhibitory effect on RNA synthesis, which was partly reduced by co-expression with HSPB3, but not with the mutants R7S or R116P (see Figure 35B). Incorporation of EU was quantified by calculating the ratio between EU incorporation in the nucleoplasm and EU incorporation in nucleoli that was not affected by overexpression of HSPB2 and HSPB3. Nucleoli contains RNA pol I; thus, combined these results would suggest that the IN accumulation of HSPB2 or HSPB3 has deleterious effects on RNA transcription by specifically acting on RNA pol II-mediated transcription.

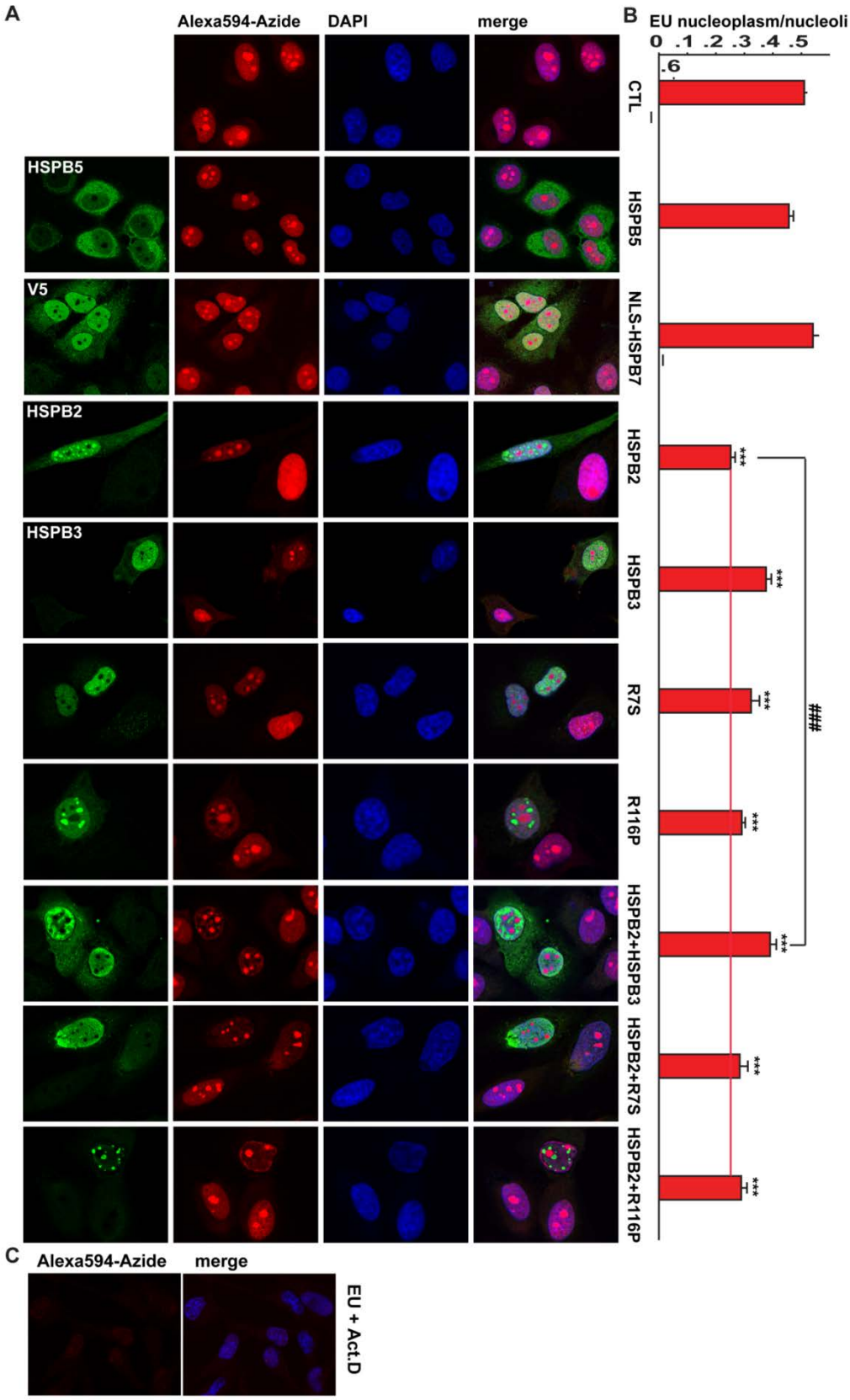

Figure 35: A: HeLa cells were transfected for 48 h with myc-HSPB3 (wt and mutants, alone or in combination with HSPB2), HSPB5 or NLS-HSPB7 (used as controls). 6h prior to fixation, cells were incubated with 200µM 5-ethynyluridine (EU), fixed, stained with Alexa594-Azide and subsequently stained for HSPB3 or V5-NLS-HSPB7 (green). **B:** Quantification of EU incorporation from **A**. **C** HeLa cells were treated with the RNA polymerase II inhibitor actinomycin D for 1 h, fixed and stained with Alexa594-Azide.

We next measured RNA pol II-mediated synthesis with EU in human cycling myoblasts infected with HSPB2, myc R7S or myc-R116P.

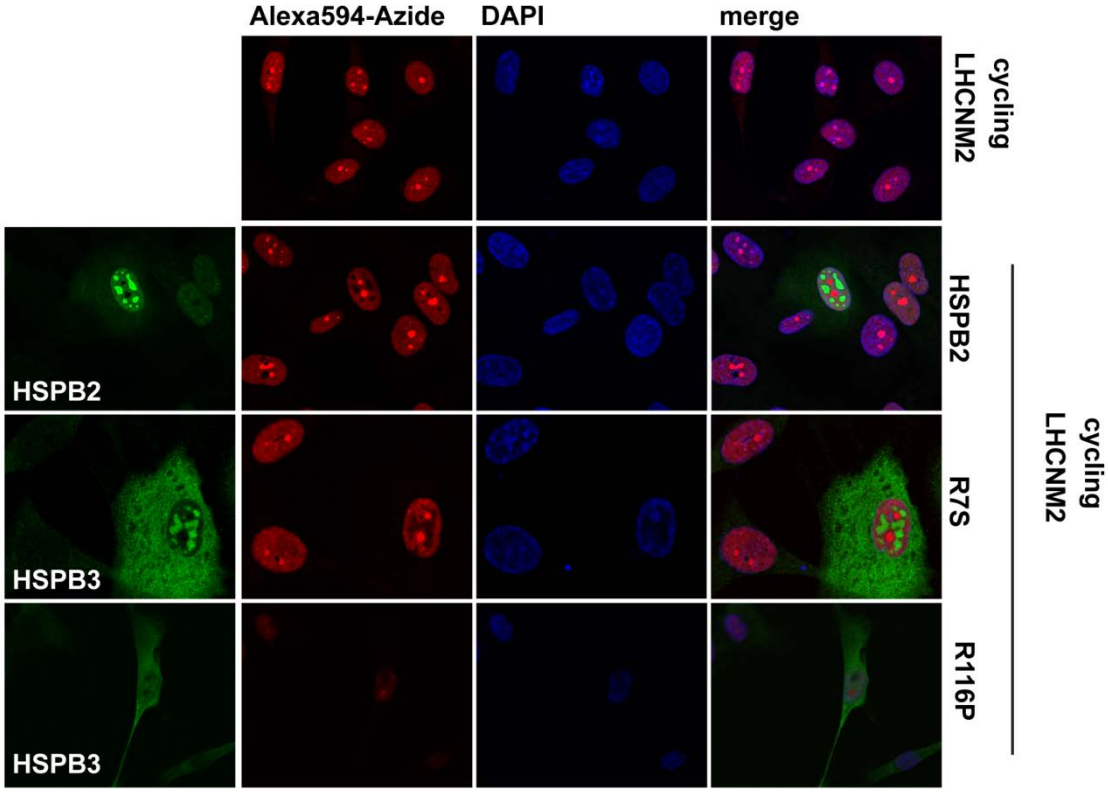

Figure 36: Cycling LHCN-M2 cells were infected with mock (cycling) or HSPB2, myc-R7S and myc-R116P lentiviral particles. 6 h prior to fixation, cells were incubated with 200μM 5-ethynyluridine (EU), fixed, stained with Alexa594-Azide and subsequently stained for HSPB3 or HSPB2 (green).

HSPB2 and HSPB3, although altering nuclear shape and function, do not induce apoptosis but decrease the mitotic index

We then asked whether overexpression of HSPB2 and HSPB3, by affecting nuclear shape, integrity and function, may lead to cell toxicity and apoptosis. The nuclei of apoptotic cells have often a "horse-shoe" like appearance and shrink (Elmore 2007). From our immunofluorescence studies, we had no evidence of presence of apoptotic nuclei/cells in HSPB2 or HSPB3 expressing cells. To study whether HSPB2 or HSPB3 may lead to the activation of apoptosis, we monitored the cleavage of caspase-3, by immunofluorescence and the cleavage of PARP, by western. We treated HeLa cells overnight with doxorubicin (10μM) in order to induce the cleavage of caspase-3 and to verify the specificity of the antibody used to stain cleaved-caspase-3. As expected, upon treatment with doxorubicin, all cells showed

condensed chromatin with accumulation of cleaved-caspase-3 inside the nuclei (see Figure 37A). Instead, overexpression of HSPB2 and HSPB3 did not induce caspase-3 cleavage (see Figure 37B). Concerning PARP cleavage, this was induced by treating HeLa cells overnight with staurosporine (5μM); this treatment lead to the accumulation of the cleaved fragment (c.f.) at around 90 kDa (see Figure 37D). PARP cleavage was not detected in Hek293T cells overexpressing HSPB2 or HSPB3 (wt and mutants), alone or combined (see Figure 37C). Next, since in HeLa cells the transfection efficiency is lower as compared to Hek293T cells (where it reaches 70-90%; data not shown). We co-transfected HeLa cells with GFP and HSPB2 or HSPB3 and we selected by FACS sorting the GFP-positive cells (which were also positive for HSPB2 or HSPB3). Cleaved PARP was not detected in all conditions analyzed: GFP alone (control) or GFP expressed with HSPB2 and HSPB3 (see Figure 37D).

We next asked whether, by affecting nuclear shape and function, overexpression of HSPB2 and HSPB3 (wt and mutants) could delay cell division. Phosphorylation on serine 10 of histone 3 (pS10-H3) plays a crucial role in chromosome condensation during mitosis and is widely used as marker to identify mitotic cells. Using an antibody specific for pS10-H3, we found that 48 h post-transfection, ca. 16% of cells transfected with HSPB5, used as positive control, were undergoing mitosis; instead, we could not find cells overexpressing HSPB2 or HSPB3 (wt and mutants) positive for pS10-H3 (see Figure 37F). The exit from cell cycle is an important prerequisite to start the differentiation process. If HSPB2 and HSPB3 promote the exit from cell cycle, this might explain why their expression levels are so tightly regulated in cycling cells, while being induced during differentiation (which follows cell cycle exit).

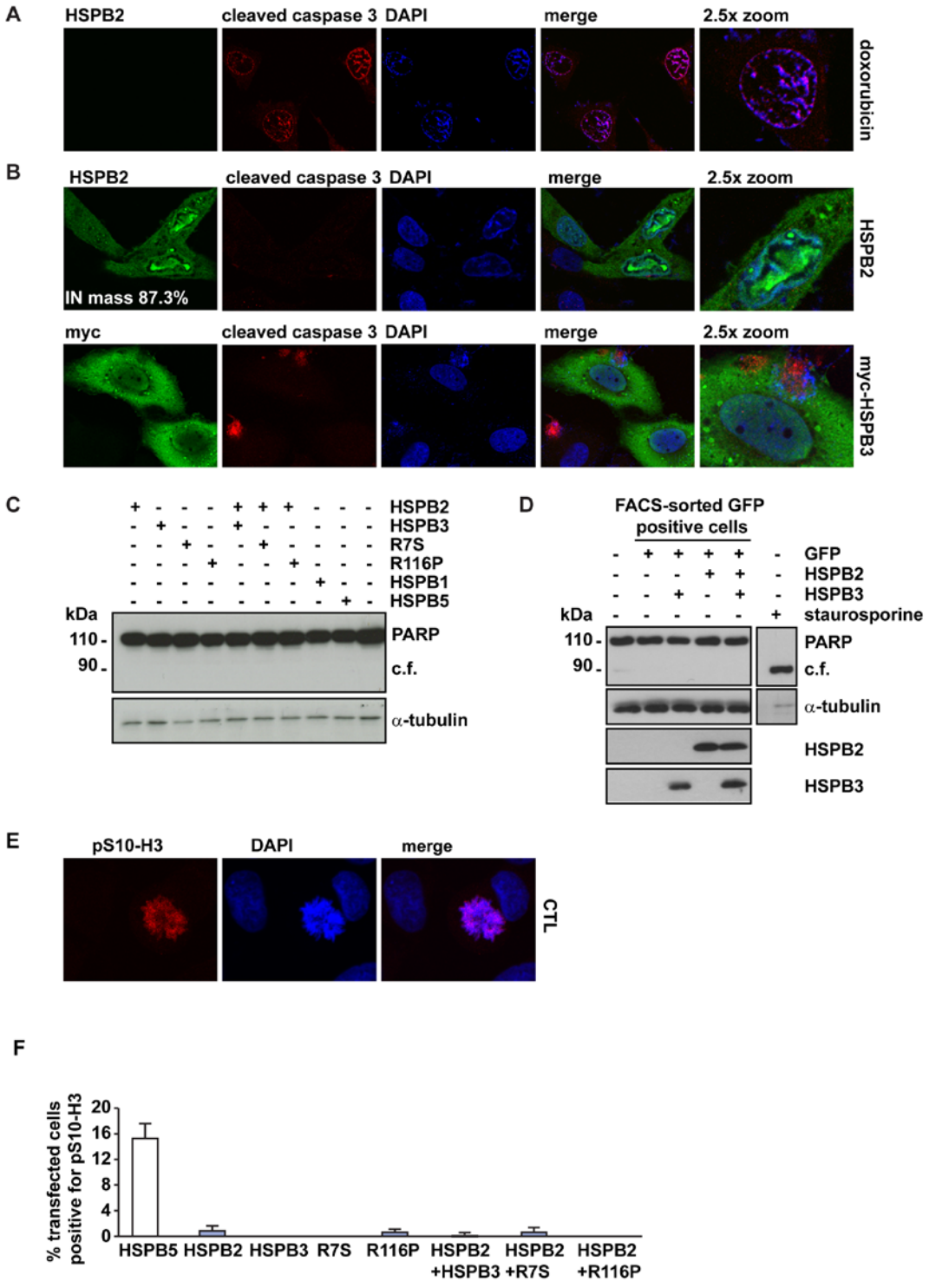

Figure 37: **A:** Cells were treated o/n with 10µM of doxorubicin to induce cleavage of caspase-3. **B:** Cells were transfected with HSPB2 and myc-HSPB3, were fixed and labelled with cleaved-caspase-3. **C:** Hek293T cells were transfected with HSPB2 and myc-HSPB3 (wt and mutants) alone or in combination, and with HSPB5 and HSPB1 (used as controls). Total lysate from each condition were analyzed by western blot for the induction of PARP cleavage. **D:** HeLa cells were treated o/n with 5µM of staurosporine to induce PARP cleavage, or transfected with GFP in combination with HSPB2 and myc-HSPB3 (alone or in combination). GFP positive cells were selected by FACS and then processed for SDS-PAGE and western blot to measure PARP cleavage. **E:** Control HeLa cells were labelled with pS10-H3 and DAPI. **F:** HeLa cells were transfected for 48 h with HSPB5 alone (used as control) or with HSPB2, myc-HSPB3, myc-R7S, myc-R116P, alone or combined. Cells were fixed and labelled for pS10-H3 and quantification of the percentage of transfected cells positive to pS10-H3 was reported.

HSPB2 and HSPB3 aggregate also in the nucleus of immortalized motor neuron cells

The R7S mutation of HSPB3 causes distal hereditary motor neuropathy, where both the motor neurons and the skeletal muscle cells are affected. In fact, the disease leads to a progressive degeneration of peripheral motor neurons and atrophy of the skeletal muscles. However, it is still unclear whether the disease originates at the level of the peripheral motor neurons to later lead to muscle atrophy or whether R7S HSPB3 affects simultaneously the viability of peripheral motor neurons and skeletal muscle cells. We thus studied the aggregation properties of HSPB2 and HSPB3, as well as their effects on lamin distribution, and speckle shape in immortalized motor neurons. For this purpose we used the NSC34 cells, a widely accepted motor neuronal cell model. Like in HeLa or Hek293T cells, the A33AfsX50 mutant was undetectable in NSC34 cells, both when expressed alone or with HSPB2.

Also in NSC34 cells, HSPB2 and HSPB3 (wt and mutants) were highly enriched in the nuclear fraction. Interestingly, similarly to what observed in Hek293T cells, also in NSC34 cells the amount of R7S present in the nuclear fraction is higher as compared to HSPB3 wt. This suggests that the R7S mutation may enhance the propensity of HSPB3 to accumulate and aggregate at the perinuclear and nuclear level.

Also, in NSC34 immortalized motor neurons, HSPB2 aggregated inside the nucleus and sequestered endogenous lamin A/C (see Figure 38A). Concerning the HSPB3 mutants, also in this motor neuronal cell line, R7S formed the typical PN aggregate, which co-aggregated with lamin B1 and partially damaged the nuclear meshwork, while R116P formed IN large aggregates that displaced the DNA (see Figure 38B). Speckle round-up was also observed in NSC34 cells expressing HSPB2, HSPB3, R7S or R116P (see Figure 38C). Globally, our results demonstrate the high propensity of HSPB2 and HSPB3 (wt and mutants) to accumulate and aggregate inside the nucleus and at the perinuclear region of the cells, thereby influencing nuclear architecture and function. These properties are intrinsic to HSPB2 and HSPB3 and do not depend on the cell type where they are overexpressed (but rather on their total level of expression).

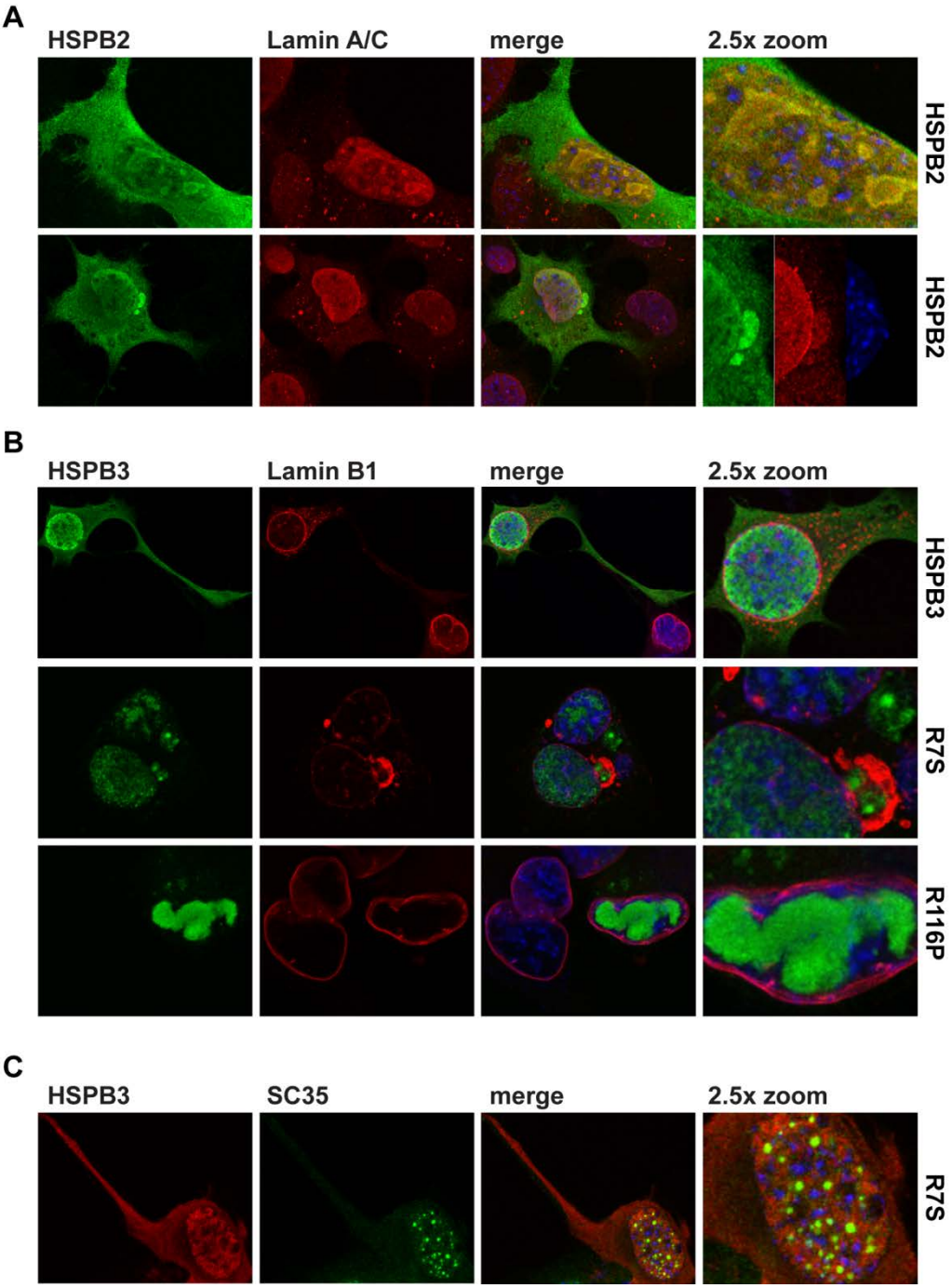

Figure 38. A: NSC34 cells were transfected with HSPB2, fixed and labelled with α-HSPB2 and α-lamin A/C. **B:** NSC34 cells were transfected with myc-HSPB3, myc-R7S and myc-R116P, fixed and labelled with α-HSPB3 and α-lamin B1. **C:** NSC34 cells were transfected with R7S, fixed and labelled with α-HSPB3 and α-SC35.

DISCUSSION

The mammalian family of small heat shock proteins (HSPB) consists of ten members (HSPB1–HSPB10), which are characterized by different functions amongst which the chaperone activity is one of the best studied. In contrast to the major heat shock protein families (e.g. HSP70, HSP90), the HSPB proteins do not require ATP to bind to substrate proteins and maintain them in a refolding competent state, thereby exerting chaperone activity. However, refolding of the client bound by the HSPBs or targeting to degradation (when the client is irreversibly damaged) requires the assistance of ATP-driven chaperone machineries such as e.g. Hsp70, Hsp90.

HSPBs display different expression profiles. Some members of this family are ubiquitously expressed, like e.g. HSPB1, HSPB5 and HSPB8, while some other members are expressed exclusively in specific cell types/tissues, like e.g. HSPB2, HSPB3, HSPB4, HSPB9 and HSPB10. Not all the members of the HSPB family have been widely studied so far. Most of the research focused in the last 20 years on HSPB1, HSPB4, HSPB5 and more recently HSPB8. Instead, HSPB2 and HSPB3 have received little attention by the scientific community and their physiological functions are largely unknown. HSPB2 and HSPB3 form a complex that is expressed in differentiated muscle cells (Sobott et al. 2005; den Engelsman et al. 2009). Recently, a missense mutation of HSPB3, the R7S mutation, has been associated to distal hereditary motor neuropathy type 2C (dHMN 2C) (Kolb et al. 2010). This finding highlights that HSPB3 or the HSPB2-HSPB3 complex would exert important functions for the maintenance of motor neuron and muscle cell viability, since motor neuropathy leads to motor neuron degeneration and atrophy of the skeletal muscles. However, although it is directly associated with dHMN 2C, how mechanistically the R7S mutation leads to motor neuron degeneration is still unknown.

In light of the expression profile of HSPB2 and HSPB3, restricted mainly to differentiated muscles and of the association of HSPB3 with motor neuropathy, Prof. Carra in collaboration with Prof. Tupler sequenced 400 DNAs from patients affected by myopathy of unidentified origin in search of mutations in the genes encoding for HSPB2 and HSPB3. This analysis allowed to discover two new mutations in the gene encoding for HSPB3 in two patients with myopathy signs: p.R116P and p.A33AfsX50 (c.774_775het_insC). The R116P mutation affects a key amino acid in the α-crystallin domain, whose mutation in other HSPBs causes neuromuscular diseases (Datskevich et al. 2012; Boncoraglio et al. 2012 and Ghaoui et

al. 2016); the second mutation identified is p.A33AfsX50, a missense mutation that leads to a premature stop codon (unpublished Carra).

In this thesis we characterized the stability, sub-cellular localization and functions of the wildtype forms of HSPB2 and HSPB3, as well as of the HSPB3 mutants found in patients with neuromuscular/muscular disease.

For the characterization of these proteins, we used different mammalian cell lines such as HeLa and Hek293T, where the characterization of other HSPBs has been previously done with encouraging results. Then we validated the results obtained in HeLa cells using human myoblasts (LHCN-M2) that we maintained into cycling conditions, as well as in differentiated state. LHCN-M2 represents the more appropriate model to study the functions of HSPB2 and HSPB3, due to their restricted expression profile (Maeda et al. 1995; Whiting et al. 1995; Lam et al. 1996). We verified indeed that both HSPB2 and HSPB3 are expressed in human skeletal muscles and are induced in LHCN-M2 cells during differentiation (see Figures 6A and B and 13).

Several mechanisms have been described that can partly explain how various mutations in specific HSPBs result in neuromuscular/muscular or neurologic diseases. HSPB mutations associated with disease can affect the interaction of mutant HSPB with specific partners or clients. For example, enhanced interaction of mutant HSPB1 with tubulin has been observed in neuronal cultures and transgenic mice expressing a mutant of HSPB1 associated with CMT disease; as a consequence microtubules are hyper-stabilized with alterations of microtubule dynamics; this in turn may contribute to increase neuronal vulnerability (Almeida-Souza et al. 2011). Thus, we analysed the stability of the HSPB3 mutants and their ability to bind to HSPB2 and to form the typical complex observed in differentiated muscle cells. Our results show that R7S and R116P are stable, while the truncated form A33AfsX50 is recognized by the PQC system and rapidly degraded after synthesis. For this reason we excluded this mutant from the characterization. Concerning the ability to form a complex with HSPB2, R7S still interacted with HSPB2, with binding affinity similar to the one of wildtype HSPB3. Instead R116P could not associate with HSPB2. Combined with the extremely low stability of A33AfsX50, which is rapidly degraded after synthesis, our results suggest that both mutations found in patients prevalently affected by myopathy lead to complex disruption (either for lack of HSPB3 or for abrogated binding of HSPB3 R116P to HSPB2), while the mutation that causes motor neuropathy (R7S) has no significant impact of the formation of the HSPB2-HSPB3 complex. Thus altered interaction of HSPB3 mutants with HSPB2 can lead

to an imbalance in the amount of “free” HSPB2 and HSPB3, which can in turn affect their function and interaction with other partners or clients (similarly to what has been described for mutant HSPB1). In agreement, we found that an excess of “free” HSPB2 alters the distribution of lamin A/C and prelamin A with consequences on the integrity of the nuclear envelope and nuclear function (see later). Such imbalance in the association of HSPB2 with HSPB3 could thus contribute to motor neuron and skeletal muscle cell vulnerability by affecting their interaction with specific clients. In line with such an interpretation, HSPB2 “free” of HSPB3 can directly bind to lamin A (although weakly) with profound consequences on lamin A/C IN distribution.

Alternatively, but not mutually exclusive, mutations in several chaperones that have been associated with neuromuscular and muscular diseases often lead to the accumulation of protein aggregates that contain the mutated protein itself (Vicart et al. 1998; Perng et al. 1999a). For example, mutated HSPB5 associated with myofibrillar myopathy leads to the accumulation of aggregates that contain both mutated R120G HSPB5 and desmin, an intermediate filament protein essential for the maintenance of the overall structure and for the cytoskeletal organization of striated muscle cells. Desmin is one of the first proteins expressed upon satellite cell activation (Lazarides and Hubbard 1976; Kaufman et al. 1991) and it plays an important role in the maintenance of muscular tone and differentiation potential (Vicart et al. 1996). The mutant R120G of HSPB5 shows higher affinity for desmin, compared to HSPB5 wt, and it promotes desmin aggregation (Perng et al. 1999). Together with loss of HSPB5 function, its aggregation and the sequestration of desmin by mutant HSPB5 contribute to muscle cell degeneration (Kumar et al. 1999; Perng et al. 1999; Bova et al. 1999; Chávez Zobel et al. 2003). In addition to the maintenance of the muscular tone, desmin plays also a role in maintaining the appropriate differentiation potential of muscle cells. In fact, the forced expression of desmin in myoblasts that lack lamins A and C and which are characterized by dramatically compromised differentiation potential, restores differentiation potential (Melcon et al. 2006). However, the exact function of desmin in myogenesis remains unclear (Li et al. 1994; Weitzer et al. 1995; Smythe et al. 2001).

Our analysis of the sub-cellular distribution of HSPB2 and HSPB3 wt and mutants revealed that both wildtype and mutant HSPB2 and HSPB3 tend to aggregate in mammalian cells upon overexpression. In agreement with previous findings concerning other disease associated mutants of HSPBs, also R7S and R116P increased the tendency of HSPB3 to aggregate (although, surprisingly already the wildtype forms of HSPB2 and HSPB3, when

expressed at relatively high levels, have high tendency to aggregate). Our fluorescence microscopy studies allowed us to demonstrate that, in contrast to the majority of HSPBs that are mainly cytosolic, such as e.g. HSPB1 and HSPB5, both HSPB2 and HSPB3 (wt and mutants) are enriched in the nucleus. Curiously, aggregation of HSPB2 and HSPB3 occurs mainly in the intranuclear and perinuclear compartments of the cells, respectively. The observation that the R116P mutant aggregates exclusively inside the nucleus, combined with our finding that the R7S forms a typical large aggregate accumulating at the perinuclear region of the cells and that an excess of "free" HSPB2 decreases nuclear stability and causes the deformation of the nucleus strongly support that the nucleus is the target of HSPB3-associated diseases.

Concerning the physiological functions of HSPB2 and HSPB3, it is unlikely that HSPB2 and HSPB3 are required for skeletal muscle differentiation. This interpretation is supported by several findings. First, mice knockout of both HSPB2 and HSPB5 develop skeletal differentiated muscles (Brady et al. 2001). Second, knockout of HSPB2 in cardiac myocytes also does not affect their maturation and differentiation. However, HSPB2 and HSPB3 are induced during the process of differentiation, which suggests that they might support specific function connected with (but not necessarily required for) muscle differentiation. In parallel, knockout of HSPB2 and HSPB5 leads to progressive muscle atrophy, while knockout of HSPB2 in cardiomyocytes renders these cells more vulnerable to stress. Combined these data support that, rather than being involved in the process of muscle differentiation per se, several HSPBs, amongst which are HSPB2 and HSPB3, would participate in stress tolerance. In light of our data showing that HSPB2 and HSPB3 accumulate in the nuclei affecting lamin distribution, HSPB2 and HSPB3 might modulate nuclear structure and function to ultimately allow the cells to rapidly respond to stress. However, our studies have been performed under overexpression conditions and allowed us to identify target proteins, whose subcellular distribution and function is affected by high levels of HSPB2 and HSPB3 (and not by other HSPBs such as e.g. HSPB1, HSPB5 or HSPB7). To shed light on the physiological functions of HSPB2 and HSPB3 more studies in human myoblasts and under conditions where the expression of HSPB2 and HSPB3 is silenced are needed.

Concerning the direct association of or implication of HSPB3 mutants in neuromuscular/muscular diseases, our results strongly suggest that the nucleus may represent the target of mutant HSPB3 and that alteration of nuclear shape and function due to imbalances in HSPB2-HSPB3 levels may contribute to HSPB3-associated diseases. The mutants of HSPB3 characterized in this study all increase the aggregation propensities of

HSPB3 and/or, indirectly, HSPB2. Imbalances in the expression levels and interaction of HSPB2 and HSPB3 and accumulation of HSPB2 and HSPB3 aggregates may affect nuclear functions in different ways. First, by aggregating at the perinuclear region of the cells and inside the nucleus, HSPB3 and a free exceeding pool of HSPB2 change the distribution of mature lamin A/C and cause the accumulation of prelamin A. Second, by accumulating inside the nucleus HSPB2 and HSPB3 inhibit RNA transcription. These two effects are likely interconnected, since prelamin A maturation and lamin A/C and lamin B1 distribution and levels regulate, indirectly, RNA transcription. In fact, it has been demonstrated in several cell lines that, besides maintaining the nuclear architecture and providing mechanical stability, nuclear lamins are distributed throughout the nucleoplasm, where they modulate chromatin remodelling, DNA replication and RNA transcription. For example, alteration of lamin organization inhibits the elongation phase resulting in a dramatic reduction of DNA replication (Spann et al. 1997; Moir et al. 2000). Lamin function appears particularly important for the function and viability of skeletal muscle cells. In fact, the remodelling of the nucleoskeleton and of lamins is essential to ensure the proper differentiation of skeletal muscle cells (Markiewicz et al. 2005). Most importantly, alterations of lamin distribution cause neuromuscular and muscular diseases. For example, mutations of *LMNA* gene and NE proteins have been associated with numerous forms of myopathies, called "laminopathies" and neuromuscular diseases such as the Charcot-Marie-Tooth disease (De Sandre-Giovannoli et al. 2002). Laminopathies include for example the Emery-Dreifuss Muscular Dystrophy (EDMD) (Bonne et al. 1999; Sullivan et al. 1999), the limb-girdle muscular dystrophy type 1B (Van der Kooi et al. 1997; Muchir et al. 2000), which both affect the striated skeletal and cardiac muscles, and congenital muscular dystrophy linked to the *LMNA* (L-CMD) (Mercuri et al. 2004; Quijano-Roy et al. 2008). Thus, in light of a direct association of mutation of lamins and integral proteins of the membrane (e.g. emerin) with muscular diseases it is tempting to speculate that the nucleus is the cellular target of HSPB3 mutations and that HSPB2 and HSPB3 play specific, yet unknown functions at the nuclear level that are (at least in part) altered by the HSPB3 mutants, thereby contributing to disease progression.

From the mechanistic point of view, mutations of lamins and emerin cause an increase of nuclear deformability and fragility to mechanical stress of skeletal muscle cells and impair the activation of mechanosensitive genes, thereby increasing the vulnerability of these cells to repetitive strain. HSPB3 mutants by aggregating and by affecting the distribution of lamins (and prelamin A) might indirectly impair the expression of specific genes upon stress, thereby

conferring vulnerability to differentiated skeletal muscle cells. Moreover, both mutations in *LMNA* and *Emd* genes as well as the accumulation of prelamin A have been associated with altered muscle cells regeneration (Lammerding et al. 2005; Ozawa et al. 2006). HSPB3 mutants could, eventually, also interfere with this process.

Our immunofluorescence data show that HSPB3 wt and mutants, by aggregating at the nuclear/perinuclear level, lead to a perturbation of prelamin A localization and maturation, causing its accumulation. On the other hand R116P mutant increases the "free" pool of HSPB2 that can subsequently sequester prelamin A and lamin A/C, thereby affecting also the recruitment of integral proteins such as emerin and SUN2 at the NE. As a consequence, the interplay between the nucleoskeleton and the cytoskeleton could also be compromised. This interplay is fundamental for the maintenance of the muscular tone and becomes particularly important during stress conditions (e.g. mechanical stress). The compromised interplay between the nucleoskeleton and the cytoskeleton leads to nuclear instability, fragility and deformability, resulting in muscle weakness and degeneration. However, at present we have no evidence supporting an (indirect) effect of HSPB3 mutants on the interplay between the nucleoskeleton and the cytoskeleton and mechanotransduction. Instead all our results really point to alteration of lamin A/C and, to a lesser extent, of lamin B1 as key event that may trigger HSPB3-mediated toxicity.

Next, we have preliminary evidence suggesting the potential impact of HSPB3 mutants on RNA transcription and adaptive gene expression to stress. Dysregulation of RNA transcription, especially in response to stress, might be (at least in part) responsible for motor neuron and skeletal muscle vulnerability in presence of mutant HSPB3. Our works show that, HSPB2 and HSPB3 cause a modification of the shape and size of the nuclear speckles; reminiscent of what occurs upon transcription inhibition with e.g. actinomycin D, or thermal shock. Upon these conditions, splicing factors and transcription factors crowd around in nuclear speckles, which become larger and rounder (Spector and Lamond, 2011). Overexpression and accumulation of HSPB2 and HSPB3 inside the nuclei results in RNA transcription inhibition, as evidenced by our assay with EU. Thus, endogenously expressed HSPB2 and HSPB3 could participate in the regulation of transcription and mRNA splicing, and could inhibit transcription in the nucleus, a function that could be dysregulated by HSPB3 mutants. Inhibition of RNA transcription and speckle round-up in HSPB2 and HSPB3 overexpressing cells may be a consequence of the changes in lamin distribution induced by HSPB2 and HSPB3. Alternatively, HSPB2 and HSPB3 may indirectly modulate the functions

and morphology of speckles by direct interaction with specific components of speckles themselves. In fact, HSPB1 and HSPB5 can colocalize with speckles upon stress conditions (van Rijk et al. 2003; Vos et al. 2009). However, we found little/no experimental evidence that supports recruitment of HSPB2 and HSPB3 in nuclear speckles. Thus, combined our results suggest that the speckle round-up observed would be due to indirect rearrangements of prelamin A and lamins, rather than to a direct effect of HSPB2 and HSPB3 within speckles. This interpretation is corroborated by the evidence that disruption of prelamin A processing as well as mutation in *LMNA* are both associated with dysregulation of mRNA splicing. Concerning the functional consequences of speckle-round up and inhibition of RNA pol II-mediated transcription, these might be relevant to muscle cell viability. In fact, it has been demonstrated that RNA pol II is implicated in the transcription of miRNA and that LMNA-associated muscular dystrophy is characterized by dysregulation of specific miRNA, implicated in the modulation of myoblast differentiation (Sylvius et al. 2011). Moreover, overexpression of lamin A/C and silencing of lamin B1 significantly inhibit pol II-mediated RNA transcription causing speckles round-up (Kumaran and Spector 2008; Shimi et al. 2008; Tang et al. 2008). Thus, mutant HSPB3 either due to change in prelamin A distribution and levels or to imbalance in the interaction between HSPB2 and prelamin A and mature lamin A/C might lead to dysregulation of RNA transcription.

Finally, our study demonstrates that the dramatic changes in the nuclear shape and function induced by HSPB2 and HSPB3 are not associated with major toxicity. Infact, apoptotic markers were not activated in HSPB2 and HSPB3 expressing cells. However, our data suggest that the nuclear changes induced by HSPB2 and HSPB3 may affect the ability of the cells to undergo cell division. This is in line with their expression in differentiating cells, which exit the cell cycle.

In summary, although our results do not allow us to demonstrate what is the exact physiological function of HSPB2 and HSPB3, they overall allow us to propose that these chaperones display specific nuclear functions, whose regulation may contribute to maintain muscle cell shape and stability and whose dysregulation would alter nuclear remodeling and deformability, thereby contributing to neuromuscular and muscular disease.

ACKNOWLEDGMENTS

I would like to express my special appreciation to my supervisor Prof. Serena Carra for being a guide and a key figure during my PhD, thanks to her experience and support all my work has been possible. During these three years she was always there to provide necessary assistance and academic advices. I am grateful to her for sharing her time and resources to give this thesis a final shape.

I would like to thank all my colleagues for kind support and help; especially, Dr. Lonneke Heldens for having performed the initial studies on HSPB2 and HSPB3 and having identified part of their effects on nuclear shape and for the characterization of HSPB2 and HSPB3 oligomerization properties. I would like to thank Dr. Samuel Seguin for his encouragement and his advices; and Dr. Massimo Ganassi for subcloning of lentiviral vector encoding for myc-HSPB3-R7S. A special thank to Dr. Paolo Benatti for technical help in performing lentiviral particles production. I am grateful to Dr. Giuseppina Leo for technical support with confocal microscopy and Domenico Amore for technical help in performing several experiments. My special thanks are also to Dr. Milena Nasi for technical support in performing real time PCR, and Dr Sara de Biasi for help in carrying out the FACS experiment. I would like to thanks Prof. Sandra Marmiroli and Dr. Jessika Bertacchini for fruitful discussions, for support with the co-immunoprecipitation studies with flag-lamin A and for providing several useful reagents and antibodies. Moreover, I thank Prof. Sandra Marmiroli and Prof. Giovanna Cenacchi for the electronic microscopy studies.

Finally, I am grateful to Association Francaise contre les Myopathies, Telethon and MIUR (Ministry of Education, Universities and Research Italy) for their financial support to Prof. Carra lab, which was essential to carry out all the work described here.

REFERENCES

Almeida-Souza L, Asselbergh B, d'Ydewalle C, Moonens K, Goethals S, de Winter V, Azmi A, Irobi J, Timmermans JP, Gevaert K, Remaut H, Van Den Bosch L, Timmerman V, Janssens S. Small heat-shock protein HSPB1 mutants stabilize microtubules in Charcot-Marie-Tooth neuropathy. J Neurosci. 2011, 31: 15320-8.

Aquilina JA, Watt SJ. The N-terminal domain of alphaB-crystallin is protected from proteolysis by bound substrate. Biochem Biophys Res Commun. 2007, 353: 1115-20.

Arimura T, Helbling-Leclerc A, Massart C, Varnous S, Niel F, Lacène E, Fromes Y, Toussaint M, Mura AM, Keller DI, Amthor H, Isnard R, Malissen M, Schwartz K, Bonne G. Mouse model carrying H222P-Lmna mutation develops muscular dystrophy and dilated cardiomyopathy similar to human striated muscle laminopathies. Hum Mol Genet. 2005, 14:1 55-69.

Arrigo AP, Simon S, Gibert B, Kretz-Remy C, Nivon M, Czekalla A, Guillet D, Moulin M, Diaz-Latoud C, Vicart P. Hsp27 (HspB1) and alphaB-crystallin (HspB5) as therapeutic targets. FEBS Lett. 2007, 581: 3665-74.

Asthana A, Raman B, Ramakrishna T, Rao ChM. Structural aspects and chaperone activity of human HspB3: role of the "C-terminal extension". Cell Biochem Biophys. 2012, 64: 61-72.

Atomi Y, Yamada S, Strohman R, Nonomura Y. Alpha B-crystallin in skeletal muscle: purification and localization. J Biochem. 1991, 110: 812-22.

Bagneris C, Bateman OA, Naylor CE, Cronin N, Boelens WC, Keep NH, and Slingsby C. Crystal structures of alpha-crystallin domain dimers of alphaB-crystallin and Hsp20. J. Mol. Biol 2009, 392: 1242-1252.

Bailey CK, Andriola IF, Kampinga HH, Merry DE. Molecular chaperones enhance the degradation of expanded polyglutamine repeat androgen receptor in a cellular model of spinal and bulbar muscular atrophy. Hum Mol Genet. 2002, 11: 515-23.

Bakthisaran R, Tangirala R, Rao ChM. Small heat shock proteins: Role in cellular functions and pathology. Biochim Biophys Acta 2015, 1854: 291-319.

Baranova EV, Weeks SD, Beelen S, Bukach OV, Gusev NB, Strelkov SV. Three-dimensional structure of α-crystallin domain dimers of human small heat shock proteins HSPB1 and HSPB6. J Mol Biol. 2011, 411: 110-22.

Bennardini F, Wrzosek A, Chiesi M. Alpha B-crystallin in cardiac tissue. Association with actin and desmin filaments. Circ Res. 1992,71: 288-94.

Bergstrom DA, Penn BH, Strand A, Perry RL, Rudnicki MA, Tapscott SJ. Promoter-specific regulation of MyoD binding and signal transduction cooperate to pattern gene expression. Mol Cell. 2002, 9: 587-600.

Biamonti G, Giacca M, Perini G, Contreas G, Zentilin L, Weighardt F, Guerra M, Della Valle G, Saccone S, Riva S, Falaschi A. The gene for a novel human lamin maps at a highly transcribed locus of chromosome 19 which replicates at the onset of S-phase. Mol Cell Biol. 1992, 12: 3499-506.

Bione S, Maestrini E, Rivella S, Mancini M, Regis S, Romeo G, Toniolo D. Identification of a novel X-linked gene responsible for Emery-Dreifuss muscular dystrophy. Nat Genet, 1994, 8: 323-7.

Boelens WC, Van Boekel MA, De Jong WW. HspB3, the most deviating of the six known human small heat shock proteins. Biochim Biophys Acta. 1998, 1388: 513-6.

Boncoraglio A, Minoia M, Carra S. The family of mammalian small heat shock proteins (HSPBs): implications in protein deposit diseases and motor neuropathies. Int J Biochem Cell Biol. 2012, 44: 1657-69.

Bonne G, Mercuri E, Muchir A, Urtizberea A, Bécane HM, Recan D, Merlini L, Wehnert M, Boor R, Reuner U, Vorgerd M, Wicklein EM, Eymard B, Duboc D, Penisson-Besnier I, Cuisset JM, Ferrer X, Desguerre I, Lacombe D, Bushby K, Pollitt C, Toniolo D, Fardeau M, Schwartz K, Muntoni F. Clinical and molecular genetic spectrum of autosomal dominant Emery-Dreifuss muscular dystrophy due to mutations of the lamin A/C gene. Ann Neurol. 2000, 48: 170-80.

Bova MP, Yaron O, Huang Q, Ding L, Haley DA, Stewart PL, Horwitz J. Mutation R120G in alphaB-crystallin, which is linked to a desmin-related myopathy, results in an irregular structure and defective chaperone-like function. Proc Natl Acad Sci U S A. 1999, 96: 6137-42.

Bova MP, McHaourab HS, Han Y, Fung BK. Subunit exchange of small heat shock proteins. Analysis of oligomer formation of alphaA-crystallin and Hsp27 by fluorescence resonance energy transfer and site-directed truncations. J Biol Chem. 2000, 275: 1035-42.

Brady JP, Garland DL, Green DE, Tamm ER, Giblin FJ, Wawrousek EF. AlphaB-crystallin in lens development and muscle integrity: a gene knockout approach. Invest Ophthalmol Vis Sci. 2001, 42: 2924-34.

Brameier MF, Banzhaf W. Linear Genetic Programming. 2007.

Braun T, Gautel M. Transcriptional mechanisms regulating skeletal muscle differentiation, growth and homeostasis. Nat. Rev. Mol. Cell Biol. 2011, 12: 349–361

Brooks GA, Hittelman KJ, Faulkner JA, Beyer RE. Tissue temperatures and whole-animal oxygen consumption after exercise. Am J Physiol. 1971, 221: 427-31.

Bruey JM, Ducasse C, Bonniaud P, Ravagnan L, Susin SA, Diaz-Latoud C, Gurbuxani S, Arrigo AP, Kroemer G, Solary E, Garrido C. Hsp27 negatively regulates cell death by interacting with cytochrome c. Nat Cell Biol. 2000, 2: 645–52.

Bryantsev AL, Kurchashova SY, Golyshev SA, Polyakov VY, Wunderink HF, Kanon B, Budagova KR, Kabakov AE, Kampinga HH. Regulation of stress-induced intracellular sorting and chaperone function of Hsp27 (HspB1) in mammalian cells. Biochem J. 2007, 407: 407-17.

Byung CY, Seung YP, Young-Don L, Jung NL, Yu JH, Heung KP. The Expression of Heat Shock Protein 60 kDa in Tissues and Cell Lines of Breast Cancer. J Breast Cancer 2008; 11: 161-71.

Capanni C, Del Coco R, Squarzoni S, Columbaro M, Mattioli E, Camozzi D, Rocchi A, Scotlandi K, Maraldi N, Foisner R, Lattanzi G. Prelamin A is involved in early steps of muscle differentiation. Exp Cell Res. 2008, 314: 3628-37.

Capell BC, Collins FS. Human laminopathies: nuclei gone genetically awry. Nat Rev Genet. 2006, 7: 940-52.

Capponi S, Geroldi A, Fossa P, Grandis M, Ciotti P, Gulli R, Schenone A, Mandich P, Bellone E. HSPB1 and HSPB8 in inherited neuropathies: study of an Italian cohort of dHMN and CMT2 patients. J Peripher Nerv Syst. 2011, 16: 287-94.

Carra S, Sivilotti M, Chávez Zobel AT, Lambert H, Landry J. HspB8, a small heat shock protein mutated in human neuromuscular disorders, has in vivo chaperone activity in cultured cells. Hum Mol Genet. 2005, 14: 1659-69.

Carra S and Landry J. Small heat shock proteins in neurodegenerative diseases. Heat Shock Proteins in Biology and Medicine 2006.

Carra S, Seguin SJ, Lambert H, Landry J. HspB8 chaperone activity toward poly(Q)-containing proteins depends on its association with Bag3, a stimulator of macroautophagy. J Biol Chem. 2008, 283: 1437-44.

Carra S, Boncoraglio A, Kanon B, Brunsting JF, Minoia M, Rana A, Vos MJ, Seidel K, Sibon OC, Kampinga HH. Identification of the Drosophila ortholog of HSPB8: implication of HSPB8 loss of function in protein folding diseases. J Biol Chem. 2010, 285: 37811-22.

Cashikar AG, Duennwald M, Lindquist SL. A chaperone pathway in protein disaggregation. Hsp26 alters the nature of protein aggregates to facilitate reactivation by Hsp104. J Biol Chem. 2005, 280: 23869-75.

Caspers GJ, Bhat SP. The expanding small heat-shock protein family, and structure predictions of the conserved "a-crystallin domain". J. Mol. Evol. 1995, 40: 238–248.

Charette SJ, Lavoie JN, Lambert H, Landry J. Inhibition of Daxx-mediated apoptosis by heat shock protein 27. Mol Cell Biol. 2000, 20: 7602–12.

Chargé SB, Rudnicki MA. Cellular and molecular regulation of muscle regeneration. Physiol Rev. 2004, 84: 209-38.

Chauhan D, Li G, Hideshima T, Podar K, Mitsiades C, Mitsiades N, Catley L, Tai YT, Hayashi T, Shringarpure R, Burger R, Munshi N, Ohtake Y, Saxena S, Anderson KC. Hsp27 inhibits release of mitochondrial protein Smac in multiple myeloma cells and confers dexamethasone resistance. Blood. 2003, 102: 3379–86.

Chávez Zobel AT, Lambert H, Thériault JR, Landry J. Structural instability caused by a mutation at a conserved arginine in the alpha-crystallin domain of Chinese hamster heat shock protein 27. Cell Stress Chaperones 2005, 10: 157-66.

Chávez Zobel AT, Loranger A, Marceau N, Thériault JR, Lambert H, Landry J. Distinct chaperone mechanisms can delay the formation of aggresomes by the myopathy-causing R120G alphaB-crystallin mutant. Hum Mol Genet. 2003, 12: 1609-20.

Chen Q, Ma J, Yan M, Mothobi ME, Liu Y, Zheng F. A novel mutation in CRYAB associated with autosomal dominant congenital nuclear cataract in a Chinese family. Mol Vis. 2009, 15: 1359-65.

Chowdary TK, Raman B, Ramakrishna T, Rao CM. Mammalian Hsp22 is a heat-inducible small heat-shock protein with chaperone-like activity. Biochem J. 2004, 381: 379–87.

Cobb BA, Petrash JM. Characterization of alpha-crystallin-plasma membrane binding. J Biol Chem. 2000, 275: 6664-72.

Conroy SE, Sasieni PD, Amin V, Wang DY, Smith P, Fentiman IS, Latchman DS. Antibodies to heat-shock protein 27 are associated with improved survival in patients with breast cancer. Br J Cancer. 1998, 77: 1875-9.

Cowling BS, McGrath MJ, Nguyen MA, Cottle DL, Kee AJ, Brown S, Schessl J, Zou Y, Joya J, Bönnemann CG, Hardeman EC, Mitchell CA. Identification of FHL1 as a regulator of skeletal muscle mass: implications for human myopathy. J Cell Biol. 2008; 183: 1033–1048.

Crisp M, Liu Q, Roux K, Rattner JB, Shanahan C, Burke B, Stahl PD, Hodzic D. Coupling of the nucleus and cytoplasm: role of the LINC complex. J Cell Biol. 2006, 172: 41-53.

Cummings CJ, Zoghbi HY. Trinucleotide repeats: mechanisms and pathophysiology. Annu Rev Genomics Hum Genet. 2000, 1: 281-328.

Cummings CJ, Sun Y, Opal P, Antalffy B, Mestril R, Orr HT, Dillmann WH, Zoghbi HY. Over-expression of inducible HSP70 chaperone suppresses neuropathology and improves motor function in SCA1 mice. Hum Mol Genet 2001, 10: 1511-8.

Das KP, Surewicz WK. Temperature-induced exposure of hydrophobic surfaces and its effect on the chaperone activity of alpha-crystallin. FEBS Lett 1995, 369: 321-5.

Datskevich PN, Nefedova VV, Sudnitsyna MV, Gusev NB. Mutations of small heat shock proteins and human congenital diseases. Biochemistry (Mosc). 2012, 77: 1500-14.

Datta SA, Rao CM. Differential temperature-dependent chaperone-like activity of alphaA- and alphaB-crystallin homoaggregates. J Biol Chem 1999, 274: 34773-8.

de Jong WW, Caspers GJ, Leunissen JA. Genealogy of the alpha-crystallin—small heat-shock protein superfamily. International Journal of Biological Macromolecules 1998, 22: 151–162.

De Maio A. Heat shock proteins: Facts, thoughts, and dreams. Shock 1999, 11: 1–12.

De Maio A. Extracellular heat shock proteins, cellular export vesicles, and the Stress Observation System: a form of communication during injury, infection, and cell damage. It is never known how far a controversial finding will go! Dedicated to Ferruccio Ritossa. Cell Stress Chaperones 2011; 16: 235-49.

De Sandre-Giovannoli A, Chaouch M, Kozlov S, Vallat JM, Tazir M, Kassouri N, Szepetowski P, Hammadouche T, Vandenberghe A, Stewart CL, Grid D, Lévy N. Homozygous defects in LMNA, encoding lamin A/C nuclear-envelope proteins, cause autosomal recessive axonal neuropathy in human (Charcot-Marie-Tooth disorder type 2) and mouse. Am J Hum Genet, 2002, 70: 726-36.

de Wit NJ, Verschuure P, Kappé G, King SM, de Jong WW, van Muijen GN, Boelens WC. Testis-specific human small heat shock protein HSPB9 is a cancer/testis antigen, and potentially interacts with the dynein subunit TCTEL1. Eur J Cell Biol. 2004, 83: 337-45.

Dechat T, Adam SA, Taimen P, Shimi T, Goldman RD. Nuclear lamins. Cold Spring Harb Perspect Biol. 2010, 2: a000547.

den Engelsman J, Bennink EJ, Doerwald L, Onnekink C, Wunderink L, Andley UP, Kato K, de Jong WW, Boelens WC. Mimicking phosphorylation of the small heat-shock protein alphaB-crystallin recruits the F-box protein FBX4 to nuclear SC35 speckles. Eur J Biochem. 2004, 271: 4195-203.

den Engelsman J, Boros S, Dankers PY, Kamps B, Vree Egberts WT, Böde CS, Lane LA, Aquilina JA, Benesch JL, Robinson CV, de Jong WW, Boelens WC. The small heat-shock proteins HSPB2 and HSPB3 form well-defined heterooligomers in a unique 3 to 1 subunit ratio. J Mol Biol. 2009, 393: 1022-32.

Devi RR, Yao W, Vijayalakshmi P, Sergeev YV, Sundaresan P, Hejtmancik JF. Crystallin gene mutations in Indian families with inherited pediatric cataract. Mol Vis. 2008, 14: 1157-70.

Dreiza CM, Brophy CM, Komalavilas P, Furnish EJ, Joshi L, Pallero MA, Murphy-Ullrich JE, von Rechenberg M, Ho YS, Richardson B, Xu N, Zhen Y, Peltier JM, Panitch A. Transducible heat shock protein 20 (HSP20) phosphopeptide alters cytoskeletal dynamics. FASEB J. 2005, 19: 261-3.

Dyson N. The regulation of E2F by pRB-family proteins. Genes Dev. 1998, 12: 2245-2262.

Ehrnsperger M, Gräber S, Gaestel M, Buchner J. Binding of non-native protein to Hsp25 during heat shock creates a reservoir of folding intermediates for reactivation. EMBO J. 1997, 16: 221-9.

Elmore S. Apoptosis: a review of programmed cell death. Toxicol Pathol. 2007, 35: 495-516.

Evgrafov OV, Mersiyanova I, Irobi J, Van Den Bosch L, Dierick I, Leung CL, Schagina O, Verpoorten N, Van Impe K, Fedotov V, Dadali E, Auer-Grumbach M, Windpassinger C, Wagner K, Mitrovic Z, Hilton-Jones D, Talbot K, Martin JJ, Vasserman N, Tverskaya S, Polyakov A, Liem RK, Gettemans J, Robberecht W, De Jonghe P, Timmerman V. Mutant small heat-shock protein 27 causes axonal Charcot-Marie-Tooth disease and distal hereditary motor neuropathy. Nat Genet. 2004, 36: 602-6.

Favreau C, Higuet D, Courvalin JC, Buendia B. Expression of a mutant lamin A that causes Emery- Dreifuss muscular dystrophy inhibits in vitro differentiation of C2C12 myoblasts. Mol Cell Biol 2004, 24: 1481–1492.

Feil IK, Malfois M, Hendle J, van Der Zandt H, Svergun DI. A novel quaternary structure of the dimeric alpha-crystallin domain with chaperone-like activity. J Biol Chem 2001, 276: 12024-9.

Folker ES, Ostlund C, Luxton GW, Worman HJ, Gundersen GG. Lamin A variants that cause striated muscle disease are defective in anchoring transmembrane actin-associated nuclear lines for nuclear movement. Proc Natl Acad Sci U S A. 2011, 108: 131-6.

Fontaine JM, Rest JS, Welsh MJ, Benndorf R. The sperm outer dense fiber protein is the 10th member of the superfamily of mammalian small stress proteins. Cell Stress Chaperones. 2003, 8: 62-9.

Fuchs M, Poirier DJ, Seguin SJ, Lambert H, Carra S, Charette SJ, Landry J. Identification of the key structural motifs involved in HspB8/HspB6–Bag3 interaction. Biochemical Journal, 2010, 425: 245-257.

Gant TM, Wilson KL. Nuclear assembly. Annu Rev Cell Dev Biol. 1997, 13: 669-95.

Garrido C, Fromentin A, Bonnotte B, Favre N, Moutet M, Arrigo AP, Mehlen P, Solary E. Heat shock protein 27 enhances the tumorigenicity of immunogenic rat colon carcinoma cell clones. Cancer Res. 1998, 58: 5495-9.

Garrido C, Bruey JM, Fromentin A, Hammann A, Arrigo AP, Solary E. HSP27 inhibits cytochrome c-dependent activation of procaspase-9. Faseb J. 1999, 13: 2061–70.

Gerace L, Burke B. Functional organization of the nuclear envelope. Annu Rev Cell Biol. 1988, 4: 335-74.

Ghaoui R, Palmio J, Brewer J, Lek M, Needham M, Evilä A, Hackman P, Jonson PH, Penttilä S, Vihola A, Huovinen S, Lindfors M, Davis RL, Waddell L, Kaur S, Yiannikas C, North K, Clarke N, MacArthur DG, Sue CM, Udd B. Mutations in HSPB8 causing a new phenotype of distal myopathy and motor neuropathy. Neurology 2016, 86: 391-8.

Ghosh JG, Estrada MR, Houck SA, and Clark JI. The function of the beta3 interactive domain in the small heat shock protein and molecular chaperone, human alphaB crystallin. Cell Stress Chaperones 2006, 11: 187-197.

Giese KC, Vierling E. Changes in oligomerization are essential for the chaperone activity of a small heat shock protein in vivo and in vitro. J Biol Chem. 2002, 277: 46310-8.

Giffard RG, Han RQ, Emery JF, Duan M, Pittet JF. Regulation of apoptotic and inflammatory cell signaling in cerebral ischemia: the complex roles of heat shock protein 70. Anesthesiology 2008, 109: 339-48.

Golenhofen N, Redel A, Wawrousek EF, Drenckhahn D. Ischemia-induced increase of stiffness of alphaB-crystallin/HSPB2-deficient myocardium. Pflugers Arch. 2006, 451: 518-25.

Grose JH, Langston K, Wang X, Squires S, Mustafi SB, Hayes W, Neubert J, Fischer SK, Fasano M, Saunders GM, Dai Q, Christians E, Lewandowski ED, Ping P, Benjamin IJ.

Characterization of the Cardiac Overexpression of HSPB2 Reveals Mitochondrial and Myogenic Roles Supported by a Cardiac HspB2 Interactome. PLoS One 2015, 10: e0133994.

Gusev NB, Bogatcheva NV, Marston SB. Structure and properties of small heat shock proteins (sHsp) and their interaction with cytoskeleton proteins. Biochemistry (Mosc). 2002, 67: 511-9.

Hartl FU, Bracher A, Hayer-Hartl M. Molecular chaperones in protein folding and proteostasis. Nature 2011, 475: 324–332.

Haslbeck M, Miess A, Stromer T, Walter S, Buchner J. Disassembling protein aggregates in the yeast cytosol. The cooperation of Hsp26 with Ssa1 and Hsp104. J Biol Chem. 2005, 280: 23861-8.

Haslbeck M. Recombinant expression and in vitro refolding of the yeast small heat shock protein Hsp42. Int J Biol Macromol. 2006, 38: 107-14.

Haslbeck M, Vierling E. A first line of stress defense: small heat shock proteins and their function in protein homeostasis. J Mol Biol. 2015, 427: 1537-48.

Hilton GR, Lioe H, Stengel F, Baldwin AJ, Benesch JL. Small heat-shock proteins: paramedics of the cell. Top Curr Chem. 2013, 328: 69-98.

Houlden H, Laura M, Wavrant-De Vrièze F, Blake J, Wood N, Reilly MM. Mutations in the HSP27 (HSPB1) gene cause dominant, recessive, and sporadic distal HMN/CMT type 2. Neurology. 2008, 71: 1660-8.

https://www.cgl.ucsf.edu/chimera/data/acryst2011/acrystdemo.html.

Huot J, Houle F, Spitz DR, Landry J. HSP27 phosphorylation-mediated resistance against actin fragmentation and cell death induced by oxidative stress. Cancer Res 1996, 56: 273–279.

Ikeda Y, Abe A, Ishida C, Takahashi K, Hayasaka K, Yamada M. A clinical phenotype of distal hereditary motor neuronopathy type II with a novel HSPB1 mutation. J Neurol Sci. 2009, 277: 9-12.

Inagaki N, Hayashi T, Arimura T, Koga Y, Takahashi M, Shibata H, Teraoka K, Chikamori T, Yamashina A, Kimura A. Alpha B-crystallin mutation in dilated cardiomyopathy. Biochem Biophys Res Commun. 2006, 342: 379-86.

Irobi J, Van Impe K, Seeman P, Jordanova A, Dierick I, Verpoorten N, Michalik A, De Vriendt E, Jacobs A, Van Gerwen V, Vennekens K, Mazanec R, Tournev I, Hilton-Jones D, Talbot K, Kremensky I, Van Den Bosch L, Robberecht W, Van Vandekerckhove J, Van

Broeckhoven C, Gettemans J, De Jonghe P, Timmerman V. Hot-spot residue in small heat-shock protein 22 causes distal motor neuropathy. Nat Genet. 2004, 36: 597-601.

Ishiwata T, Orosz A, Wang X, Mustafi SB, Pratt GW, Christians ES, Boudina S, Abel ED, Benjamin IJ. HSPB2 is dispensable for the cardiac hypertrophic response but reduces mitochondrial energetics following pressure overload in mice. PLoS One 2012, 7: e42118.

Ito H, Kamei K, Iwamoto I, Inaguma Y, Nohara D, Kato K. Phosphorylation-induced change of the oligomerization state of a B-crystallin. J. Biol. Chem. 2001, 276: 5346– 5352.

Iwaki T, Iwaki A, Tateishi J, Goldman JE. Sense and antisense modification of glial alpha B-crystallin production results in alterations of stress fiber formation and thermoresistance. J Cell Biol. 1994, 125: 1385-93.

Iwaki A, Nagano T, Nakagawa M, Iwaki T, Fukumaki Y. Identification and characterization of the gene encoding a new member of the alpha-crystallin/small hsp family, closely linked to the alphaB-crystallin gene in a head-to-head manner. Genomics 1997, 45: 386-94.

Jaalouk DE, Lammerding J. Mechanotransduction gone awry. Nat Rev Mol Cell Biol. 2009, 10: 63-73.

Jakob U, Gaestel M, Engel K, Buchner J. Small heat shock proteins are molecular chaperones. J Biol Chem 1993, 268: 1517–20.

James PA, Rankin J, Talbot K. Asymmetrical late onset motor neuropathy associated with a novel mutation in the small heat shock protein HSPB1 (HSP27). J Neurol Neurosurg Psychiatry 2008, 79: 461-3.

Jana NR, Tanaka M, Wang GH, Nukina N. Polyglutamine length-dependent interaction of Hsp40 and Hsp70 family chaperones with truncated N-terminal huntingtin: their role in suppression of aggregation and cellular toxicity. Hum Mol Genet. 2000, 9: 2009-18.

Jansen G, Groenen PJ, Bächner D, Jap PH, Coerwinkel M, Oerlemans F, van den Broek W, Gohlsch B, Pette D, Plomp JJ, Molenaar PC, Nederhoff MG, van Echteld CJ, Dekker M, Berns A, Hameister H, Wieringa B. Abnormal myotonic dystrophy protein kinase levels produce only mild myopathy in mice. Nat Genet. 1996, 13: 316-24.

Jantschitsch C, Kindas-Mügge I, Metze D, Amann G, Micksche M, Trautinger F. Expression of the small heat shock protein HSP 27 in developing human skin. Br J Dermatol. 1998, 139: 247-53.

Jao CY, Salic A. Exploring RNA transcription and turnover in vivo by using click chemistry. Proc Natl Acad Sci U S A. 2008, 105: 15779-84.

Jehle S, Rajagopal P, Bardiaux B, Markovic S, Kühne R, Stout JR, Higman VA, Klevit RE, van Rossum BJ, Oschkinat H. Solid-state NMR and SAXS studies provide a structural basis for the activation of alphaB-crystallin oligomers. Nat Struct Mol Biol. 2010, 17: 1037-42.

Jehle S, Vollmar BS, Bardiaux B, Dove KK, Rajagopal P, Gonen T, Oschkinat H, Klevit RE. N-terminal domain of alphaB-crystallin provides a conformational switch for multimerization and structural heterogeneity. Proc Natl Acad Sci U S A. 2011, 108: 6409-14

Kadono T, Zhang XQ, Srinivasan S, Ishida H, Barry WH, Benjamin IJ. CRYAB and HSPB2 deficiency increases myocyte mitochondrial permeability transition and mitochondrial calcium uptake. J Mol Cell Cardiol. 2006, 40: 783-9.

Kampinga HH, Brunsting JF, Stege GJ, Burgman PW, Konings AW. Thermal protein denaturation and protein aggregation in cells made thermotolerant by various chemicals: role of heat shock proteins. Exp Cell Res. 1995, 219: 536-46.

Kamradt MC, Chen F, Sam S, Cryns VL. The small heat shock protein αB-crystallin negatively regulates apoptosis during myogenic differentiation by inhibiting caspase-3 activation. J Biol Chem. 2002, 277: 38731–38736.

Kamradt MC, Lu M, Werner ME, Kwan T, Chen F, Strohecker A, Oshita S, Wilkinson JC, Yu C, Oliver PG, Duckett CS, Buchsbaum DJ, LoBuglio AF, Jordan VC, Cryns VL. The small heat shock protein αB-crystallin is a novel inhibitor of TRAIL-induced apoptosis that suppresses the activation of caspase-3. J Biol Chem. 2005, 280: 11059–11066.

Kato K, Ito H, Kamei K, Inaguma Y, Iwamoto I, Saga S. Phosphorylation of alphaB-crystallin in mitotic cells and identification of enzymatic activities responsible for phosphorylation. J Biol Chem. 1998, 273: 28346-54.

Kato K, Ito H, Iwamoto I, Lida K, Inaguma Y. Protein kinase inhibitors can suppress stress-induced dissociation of Hsp27. Cell Stress Chaperones. 2001, 6: 16-20.

Kaufman SJ, George-Weinstein M, Foster RF. In vitro development of precursor cells in the myogenic lineage. Dev Biol. 1991, 146: 228-38.

Kaufmann U, Kirsch J, Irintchev A, Wernig A, Starzinski-Powitz A. The M-cadherin catenin complex interacts with microtubules in skeletal muscle cells: Implications for the fusion of myoblasts. J. Cell. Sci. 1999, 112: 55–68.

Kim KK, Kim R, Kim SH. Crystal structure of a small heat-shock protein. Nature 1998, 394: 595–599.

Kirschner M, Winkelhaus S, Thierfelder JM, Nover L. Transient expression and heat-stress-induced co-aggregation of endogenous and heterologous small heat-stress proteins in tobacco protoplasts Plant Journal. 2000, 24: 397–411

Kolb SJ, Snyder PJ, Poi EJ, Renard EA, Bartlett A, Gu S, Sutton S, Arnold WD, Freimer ML, Lawson VH, Kissel JT, Prior TW. Mutant small heat shock protein B3 causes motor neuropathy: utility of a candidate gene approach. Neurology 2010, 74: 502-6.

Krief S, Faivre JF, Robert P, Le Douarin B, Brument-Larignon N, Lefrere I, Bouzyk MM, Anderson KM, Greller LD, Tobin FL, Souchet M, Bril A. Identification and characterization of cvHsp - A novel human small stress protein selectively expressed in cardiovascular and insulin-sensitive tissues. J Biol Chem. 1999, 274: 36592–36600.

Kriehuber T, Rattei T, Weinmaier T, Bepperling A, Haslbeck M, Buchner J. Independent evolution of the core domain and its flanking sequences in small heat shock proteins. FASEB J. 2010, 24: 3633-42.

Kumar LV, Ramakrishna T, Rao CM. Structural and functional consequences of the mutation of a conserved arginine residue in alphaA and alphaB crystallins. J Biol Chem. 1999, 274: 24137-41.

Kumaran RI, Muralikrishna B, Parnaik VK. Lamin A/C speckles mediate spatial organization of splicing factor compartments and RNA polymerase II transcription. J Cell Biol. 2002, 159: 783-93.

Kumaran RI, Spector DL. A genetic locus targeted to the nuclear periphery in living cells maintains its transcriptional competence. J Cell Biol. 2008, 180: 51–65.

Kumarasamy A, Abraham EC. Interaction of C-terminal truncated human alphaA-crystallins with target proteins. PLoS One 2008, 3: e3175.

Laemmli UK, Beguin F, Gujer-Kellenberger G. A factor preventing the major head protein of bacteriophage T4 from random aggregation. J Mol Biol. 1970, 47: 69-85.

Laganowsky A, Benesch JL, Landau M, Ding L, Sawaya MR, Cascio D, Huang Q, Robinson CV, Horwitz J, Eisenberg D. Crystal structures of truncated alphaA and alphaB crystallins reveal structural mechanisms of polydispersity important for eye lens function. Protein Sci. 2010, 19: 1031-43.

Lam WY, Wing Tsui SK, Law PT, Luk SC, Fung KP, Lee CY, Waye MM. Isolation and characterization of a human heart cDNA encoding a new member of the small heat shock protein family--HSPL27. Biochim Biophys Acta. 1996, 1314: 120-4.

Lambert H, Charette SJ, Bernier AF, Guimond A, Landry J. HSP27 multimerization mediated by phosphorylation-sensitive intermolecular interactions at the amino terminus. J Biol Chem. 1999, 274: 9378-85.

Lammerding J, Hsiao J, Schulze PC, Kozlov S, Stewart CL, Lee RT. Abnormal nuclear shape and impaired mechanotransduction in emerin-deficient cells. J. Cell Biol. 2005, 170: 781–791.

Landry J, Chrétien P, Lambert H, Hickey E, Weber LA. Heat shock resistance conferred by expression of the human HSP27 gene in rodent cells. J Cell Biol. 1989, 109: 7-15.

Landry J, Lambert H, Zhou M, Lavoie JN, Hickey E, Weber LA, Anderson CW. Human HSP27 is phosphorylated at serines 78 and 82 by heat shock and mitogen-activated kinases that recognize the same amino acid motif as S6 kinase II. J Biol Chem. 1992, 267: 794-803.

Lavoie JN, Gingras-Breton G, Tanguay RM, Landry J. Induction of Chinese hamster HSP27 gene expression in mouse cells confers resistance to heat shock. HSP27 stabilization of the microfilament organization. 1993, J Biol Chem 268: 3420–3429.

Lavoie JN, Hickey E, Weber LA, Landry J. Modulation of actin microfilament dynamics and fluid phase pinocytosis by phosphorylation of heat shock protein 27. J Biol Chem. 1993a, 268: 24210–24214.

Lavoie JN, Lambert H, Hickey E, Weber LA, Landry J. Modulation of cellular thermoresistance and actin filament stability accompanies phosphorylation-induced changes in the oligomeric structure of heat shock protein 27. Mol Cell Biol. 1995, 15: 505-16.

Lazarides E, Hubbard BD. Immunological characterization of the subunit of the 100 A filaments from muscle cells. Proc. Natl. Acad. Sci. 1976, 73: 4344–4348

Lein ES, Hawrylycz MJ, Ao N, Ayres M, Bensinger A, Bernard A, Boe AF, Boguski MS, Brockway KS, Byrnes EJ, Chen L, Chen L, Chen TM, Chin MC, Chong J, Crook BE, Czaplinska A, Dang CN, Datta S, Dee NR, Desaki AL, Desta T, Diep E, Dolbeare TA, Donelan MJ, Dong HW, Dougherty JG, Duncan BJ, Ebbert AJ, Eichele G, Estin LK, Faber C, Facer BA, Fields R, Fischer SR, Fliss TP, Frensley C, Gates SN, Glattfelder KJ, Halverson KR, Hart MR, Hohmann JG, Howell MP, Jeung DP, Johnson RA, Karr PT, Kawal R, Kidney JM, Knapik RH, Kuan CL, Lake JH, Laramee AR, Larsen KD, Lau C, Lemon TA, Liang AJ, Liu Y, Luong LT, Michaels J, Morgan JJ, Morgan RJ, Mortrud MT, Mosqueda NF, Ng LL, Ng R, Orta GJ, Overly CC, Pak TH, Parry SE, Pathak SD, Pearson OC, Puchalski RB, Riley ZL, Rockett HR, Rowland SA, Royall JJ, Ruiz MJ, Sarno NR, Schaffnit K, Shapovalova NV, Sivisay T, Slaughterbeck CR, Smith SC, Smith KA, Smith BI, Sodt AJ, Stewart NN, Stumpf KR, Sunkin SM, Sutram M, Tam A, Teemer CD, Thaller C, Thompson CL, Varnam LR, Visel A, Whitlock RM, Wohnoutka PE, Wolkey CK, Wong VY, Wood M, Yaylaoglu MB, Young RC,

Youngstrom BL, Yuan XF, Zhang B, Zwingman TA, Jones AR. Genome-wide atlas of gene expression in the adult mouse brain. Nature 2007, 445: 168-76.

Li H, Choudhary SK, Milner DJ, Munir MI, Kuisk IR, Capetanaki Y. Inhibition of desmin expression blocks myoblast fusion and interferes with the myogenic regulators MyoD and myogenin. J. Cell Biol. 1994, 124: 827–841.

Liang P, MacRae TH. Molecular chaperones and the cytoskeleton. J Cell Sci. 1997, 110: 1431-40.

Lindner RA, Carver JA, Ehrnsperger M, Buchner J, Esposito G, Behlke J, Lutsch G, Kotlyarov A, Gaestel M. Mouse Hsp25, a small shock protein. The role of its C-terminal extension in oligomerization and chaperone action. Eur J Biochem. 2000, 267: 1923-32.

Locke M, Noble EG, Atkinson BG. Exercising mammals synthesize stress proteins. Am J Physiol. 1990, 258: C723-9.

Locke M, Noble EG, Atkinson BG. Inducible isoform of HSP70 is constitutively expressed in a muscle fiber type specific pattern. Am J Physiol. 1991, 261: C774-9.

Lutsch G, Vetter R, Offhauss U, Wieske M, Gröne HJ, Klemenz R, Schimke I, Stahl J, Benndorf R. Abundance and location of the small heat shock proteins HSP25 and alphaB-crystallin in rat and human heart. Circulation 1997, 96: 3466-76.

Macleod K. pRb and E2f-1 in mouse development and tumorigenesis. Curr. Opin. Genet. Dev. 1999, 9: 31-39.

Maeda M, Taft CS, Bush EW, Holder E, Bailey WM, Neville H, Perryman MB, Bies RD. Identification, tissue-specific expression, and subcellular localization of the 80- and 71-kDa forms of myotonic dystrophy kinase protein. J Biol Chem. 1995, 270: 20246-9.

Maraldi NM, Squarzoni S, Sabatelli P, Capanni C, Mattioli E, Ognibene A, Lattanzi G. Laminopathies: involvement of structural nuclear proteins in the pathogenesis of an increasing number of human diseases. J Cell Physiol. 2005, 203: 319-27.

Marin-Vinader L, Shin C, Onnekink C, Manley JL, Lubsen NH. Hsp27 enhances recovery of splicing as well as rephosphorylation of SRp38 after heat shock. Mol Biol Cell. 2006, 17: 886-94.

Markiewicz E, Ledran M, Hutchison CJ. Remodelling of the nuclear lamina and nucleoskeleton is required for skeletal muscle differentiation in vitro. J Cell Sci 2005, 118: 409–420.

Mattioli E, Columbaro M, Capanni C, Maraldi NM, Cenni V, Scotlandi K, Marino MT, Merlini L, Squarzoni S, Lattanzi G. Prelamin A-mediated recruitment of SUN1 to the nuclear

envelope directs nuclear positioning in human muscle. Cell Death Differ. 2011, 18: 1305-15.

Mchaourab HS, Dodson EK, Koteiche HA. Mechanism of chaperone function in small heat shock proteins. Two-mode binding of the excited states of T4 lysozyme mutants by alphaA-crystallin. J Biol Chem. 2002, 277: 40557-66.

McKinsey TA, Zhang CL, Olson EN. Control of muscle development by dueling HATs and HDACs. Curr. Opin. Genet. Dev. 2001, 11: 497-504.

Méjat A, Decostre V, Li J, Renou L, Kesari A, Hantaï D, Stewart CL, Xiao X, Hoffman E, Bonne G, Misteli T. Lamin A/C-mediated neuromuscular junction defects in Emery-Dreifuss muscular dystrophy. J Cell Biol. 2009, 184: 31-44.

Méjat A, Misteli T. LINC complexes in health and disease. Nucleus. 2010, 1: 40-52.

Melcon G, Kozlov S, Cutler DA, Sullivan T, Hernandez L, Zhao P, Mitchell S, Nader G, Bakay M, Rottman JN, Hoffman EP, Stewart CL. Loss of emerin at the nuclear envelope disrupts the Rb1/E2F and MyoD pathways during muscle regeneration. Hum Mol Genet. 2006, 15 :637-51.

Merck KB, De Haard-Hoekman WA, Oude Essink BB, Bloemendal H, De Jong WW. Expression and aggregation of recombinant alpha A-crystallin and its two domains. Biochim Biophys Acta 1992, 1130: 267-76.

Mercuri E, Poppe M, Quinlivan R, Messina S, Kinali M, Demay L, Bourke J, Richard P, Sewry C, Pike M, Bonne G, Muntoni F, Bushby K. Extreme variability of phenotype in patients with an identical missense mutation in the lamin A/C gene: from congenital onset with severe phenotype to milder classic Emery-Dreifuss variant. Arch Neurol. 2004, 61: 690-4.

Michaud S, Lavoie S, Guimond MO, Tanguay RM. The nuclear localization of Drosophila Hsp27 is dependent on a monopartite arginine-rich NLS and is uncoupled from its association to nuclear speckles. Biochim Biophys Acta. 2008, 1783: 1200-10.

Mogk A, Deuerling E, Vorderwülbecke S, Vierling E, Bukau B. Small heat shock proteins, ClpB and the DnaK system form a functional triade in reversing protein aggregation. Mol Microbiol. 2003, 50: 585-95.

Mogk A, Schlieker C, Friedrich KL, Schönfeld HJ, Vierling E, Bukau B. Refolding of substrates bound to small Hsps relies on a disaggregation reaction mediated most efficiently by ClpB/DnaK. J Biol Chem. 2003a, 278: 31033-42

Moir RD, Spann TP, Goldman RD. The dynamic properties and possible functions of nuclear lamins. Int Rev Cytol. 1995, 162B: 141-82.

Molkentin JD, Black BL, Martin JF, Olson EN. Cooperative activation of muscle gene expression by MEF2 and myogenic bHLH proteins. Cell. 1995, 83:1125–1136

Morrison LE, Whittaker RJ, Klepper RE, Wawrousek EF, Glembotski CC. Roles for alphaB-crystallin and HSPB2 in protecting the myocardium from ischemia-reperfusion-induced damage in a KO mouse model. Am J Physiol Heart Circ Physiol. 2004, 286: H847-55.

Mounier N, Arrigo AP. Actin cytoskeleton and small heat shock proteins: how do they interact? Cell Stress & Chaperones 2002, 7: 167–176

Muchir A, Bonne G, van der Kooi AJ, van Meegen M, Baas F, Bolhuis PA, de Visser M, Schwartz K. Identification of mutations in the gene encoding lamins A/C in autosomal dominant limb girdle muscular dystrophy with atrioventricular conduction disturbances (LGMD1B). Hum Mol Genet. 2000, 9: 1453-9.

Mymrikov EV, Seit-Nebi AS, Gusev NB. Large potentials of small heat shock proteins. Physiol Rev. 2011, 91: 1123-59.

Nahle Z, Polakoff J, Davuluri RV, McCurrach ME, Jacobson MD, Narita M, Zhang MQ, Lazebnik Y, Bar-Sagi D, Lowe SW. Direct coupling of the cell cycle and cell death machinery by E2F. Nat. Cell Biol. 2002, 4: 859-864.

Nakagawa M, Tsujimoto N, Nakagawa H, Iwaki T, Fukumaki Y, Iwaki A. Association of HSPB2, a member of the small heat shock protein family, with mitochondria. Exp Cell Res. 2001, 271: 161-8.

Nicholl ID, Quinlan RA. Chaperone activity of alpha-crystallins modulates intermediate filament assembly. EMBO J. 1994, 13: 945-53.

Novitch BG, Spicer DB, Kim PS, Cheung WL, Lassar AB. pRb is required for MEF2-dependent gene expression as well as cell-cycle arrest during skeletal muscle differentiation. Curr. Biol. 1999, 9: 449-459.

Olson EN, Klein WH. bHLH factors in muscle development: dead lines and commitments, what to leave in and what to leave out. Genes Dev. 1994, 8: 1–8.

Oustanina S, Hause G, Braun T. Pax7 directs postnatal renewal and propagation of myogenic satellite cells but not their specification. EMBO J. 2004, 23: 3430-9.

Ozawa R, Hayashi YK, Ogawa M, Kurokawa R, Matsumoto H, Noguchi S, Nonaka I, Nishino I. Emerin-lacking mice show minimal motor and cardiac dysfunctions with nuclear-associated vacuoles. Am. J.Pathol. 2006, 168: 907–917.

Pandey P, Saleh A, Nakazawa A, Kumar S, Srinivasula SM, Kumar V,Weichselbaum R, Nalin C, Alnemri ES, Kufe D, Kharbanda S. Negative regulation of cytochrome c-mediated oligomerization of Apaf-1 and activation of procaspase-9 by heat shock protein 90. EMBO J. 2000, 19: 4310–22.

Parcellier A, Schmitt E, Gurbuxani S, Seigneurin-Berny D, Pance A, Chantome A, Plenchette S, Khochbin S, Solary E, Garrido C. HSP27 is a ubiquitin-binding protein involved in I-kappaBalpha proteasomal degradation. Mol Cell Biol. 2003, 23: 5790–802.

Parker MH, Seale P, Rudnicki MA. Looking back to the embryo: defining transcriptional networks in adult myogenesis. Nat Rev Genet. 2003, 4: 497-507.

Pasta SY, Raman B, Ramakrishna T, Rao CM. The IXI/V motif in the C-terminal extension of alpha-crystallins: Alternative interactions and oligomeric assemblies. Molecular Vision 2004, 10: 655–662.

Paulin D, Li Z. Desmin: a major intermediate filament protein essential for the structural integrity and function of muscle. Exp Cell Res. 2004, 301: 1-7.

Peckham M. Engineering a multi-nucleated myotube, the role of the actin cytoskeleton. J Microsc. 2008, 231: 486-93.

Perng MD, Cairns L, van den IJssel P, Prescott A, Hutcheson AM, Quinlan RA. Intermediate filament interactions can be altered by HSP27 and alphaB-crystallin. J Cell Sci. 1999, 112: 2099-112.

Perng MD, Muchowski PJ, van Den IJssel P, Wu GJ, Hutcheson AM, Clark JI, Quinlan RA The cardiomyopathy and lens cataract mutation in alphaB-crystallin alters its protein structure, chaperone activity, and interaction with intermediate filaments in vitro. J Biol Chem. 1999a, 274: 33235-43.

Perng MD, Wen SF, van den IJssel P, Prescott AR, Quinlan RA. Desmin aggregate formation by R120G alphaB-crystallin is caused by altered filament interactions and is dependent upon network status in cells. Mol Biol Cell. 2004, 15: 2335-46.

Pilotto A, Marziliano N, Pasotti M, Grasso M, Costante AM, Arbustini E. alphaB-crystallin mutation in dilated cardiomyopathies: low prevalence in a consecutive series of 200 unrelated probands. Biochem Biophys Res Commun. 2006, 346: 1115-7.

Piotrowicz RS, Hickey E, Levin EG. Heat shock protein 27 kDa expression and phosphorylation regulates endothelial cell migration. FASEB J 1998, 12: 1481–1490.

Piotrowicz RS, Levin EG. Basolateral membrane-associated 27-kDa heat shock protein and microfilament polymerization. J Biol Chem 1997, 272: 25920–25927.

Puri PL, Iezzi S, Stiegler P, Chen TT, Schiltz RL, Muscat GE, Giordano A, Kedes L, Wang JY, Sartorelli V. Class I histone deacetylases sequentially interact with MyoD and pRb during skeletal myogenesis. Mol. Cell. 2001, 8: 885-897.

Quijano-Roy S, Mbieleu B, Bönnemann CG, Jeannet PY, Colomer J, Clarke NF, Cuisset JM, Roper H, De Meirleir L, D'Amico A, Ben Yaou R, Nascimento A, Barois A, Demay L, Bertini E, Ferreiro A, Sewry CA, Romero NB, Ryan M, Muntoni F, Guicheney P, Richard P, Bonne G, Estournet B. De novo LMNA mutations cause a new form of congenital muscular dystrophy. Ann Neurol. 2008, 64: 177-86.

Raman B, Ramakrishna T, Rao CM. Temperature dependent chaperone-like activity of alpha-crystallin. FEBS Lett 1995, 365: 133-6.

Raman B, Rao CM. Chaperone-like activity and quaternary structure of alpha-crystallin. J Biol Chem. 1994, 269: 27264-8.

Raman B, Rao CM. Chaperone-like activity and temperature-induced structural changes of alpha-crystallin. J Biol Chem 1997, 272: 23559-64.

Rao PV, Horwitz J, Zigler JS, Jr. Chaperone-like activity of a-crystallin. J. Biol. Chem. 1994, 269: 13266–13272.

Relaix F, Rocancourt D, Mansouri A, Buckingham M. A Pax3/Pax7-dependent population of skeletal muscle progenitor cells. Nature 2005, 435: 948-53.

Requena JM, Montalvo AM, Fraga J. Molecular Chaperones of Leishmania: Central Players in Many Stress-Related and -Unrelated Physiological Processes. BioMed Research International 2015.

Rusmini P, Polanco MJ, Cristofani R, Cicardi ME, Meroni M, Galbiati M, Piccolella M, Messi E, Giorgetti E, Lieberman AP Milioto C, Rocchi A, Aggarwal T, Pennuto M, Crippa V, Poletti A. Aberrant Autophagic Response in The Muscle of A Knock-in Mouse Model of Spinal and Bulbar Muscular Atrophy. Sci Rep. 2015, 5: 15174.

Saibil H. “Chaperone machines for protein folding, unfolding and disaggregation”. Nature Reviews Molecular Cell Biology 2013, 14: 630–642.

Saji H, Iizuka R, Yoshida T, Abe T, Kidokoro S, Ishii N, Yohda M. Role of the IXI/V motif in oligomer assembly and function of StHsp14.0, a small heat shock protein from the acidothermophilic archaeon, Sulfolobus tokodaii strain 7. Proteins. 2008, 71: 771-82.

Schäfer C, Clapp P, Welsh MJ, Benndorf R, Williams JA. HSP27 expression regulates CCK-induced changes of the actin cytoskeleton in CHO-CCK-A cells. Am J Physiol. 1999, 277: C1032-43.

Shaklai S, Amariglio N, Rechavi G, Simon AJ. Gene silencing at the nuclear periphery. Febs J. 2007, 274: 1383-92.

Shashidharamurthy R, Koteiche HA, Dong J, McHaourab HS. Mechanism of chaperone function in small heat shock proteins: dissociation of the HSP27 oligomer is required for recognition and binding of destabilized T4 lysozyme. J Biol Chem. 2005, 280: 5281-9.

Shemetov AA, Gusev NB. Biochemical characterization of small heat shock protein HspB8 (Hsp22)-Bag3 interaction. Arch Biochem Biophys. 2011, 513: 1-9.

Shimi T, Pfleghaar K, Kojima Shin-ichiro, Pack Chan-Gi, Solovei I, Goldman AE, Adam SA, Dale K. Shumaker DK, Kinjo M, Cremer T, Goldman RD. The A- and B-type nuclear lamin networks: microdomains involved in chromatin organization and transcription. Genes Dev. 2008, 22: 3409–3421.

Sinensky M, Fantle K, Trujillo M, McLain T, Kupfer A, Dalton M. The processing pathway of prelamin A. J Cell Sci. 1994, 107: 61-7.

Sittler A, Lurz R, Lueder G, Priller J, Lehrach H, Hayer-Hartl MK, Hartl FU, Wanker EE. Geldanamycin activates a heat shock response and inhibits huntingtin aggregation in a cell culture model of Huntington's disease. Hum Mol Genet. 2001, 10: 1307-15.

Smith JB, Liu Y, Smith DL. Identification of possible regions of chaperone activity in lens alpha-crystallin. Exp Eye Res. 1996, 63: 125-8.

Smythe GM, Davies MJ, Paulin D, Grounds MD. Absence of desmin slightly prolongs myoblast proliferation and delays fusion in vivo in regenerating grafts of skeletal muscle. Cell Tissue Res. 2001, 304: 287–294.

Sobott F, McCammon MG, Hernández H, Robinson CV. The flight of macromolecular complexes in a mass spectrometer. Philos Trans A Math Phys Eng Sci. 2005, 363: 379-89.

Spann TP, Goldman AE, Wang C, Huang S, Goldman RD. Alteration of nuclear lamin organization inhibits RNA polymerase II-dependent transcription. J Cell Biol. 2002, 156: 603-8.

Spector DL, Lamond AI. Nuclear speckles. Cold Spring Harb Perspect Biol. 2011.

Sreelakshmi Y, and Sharma KK. Recognition sequence 2 (residues 60-71) plays a role in oligomerization and exchange dynamics of alphaB-crystallin. Biochemistry 2005, 44: 12245-12252.

Stenoien DL, Cummings CJ, Adams HP, Mancini MG, Patel K, DeMartino GN, Marcelli M, Weigel NL, Mancini MA. Hum Mol Genet 1999, 8: 731–41.

Studer S, Obrist M, Lentze N, Narberhaus F. A critical motif for oligomerization and chaperone activity of bacterial alpha-heat shock proteins. European Journal of Biochemistry 2002, 269: 3578–3586.

Stuurman N, Heins S, Aebi U. Nuclear lamins: their structure, assembly, and interactions. J Struct Biol. 1998, 122: 42-66.

Sugiyama Y, Suzuki A, Kishikawa M, Akutsu R, Hirose T, Waye MM, Tsui SK, Yoshida S, Ohno S. Muscle develops a specific form of small heat shock protein complex composed of MKBP/HSPB2 and HSPB3 during myogenic differentiation. J Biol Chem. 2000, 275: 1095-104.

Sullivan T, Escalante-Alcalde D, Bhatt H, Anver M, Bhat N, Nagashima K, Stewart CL, Burke B. Loss of A-type lamin expression compromises nuclear envelope integrity leading to muscular dystrophy. J Cell Biol. 1999, 147: 913-20.

Sun Y, MacRae TH. Small heat shock proteins: molecular structure and chaperone function. Cell Mol Life Sci. 2005, 62: 2460-76.

Suzuki A, Sugiyama Y, Hayashi Y, Nyu-i N, Yoshida M, Nonaka I, Ishiura S, Arahata K, Ohno S. MKBP, a novel member of the small heat shock protein family, binds and activates the myotonic dystrophy protein kinase. J Cell Biol. 1998, 140: 1113-24.

Sylvius N, Bonne G, Straatman K, Reddy T, Gant TW, Shackleton S. MicroRNA expression profiling in patients with lamin A/C-associated muscular dystrophy. Faseb J. 2011, 25: 3966-78.

Tang BS, Zhao GH, Luo W, Xia K, Cai F, Pan Q, Zhang RX, Zhang FF, Liu XM, Chen B, Zhang C, Shen L, Jiang H, Long ZG, Dai HP. Small heat-shock protein 22 mutated in autosomal dominant Charcot-Marie-Tooth disease type 2L. Hum Genet. 2005, 116: 222-4.

Tang CW, Maya-Mendoza A, Martin C, Zeng K, Chen S, Feret D, Wilson SA, Jackson DA. The integrity of a lamin-B1-dependent nucleoskeleton is a fundamental determinant of RNA synthesis in human cells. J Cell Sci. 2008, 121: 1014-24.

Tavaria M, Gabriele T, Kola I, Anderson RL A hitchhiker's guide to the human Hsp70 family. Cell Stress Chaperones 1996, 1: 23–28.

Taylor RP, Benjamin IJ. Small heat shock proteins: a new classification scheme in mammals. J Mol Cell Cardiol. 2005, 38: 433-44.

Treweek TM, Rekas A, Walker MJ, Carver JA. A quantitative NMR spectroscopic examination of the flexibility of the C-terminal extensions of the molecular chaperones, αA- and αB-crystallin. Exp Eye Res. 2010, 91: 691-9.

van de Klundert FA, Gijsen ML, van den IJssel PR, Snoeckx LH, de Jong WW. alpha B-crystallin and hsp25 in neonatal cardiac cells--differences in cellular localization under stress conditions. Eur J Cell Biol. 1998, 75: 38-45.

Van der Kooi AJ, van Meegen M, Ledderhof TM, McNally EM, de Visser M, Bolhuis PA. Genetic localization of a newly recognized autosomal dominant limb-girdle muscular dystrophy with cardiac involvement (LGMD1B) to chromosome 1q11-21. Am J Hum Genet. 1997, 60: 891-5.

van Heijst JW, Niessen HW, Musters RJ, van Hinsbergh VW, Hoekman K, Schalkwijk CG. Argpyrimidine-modified Heat shock protein 27 in human non-small cell lung cancer: a possible mechanism for evasion of apoptosis. Cancer Lett 2006, 241: 309–19.

van Montfort RL, Basha E, Friedrich KL, Slingsby C, Vierling E. Crystal structure and assembly of a eukaryotic small heat shock protein. Nat. Struct. Biol. 2001, 8: 1025-1030.

Van Montfort R, Slingsby C, Vierling E. Structure and function of the small heat shock protein/alpha-crystallin family of molecular chaperones. Adv Protein Chem. 2001a, 59: 105-56.

van Rijk AE, Stege GJ, Bennink EJ, May A, Bloemendal H. Nuclear staining for the small heat shock protein alphaB-crystallin colocalizes with splicing factor SC35. Eur J Cell Biol. 2003, 82: 361-8.

Vaughan A, Alvarez-Reyes M, Bridger JM, Broers JL, Ramaekers FC, Wehnert M, Morris GE, Whitfield WGF, Hutchison CJ. Both emerin and lamin C depend on lamin A for localization at the nuclear envelope. J Cell Sci. 2001, 114: 2577-90.

Verghese J, Abrams J, Wang Y, Morano KA. “Biology of the heat shock response and protein chaperones: budding yeast (Saccharomyces cerevisiae) as a model system,” Microbiology and Molecular Biology Reviews. 2012, 76: 115–158.

Vicart P, Dupret JM, Hazan J, Li Z, Gyapay G, Krishnamoorthy R, Weissenbach J, Fardeau M, Paulin D. Human desmin gene: cDNA sequence, regional localization and exclusion of the locus in a familial desmin-related myopathy. Hum Genet. 1996, 98: 422-9.

Vicart P, Caron A, Guicheney P, Li Z, Prevost MC, Faure A, Chateau D, Chapon F, Tomé F, Dupret JM, Paulin D, Fardeau M. A missense mutation in the alpha B-crystallin chaperone gene causes a desmin-related myopathy. Nat Genet 1998, 20: 92–5.

Vos MJ, Hageman J, Carra S, Kampinga HH. Structural and Functional Diversities between Members of the Human HSPB, HSPH, HSPA, and DNAJ Chaperone Families. Biochemistry, 2008, 47: pp 7001–7011.

Vos MJ, Kanon B, Kampinga HH. HSPB7 is a SC35 speckle resident small heat shock protein. Biochim Biophys Acta. 2009, 1793: 1343-53.

Vos MJ, Zijlstra MP, Kanon B, van Waarde-Verhagen MA, Brunt ER, Oosterveld-Hut HM, Carra S, Sibon OC, Kampinga HH. HSPB7 is the most potent polyQ aggregation suppressor within the HSPB family of molecular chaperones. Hum Mol Genet. 2010, 19: 4677-93.

Wang K, Spector A. Alpha-crystallin stabilizes actin filaments and prevents cytochalasin-induced depolymerization in a phosphorylation-dependent manner. Eur J Biochem. 1996, 242: 56-66.

Wang X, McManus M. Lentivirus production. J Vis Exp. 2009.

Weitzer G, Milner DJ, Kim JU, Bradley A, Capetanaki Y. Cytoskeletal control of myogenesis: A desmin null mutation blocks the myogenic pathway during embryonic stem cell differentiation. Dev. Biol. 1995, 172: 422–439.

Whiting EJ, Waring JD, Tamai K, Somerville MJ, Hincke M, Staines WA, Ikeda JE, Korneluk RG. Characterization of myotonic dystrophy kinase (DMK) protein in human and rodent muscle and central nervous tissue. Hum Mol Genet. 1995, 4: 1063-72.

Worman HJ, Gundersen GG. Here come the SUNs: a nucleocytoskeletal missing link, Trends Cell Biol. 2006, 16: 67–69.

Zeschnigk M, Kozian D, Kuch C, Schmoll M, Starzinski-Powitz A. Involvement of M-cadherin in terminal differentiation of skeletal muscle cells. J. Cell Sci. 1995, 108: 2973–2981

Zhu CH, Mouly V, Cooper RN, Mamchaoui K, Bigot A, Shay JW, Di Santo JP, Butler-Browne GS, Wright WE. Cellular senescence in human myoblasts is overcome by human telomerase reverse transcriptase and cyclin-dependent kinase 4: consequences in aging muscle and therapeutic strategies for muscular dystrophies. Aging Cell. 2007, 6: 515-23.

Zwerger M, Jaalouk DE, Lombardi ML, Isermann P, Mauermann M, Dialynas G, Herrmann H, Wallrath LL, Lammerding J. Myopathic lamin mutations impair nuclear stability in cells and tissue and disrupt nucleo-cytoskeletal coupling. Hum Mol Genet. 2013, 22: 2335-49.